UNIVERSITATEA DE MEDICINĂ ȘI FARMACIE
GRIGORE T. POPA IAȘI

HABILITATION THESIS

Lecturer:
Constantin VOLOVĂȚ, MD, PhD

Iași

2023

UNIVERSITATEA DE MEDICINĂ ȘI FARMACIE
GRIGORE T. POPA IAȘI

PRECISION ONCOLOGY: INTEGRATING NANO-CARRIERS, BIOMARKERS, AND GROWTH FACTORS FOR ENHANCED THERAPEUTIC STRATEGIES

Lecturer:
Constantin VOLOVĂȚ, MD, PhD

2023

Table of Contents:

ABBREVIATIONS

ADR - adrenal

AI - artificial intelligence

ALC - absolute lymphocyte count

ALT - alanine aminotransferase

ANC - absolute neutrophil count

APC - antigen-presenting cells

AST - aspartate aminotransferase

BMI - body mass index

BRA - brain

CALR - calreticulin

CAT - catalase

CATLA-4 - cytotoxic T-lymphocyte-associated protein 4

CCPD - cytosine-phosphate-guanine oligodeoxynucleotide

CEOG PS - Eastern Cooperative Oncology Group Performance Score

CI - confidence interval

Cldn7 - Claudin-7

CRC - colorectal cancer

CPHSR - Cox Proportional Hazards Survival Regression

CTL - cytotoxic lymphocyte

CXCL10 - C-X-C motif chemokine 10

DAMPs - damage-associated molecular patterns

DNA - deoxyribonucleic acid

DSN - duration of severe neutropenia

ECG - echocardiographic

EMA - European Medicines Agency

EMT - epithelial-to-mesenchymal transition

EPR - enhanced permeability and retention effect

EVs - extracellular vesicles

FDA - Food and Drug Administration

FN - febrile neutropenia

GM-CSF - granulocyte-macrophage colony-stimulating factor

HAase - hyaluronidase

HB - hemoglobin

HEP - hepatic

HMGB1 - high-mobility group box 1

ICD - immunogenic cell death

ICI - immune checkpoint inhibitor

IDO - indoleamine 2,3-dioxygenase

IFN-α/β - interferon-alpha/beta

IFN-γ - interferon-gamma

IL-12 - interleukin-12

ITT - intent-to-treat

kNN - K-nearest neighbor

LNs - lymph nodes

MDDC - monocyte-derived dendritic cells

MHC - major histocompatibility complex

MDR - multidrug resistance

MDDC - monocyte-derived dendritic cells

MCV - mean corpuscular volume

MDR - multidrug resistance

MVBs - multivesicular bodies

NDDS - Nano drug delivery systems

NK/NKT cells - natural killer/natural killer T cells

NM - nanomaterial

NICE - National Institute for Health and Care Excellence

NLR - neutrophil-to-lymphocyte ratio

NMD - Nano drug delivery systems

NMR - nuclear magnetic resonance

NP - nanoparticles

NSCLC - non-small-cell lung cancer

OSS - osseous

OS - overall survival

PFS - progression-free survival

PEG - polyethylene glycol

PD-1 - programmed cell death protein 1

PD-L1 - programmed cell death ligand 1

PUL - pulmonary

RAS/MAP kinases - RAS/mitogen-activated protein kinases

RNA - ribonucleic acid

RNAi - RNA interference

ROS - reactive oxygen species

SAEs - serious adverse events

SC - subcutaneous

SCLC - small cell lung cancer

SD - standard deviation

T-VEC - Talimogene Laherparepvec

TEAE - treatment-emergent adverse event

TGF-β - transforming growth factor-beta

TIME - Tumour Immune Microenvironment

TILs - tumor-infiltrating lymphocytes

TMB - tumoral mutational burden

TME - tumor microenvironment

TNF - tumor necrosis factor

T-VEC - Talimogene Laherparepvec

TAMs - tumor-associated macrophages

TEXs - tumor-derived exosomes

TIME - Tumour Immune Microenvironment

TLR - toll-like receptor

TN - tumor necrosis factor

TNF - tumor necrosis factor

TNF - tumor necrosis factor

TNF - tumor necrosis factor

TNM - tumor-node-metastasis

TME - tumor microenvironment

VEGF - vascular endothelial growth factor

VLPs - virus-like particles

REZUMATUL TEZEI

Această teză de abilitare intitulată **„ONCOLOGIE DE PRECIZIE: INTEGRAREA NANOVECTORILOR, BIOMARKERILOR ȘI A FACTORILOR DE CREȘTERE PENTRU ÎMBUNĂTĂȚIREA STRATEGIILOR TERAPEUTICE”** redă necesitatea unei abordări multidisciplinare ale afecțiunilor oncologice în vederea identificării unor elemente inovatoare care vor putea crește performanța actului medical și care vor putea îmbunătăți prognosticul pacienților. Domeniul oncologiei se află sub auspiciul provocării permanente de inovare, constatându-se, de-a lungul timpului, numeroase progrese ale abordărilor terapeutice, iar această lucrare vine să evidențieze integrarea unor elemente de noutate în algoritmii de tratament oncologic, meniți să ofere rezultate clinice mai bune. Nanovectorii, biomarkerii serici și utilizarea factorilor de creștere reprezintă o serie de noi unelte utilizate în medicina personalizată, care oferă oportunitatea unui tratament țintit și a unor rezultate oncologice predictibile.

SECȚIUNEA I a tezei de abilitare cuprinde un rezumat al activităților mele științifice, academice și clinice realizate de-a lungul carierei și reflectate de obținerea unui număr de 1064 de citări și a unui indice Hirsch de 10.

SECȚIUNEA a-II-a din această teză reunește 3 capitole care reflectă activitatea mea științifică și interesele de cercetare recente. Primul capitol a evidențiat importanța utilizării nanovectorilor pentru imunomodulare și pentru terapia țintită în cazul diverselor tipuri de tumori maligne, cuprinzând și un model teoretic de eliberare a diclofenacului dintr-un dispozitiv special de tip hidrogel. Cel de-al doilea capitol a sintetizat rezultatele a două trialuri clinice care au urmărit identificarea unor factori de prognostic pentru cancerul colorectal și pulmonar. Al treilea capitol a descris rezultatele obținute de pe urma a 3 trialuri clinice care au măsurat eficacitatea utilizării factorilor de creștere în asociere cu chimioterapia pentru reducerea efectelor adverse specifice la pacienții cu cancer de sân sau pulmonar.

SECȚIUNEA a-III-a enunță principalele direcții de dezvoltare profesională, academică și de cercetare științifică pe care doresc să le pun în practică. Voi urmări o colaborare clinică și științifică interinstituțională, care să aducă beneficii multiple, atât pentru colectivul de cercetători, precum și pentru pacienți. Totodată, doresc să implic activ

atât studenții, cât și rezidenții în activitatea de cercetare și în multiple activități didactice centrate pe nevoia lor de a învăța și de a se perfecționa.

SECȚIUNEA a-IV-a include o listă cu articole, cărți și capitolele de carte care m-au ajutat la elaborarea acestei teze.

THESIS SUMMARY

This habilitation thesis entitled **"PRECISION ONCOLOGY: INTEGRATING NANO-CARRIERS, BIOMARKERS, AND GROWTH FACTORS FOR ENHANCED THERAPEUTIC STRATEGIES"** underscores the need for a multidisciplinary approach to oncological conditions in order to identify innovative elements that can improve medical performance and enhance patient prognosis. The field of oncology constantly faces the challenge of innovation, witnessing numerous advances in therapeutic approaches over time, and this work highlights the integration of novel elements into oncological treatment algorithms, aimed at providing better clinical outcomes. Nanocarriers, serum biomarkers, and the use of growth factors represent a set of new tools in personalized medicine, offering the opportunity for targeted treatment and predictable oncological results.

SECTION I of the habilitation thesis provides a summary of my scientific, academic, and clinical activities throughout my career, reflected in 1064 citations and a Hirsch index of 10.

SECTION II of this thesis comprises 3 chapters that reflect my scientific activity and recent research interests. The first chapter emphasizes the importance of using nanocarriers for immunomodulation and targeted therapy for various types of malignant tumors, including a theoretical model for diclofenac release from a hydrogel-based device. The second chapter synthesizes the results of two clinical trials aimed at identifying prognostic factors for colorectal and lung cancer. The third chapter describes the results obtained from three clinical trials measuring the efficacy of using growth factors in combination with chemotherapy to reduce specific adverse effects in breast and lung cancer patients.

SECTION III outlines the main directions for professional, academic, and scientific research development that I plan to pursue. I aim to foster interinstitutional clinical and scientific collaboration that brings multiple benefits, both for the research community and for patients. Additionally, I intend to actively involve both students and residents in research activities and various teaching endeavors to meet their learning and improvement needs.

SECTION IV includes a list of articles, books, and book chapters that helped me develop this thesis.

SECTION I

Synopsis of clinical, academic, and scientific achievements

A. Clinical achievements

After receiving my medical degree from the Grigore T. Popa University of Medicine and Pharmacy in Iasi in 1985, I went on to finish a residency program in oncology at the "Prof. Dr. Alexandru Trestioreanu" Oncology Institute in Bucharest, Romania, working under the direction of Professor Ion Bălănescu. My understanding of oncology and radiotherapy was able to mature during this period of time, which was quite beneficial. The wide diversity of oncologic disease that I was exposed to during my formation not only provided me with a solid clinical background, but it also assisted me in constructing the clinical approaches of these patients in a resilient manner. In addition, I improved my theoretical reasoning through countless sessions of brainstorming with my supervisors and colleagues.

When I worked as a family physician in Romanești village, which is located in the county of Iasi, from 1989 until 1991, I had the opportunity to treat patients of all ages, from infants and toddlers to adults and senior citizens. During this time, I worked to increase awareness of the importance of sanitary education and prevention in the rural area. Additionally, I made it a point to visit each and every home that fell under my area of supervision in order to assess the living conditions as well as the general health of the families there. Because we were the first people to respond in the event of an emergency, we were in need of at least the most fundamental medical kits in order to properly care for our patients. As a result, I worked together with local institutions to improve the circumstances of the cabinet where patients were evaluated.

After earning a degree as a Specialist in the field of Oncology in 1994, I began working at an oncology office at Saint Spiridon's Clinical Emergency Hospital. I was there for four years. Since then, I've kept working in this environment and in 1998 I earned a degree as a primary physician. In the year 1994, I was given the position of coordinator of the oncologic practice in the county of Iasi, and I remained in this role until the year 2001, when I made the decision to continue my work in a private setting.

The years spent in the public health care system thought me the need to develop a specialized medical platform that would enable patients access to prompt and personalized

care. Thus, I decided to construct a center of oncologic and radiotherapeutic care- Victoria Hospital, Iasi, Romania.

I obtained a master degree in Management and Public Health, and I completed a course of hospital management at the National School of Public Health and Management Bucharest that allowed me to manage and optimize the clinical activity in this center.

The development of such a project was a significant personal and professional challenge for me, and I was able to create an original concept for this unfilled niche in the regional market, which had various advantages for oncologic patients.

Throughout these years, I have had an interest in gaining experience in a variety of oncology subspecialties, and I have participated in a number of internships, both in this country and abroad. These experiences have provided me with a variety of possibilities to broaden my learning and to cultivate a variety of professional contacts with my peers. During the course of my education to become an oncology expert, I have gained experience in the oncology fields through the following internships:

1. European School of Oncology, Vienna, 1999- clinical trial course;
2. Royal Marsden Hospital, London, 1999- Glioma Perceptorship program
3. Perspectives in colorectal cancer, 2001, Dublin- oncology course;
4. National Cancer institute, 2006, Bethesda- Immunology of hyperthermia program;
5. University of Medicine from Hong Kong, 2007- Good Clinical Practice course;
6. University of Medicine from Kiel, 2008- training in melanoma treatment;
7. Grosslingen Hospital, Munich, 2008- hyperthermia in cancer treatment;
8. Instituti del Tumori, Milano, 2009- training in hepatocarcinoma treatment;
10. Institute Gustave Roussi, Paris, 2011- training in breast cancer treatment;
11. Leuven Oncology Institute, 2012- training in colorectal cancer treatment;

B. Academic achievements

I commenced my teaching endeavors in 2019, when I obtained a lecturer position at the Oncology discipline from the University of Medicine and Pharmacy “Grigore T. Popa”, Iasi, which I presently occupy with honor.

Throughout the course of my academic career, I have made contributions to the creation of curricular materials, hands-on workshops, real-world case studies, and academic seminars for oncology students. I was in charge of coordinating the *Oncology course* for the fourth-year students, and I also coordinated the *Oncological Emergencies* optional course for students in their fourth year of medical school.

I have committed a large amount of time and energy into the facilitation of medical education at the University of Medicine and Pharmacy "Grigore T. Popa" for all three categories of learners, which include undergraduate students, residents, and postgraduate physicians. I was able to make a contribution to the creation of instructional resources as well as evaluations of knowledge. Throughout the course of their academic writing endeavours, I served as a mentor to a group of 15 undergraduate students (7 general medicine students and 8 nursing students). In addition, I was responsible for facilitating the participation of locals in the development of scholarly publications and syntheses on a variety of topics.

During my career, I helped writing the following books/ book chapters:

1. **Volovat C**, Volovat SR. „Evaluarea pacientului onco-geriatric: particularitati terapeutice". In: Ioana Dana Alexa „Actualitati in geriatrie". Editura „Gr. T.Popa" UMF Iasi 2011; pg 237-245 (ISBN 978-606-544-077-7)
2. **C VOLOVAT**, S VOLOVAT. „Obezitatea si cancerul mamar". În: Carmen Vulpoi, Voichiţa Mogoş, Crisina Preda „Actualităţi in Endocrinologia Oncologică. Sillabus". Editura „Gr. T. Popa", UMF Iaşi 2014; pg: 163-170 (ISBN 978-606-544-233-4)
3. Cătălin Pricop, Dan Mischianu, Orsolya Martha. Cancerul de prostată local avansat şi metastazant Editura PIM, 2015: 322-341. (ISBN 978-606-13-2779-9)
4. **Volovat, C.,** Volovat, SR. Update in oncology. Editura „Gr. T. Popa", UMF Iaşi 2019 (2 vol) (ISBN 978-606-544-615-1/ 978-606-544-672-4)
5. **Volovat, C**., Volovat, SR., Agop, M. (2022). Nanotechnology and Immunomodulators in Cancer. In:Kesharwani, R.K., Keservani, R.K., Sharma, A.K. (eds) Immunomodulators and Human Health. Springer, Singapore. https://doi.org/10.1007/978-981-16-6379-6_5 (ISBN 978-981-16-6378-9)

It is essential to point out that I have continuously demonstrated a desire to pay attention to and incorporate comments and recommendations from my students, and that this is something that I have done consistently. In addition, I have taken an active part in a number of activities that have been organized by student associations here at our university. These events have included seminars and conferences that have been sponsored by student organizations such as SSCR (Societatea Studențească de Chirurgie din România) and SSMI (Societatea Studenților Medicinişti Iași). As a result of my participation in the aforementioned events, I have consistently been able to evoke genuine inspiration for young

students, which has served as a source of encouragement for me. The diagnosis and treatment of a variety of oncologic illnesses, as well as advances in oncologic therapy, have been among the extracurricular themes that have been discussed.

One of my primary goals at Victoria Hospital was to put together a group of people that work well together and maintain a professional demeanour. At the moment, this establishment is home to a workforce that is comprised of oncology residents, in addition to primary care physicians and medical specialists. I acted as a role model and gave direction for each of them.

My teaching and mentoring activities were also expanded into the field of oncology research. As a result, a large number of residents and young specialists are currently working under my supervision at Victoria Hospital in a variety of clinical trials, and they are working in collaboration with investigators from important medical centres all over the world.

Due to my dedication to ongoing medical education, I have proposed two post-university courses for oncology specialists. These courses are titled: *Integration of systemic treatment in the multidisciplinary treatment of hepatocarcinoma* and *Treatment of cholangiocarcinoma and liver metastases - the point of view of the medical oncologist. Notions of oncological treatment of malignant liver tumors*.

C. Scientific achievements

Scientific research was the central point of my professional career that required complex thinking and innovative approached of diagnostic and therapeutic strategies. My research career developed under the supervision of Professor Carmen Vulpoi, who helped me in the process of fulfilling my doctoral research, that evaluated quality of life and adverse effects in breast cancer patients treated with aromatase inhibitors. Our results were reunited under a doctoral thesis that was publicly presented and evaluated in 2012.

I have contributed more than 40 research publications of various categories to international journals indexed in Web of Science Core Collections, and the results of my work were disseminated at numerous national and international congresses and conferences as stated in my *curriculum vitae*.

My researcher profile is characterized by the following metrics in Web of Science: Hirsch index of 10, 41 publications and 1,064 citations, with and ascending trend of citations in the last 5 years.

Following the completion of my PhD studies, I have participated in more than 90 national and international research programs and grants as a main investigator. Some of the most recent grants include:

1. MANTA – A randomized Phase II study of Fulvestrant in combination with either the dual mTOR inhibitor AZD2014 or Everolimus or Fulvestrant alone in Estrogen receptor – positive advanced or metastatic breast cancer - 009175QM 2016-2018.
2. PAKT - A Phase II, Double Blind, Randomised, Placebo-Controlled Study of the AKT Inhibitor AZD5363 in Combination With Paclitaxel in Triple-Negative Advanced or Metastatic Breast Cancer - 009246QM 2016-2018.
3. A randomized open-label, multicenter, Phase 3 study to evaluate the efficacy and safety of Avelumab (MSB0010718C) in combination with and/or following chemotherapy in patients with previously untreated epithelial ovarian cancer 2016-2018.
4. A Randomized Phase 3 Study of MRTX849 versus Docetaxel in Patients with Previously Treated Non-Small Cell Lung Cancer with KRAS G12C Mutation.
5. A Phase 3, Randomized, Double-Blind, Placebo-Controlled Study of the Efficacy and Safety of Namodenoson in the Treatment of Advanced Hepatocellular Carcinoma in Patients with Child-Pugh Class B7 Cirrhosis
6. A Phase 3 trial of Fianlimab (REGN3767, ANTI-LAG-3) Cemiplimab versus Pembrolizumab in patients with previously untreated unresectable locally advanced or metastatic melanoma.
7. A Randomized, Open-Label, Multicenter Phase 3 Trial of Domvanalimab, Zimberelimab, and Chemotherapy Versus Nivolumab and Chemotherapy in Participants with Previously-Untreated Locally Advanced Unresectable or Metastatic Gastric, Gastroesophageal Junction, and Esophageal Adenocarcinoma.
8. HORIZON - REVERT – taRgeted thErapy for adVanced colorEctal canceR ,Horizon 2020, SC1-BHC-02-2019: Systems approaches for the discovery of combinatorial therapies.

I have always been interested in actively joining professional organizations from Romania and abroad in the oncology field, as they are complementary to and helpful to my

scientific, clinical, and academic pursuits. I belong to numerous scientific organizations such as:

- Society of Physicians and Naturalists and Medical-Surgical Journal of Iasi (1990);
- Romanian Society Against Pain (1993);
- Balkan Union of Oncology (1998);
- American Society of Clinical Oncology (2001);
- European Society of Hyperthermia (2007);
- European Society of Medical Oncology (2008);
- Multinational Association of Supportive Care in Cancer (2011)

In addition, I am a founder member of the League to Fight Cancer Moldavia (first non-governmental association of cancer patients in Romania) since 2014 and of the Romanian Society of Radiotherapy and Medical Oncology since 1997.

SECTION II

Chapter 1: Nano-vectors for drug delivery in cancer treatment

I.1.1. State of art

According to Siegel et al., cardiovascular disease is the primary cause of mortality, with cancer ranking second in terms of prevalence (1). The decline in cancer mortality rate has been observed in recent years due to advancements in medical care and improvements in living standards (2).

Nevertheless, there has been a modest decrease in the incidence of diagnosed cancers since 2020. On the other hand, there has been a gradual rise in mortality rates, which can be attributed to delayed diagnosis and treatment, concurrent viral infections, and the sluggishness in data gathering caused by the COVID-19 pandemic (3).

In the year 2022, the United States witnessed the emergence of approximately 1.91 million individuals diagnosed with cancer, with a regrettable outcome of 600,000 fatalities. According to Siegel et al., prostate cancer exhibited the highest incidence rate among males, while breast cancer was the most frequently diagnosed cancer among females. Additionally, lung cancer emerged as the leading cause of mortality attributable to cancer, resulting in an estimated 350 fatalities per day (4).

In the field of clinical oncology, various novel cancer treatment strategies have been developed, including immunotherapy, RNAi therapy, and gene editing. However, despite these advancements, chemotherapy, which involves the use of cytotoxic drugs, remains the primary therapeutic modality (5). Despite its significant role in treatment, chemotherapy is often linked to multidrug resistance (MDR), toxicity, and various side effects, leading to reduced patient adherence (6).

Multidrug resistance (MDR) poses a significant obstacle in the field of cancer therapy, resulting in diminished levels of therapeutic drugs within cells and the occurrence of detrimental systemic toxicity. These factors contribute to the potential failure of chemotherapy interventions (7).

The development of multidrug resistance (MDR) in cancer is a complex process that arises from the interplay of various mechanisms. A comprehensive understanding of these mechanisms is crucial for the advancement of effective cancer treatment strategies (8).

The upregulation of membrane transporter proteins represents a significant mechanism of drug resistance, as it leads to enhanced efflux of substances from cellular compartments (9). Furthermore, the reduction of drug uptake and the elimination of receptors and transporter proteins on the surface of the tumor have been found to lead to inadequate drug uptake, thereby impacting drug concentrations (10).

In addition, the promotion of tumor multidrug resistance (MDR) is facilitated by various factors such as DNA repair mechanisms, anti-apoptotic and pro-apoptotic proteins, the intricate tumor microenvironment (TME), and autophagy. These factors have been extensively studied and documented by researchers (11). Fortunately, nanomedicine exhibits significant promise in addressing the diverse mechanisms of multidrug resistance (MDR) that impose limitations on conventional chemotherapeutic agents.

Nano drug delivery systems (NDDS) offer a potentially effective method for precise and controlled drug administration, making them a promising avenue in the field of cancer therapy (12). Nanoparticles can be synthesized through the utilization of both organic and inorganic substances, including lipids, polymers, and gold (13).

Nanoparticles, with an average particle size of approximately 100 nm, can exploit the phenomenon known as the enhanced permeability and retention effect (EPR) to achieve passive tumor targeting and retention (14). Furthermore, the physicochemical characteristics of nanoparticles, including their size, structure, and surface charge, can be modified through the manipulation of material composition and proportion (15).

Nanoparticles possess various biological properties that confer several advantages, including targeted delivery to tumors, reduced systemic side effects, and prolonged circulation in the plasma. According to Scarano et al., nanoparticle drug delivery systems possess the capability to transport larger quantities of drugs and hinder detection by efflux pumps (16).

Due to the intricate nature of the tumor microenvironment, the administration of a single chemotherapeutic drug or sequence-specific nucleic acids may not yield satisfactory treatment outcomes. Consequently, there is a growing interest in the simultaneous delivery of multiple therapeutic agents, as highlighted by Jang et al. (17).

In addition, the utilization of combination delivery methods has been found to yield synergistic outcomes in terms of enhancing the effectiveness of tumor inhibition by targeting multiple distinct pathways. This approach also holds the potential to minimize adverse effects and optimize the therapeutic efficacy of drugs (18).

It has been demonstrated by Taratula et al. (19) and Yin et al. (20) that a combination therapy approach can effectively treat various forms of cancer . The utilization of nanoparticles as carriers for multiple cytotoxic drugs is a frequently employed approach to enhance the responsiveness of tumors to therapeutic agents.

Hence, the co-administration of cytotoxic agents and nucleic acids represents a potential therapeutic approach for combating tumors, as it has the potential to decrease drug dosage and overcome drug resistance.

In contemporary research, there has been a growing trend in the simultaneous delivery of genes and gene agents, which has demonstrated a synergistic ability to regulate gene expression within tumor cells (21). Various alternative materials, including lipids, polymers, and inorganic nano-systems, have been employed in the fabrication of co-delivery nanoparticles.

Nanovectors represent an important step in the personalized medical plan, allowing a targeted treatment of the tumors, an extention of the circulation time for several drugs, and a reduction of their clearance from the body.

The use of nanovectors for drug delivery in cancer treatment has shown promise in preclinical studies and some clinical trials. However, challenges remain, including scalability of manufacturing, safety concerns, immune responses, and regulatory considerations. As research continues, nanovectors have the potential to revolutionize cancer treatment by improving drug delivery efficiency and reducing systemic toxicity.

Personal contributions:

1. Volovat SR, Ursulescu CL, Moisii LG, **Volovat C**, Boboc D, Scripcariu D, Amurariti F, Stefanescu C, Stolniceanu CR, Agop M, Lungulescu C, Volovat CC. The Landscape of Nanovectors for Modulation in Cancer Immunotherapy. Pharmaceutics. 2022 Feb 11;14(2):397. doi: 10.3390/pharmaceutics14020397. PMID: 35214129; PMCID: PMC8875018.
2. Volovat SR, Negru S, Stolniceanu CR, **Volovat C**, Lungulescu C, Scripcariu D, Cobzeanu BM, Stefanescu C, Grigorescu C, Augustin I, Lupascu Ursulescu C, Volovat CC. Nanomedicine to modulate immunotherapy in cutaneous melanoma (Review). Exp Ther Med. 2021 May;21(5):535. doi: 10.3892/etm.2021.9967. Epub 2021 Mar 23. PMID: 33815608; PMCID: PMC8014970.

3. Ailincai D, Agop M, Marinas IC, Zala A, Irimiciuc SA, Dobreci L, Petrescu TC, **Volovat C**. Theoretical model for the diclofenac release from PEGylated chitosan hydrogels. Drug Deliv. 2021 Dec;28(1):261-271. doi: 10.1080/10717544.2021.1876181. PMID: 33501878; PMCID: PMC7850333

I.1.2. The Landscape of Nanovectors for Modulation in Cancer Immunotherapy

I.1.2.1 Introduction

Cancer immunoediting involves elimination, equilibrium, and escape. Modern cancer immunosurveillance involves molecules and cells with innate and adaptative immunity working together to detect and eliminate developing tumours. Sometimes tumour cell variants enter an equilibrium phase where the immune system controls tumour cell growth.

The immune system's elimination phase involves cytokines (IFN-α/β, IFN-γ, IL-12, and TNF), dendritic cells, macrophages, NK/NKT cells, CD4+ and CD8+ T cells, and immune effector molecules (perforin and TRAIL). The immune system's tumour detection mechanisms are unknown.

A developing tumour produces "danger signals"—cytokines like type I IFNs that activate dendritic cells, natural killer cells, and macrophages. The second phase of cancer immunoediting, equilibrium, is when the innate immune system cannot kill cancer cells but keeps them in immune-mediated tumour dormancy. The host immune system does not completely eliminate the heterogeneous tumour, but tumour cells and immune system are in a dynamic balance.

Certain tumour cells escape immune detection and destruction (22). Tumour escape from immune control is a dramatic immunoediting result. The escape phase is when the immune system fails to eliminate or control cancer cells, allowing cell variants to grow unrestricted. The immune-desert, immune-excluded, and inflamed TME immune phenotypes include adaptive and innate immune cells that affect immunotherapy. Immunological tolerance, ignorance, and T cell priming are all absent in the immune-desert phenotype (lack of antitumor immune cells) (23).

These tumours, including pancreatic and prostate cancers, have poor immune checkpoint inhibitor (ICI) responses and worse outcomes than other phenotypes due to a lack of pre-existing cytotoxic T cells and a poor T cell receptor clonal repertoire. In the immune-excluded phenotype, extravascular stroma and immature vessels block tumour

periphery or stroma immune cells. Additionally, TGF-β expression and CAF density increase (24, 25).

This phenotype is more sensitive to immune checkpoint inhibitors (ICI) than immune-desert tumours because the stroma contains CD8+ T-effector cells that can proliferate and become active. T cells from the parenchyma express proinflammatory cytokines in the third phenotype, indicating a failure of the antitumor immune response (26). Despite the abundance of T cells with tumor-associated antigen receptors, hypoxia-suppressed immune cells are also present. Melanoma and non-small-cell lung cancer have this phenotype. This phenotype has the most ICI sensitivity potential (27).

Superimposed on the three main phenotypes of TME described above, tumours were classified into “hot” and “cold” tumours, referring to T cell infiltration, and recently into four categories: hot, altered–excluded, altered–immunosuppressed, and cold (28).

The type, location, and density of immune cells in a tumour site can provide more accurate patient stratification than the classical TNM system for any cancer (29, 30).

The Immunoscore, a robust, consensus-based, standardised scoring system, was developed from the classification of tumours into “hot” and “cold” (31-33). Cancer immunotherapy is a new alternative to classical therapies that develops agents to help the immune system recognise and destroy tumour cells (34-37).

Synthetic immunotherapy, such as monoclonal antibodies (MoAbs) and chimeric antigen receptors (CARs), and molecules that enhance natural immune responses, such as immune checkpoint inhibitors (ICIs), are two types of classical cancer immunotherapy (38).

The best-known immune checkpoint inhibitors suppress T cell responses to cancers and target tumours to enable antitumor immunity by targeting PD-1 and CTLA-4. Seven checkpoint inhibitors, four cytokines, two adjuvants, and a small molecule with immunomodulatory properties have been approved by FDA, EMA, and NICE to treat more than a dozen major cancer types.

I.1.2.2. Mechanisms of Resistance to Immune-Checkpoint Blockades in Cancer

Tumour heterogeneity and the complex immune microenvironment affect treatment efficacy and are linked to individual immune system variations (39). Immunotherapeutic resistance is intrinsic or acquired. Primary resistance is cancer's non-response to immunotherapy (36, 40).

Hyperprogressive diseases (HPDs) that alter chromosome 11 region 13, (MDM)2/4 gene amplification, and EGFR gene mutation cause intrinsic resistance (41). TME

alterations (macrophage polarisation) and low tumoral mutational burden (TMB) also affect resistance (42-44).

Extrinsic immunotherapy resistance is linked to TME tumor-infiltrating lymphocytes (TILs) (45-47). It was reported that TME immunosuppression is always associated with Treg, MDSC, and TAM infiltration (48).

The immunosuppressive tumour stroma of "cold tumours" has low mutational burden and neoantigen presence (49). Tumor-associated TLSs have a good prognosis in most cancer types, suggesting they can induce a systemic and long-lasting antitumor response (50).

I.1.2.3. Bioactive Nanoparticles Designed to Modulate Cancer Immunotherapy

Cancer tumour targeting is a major scientific issue that improves treatment efficacy and reduces off-target effects. In recent years, vectorization methods have expanded with the discovery of new families of nanovectors (1–1000 nm) created by chemical engineering (e.g., nanoparticles) or biological (e.g., viruses, bacteria, and extracellular vesicles) (51).

Nanoparticles must be 1–100 nm in size, have high surface-area-to-volume ratios, and have good delivery kinetics. Nanoparticles, larger than 200 nm, are more likely to be fenestrated in the spleen and have variable intratumoral distribution depending on regional blood flow.

Small nanoparticles (<10 nm) are often cleared by the kidneys. Nanoparticles must also have non-antigenic coatings and passive targeting into highly angiogenic tumours to avoid immunogenicity.

The physiochemical properties of nanoparticles, such as size, shape, coating with tumour cell-targeting antibodies, aptamers, peptides, and/or small molecules that interact with malignant cells, tumour type, size, and stage, and mononuclear phagocytic system influence the targeting of NPs in tumours. Nanoparticles are mostly stored in the liver and spleen.

The scavenger receptors of Kupffer cells engulf NPs in liver capillaries. Large inorganic NPs stay in Kupffer cells for a long time, but organic particles degrade quickly (52). Red pulp macrophages in the spleen degrade erythrocytes, while white pulp metallophilic macrophages clear apoptotic cells (53).

Phagocytosis, micropinocytosis, endocytosis, and other mechanisms help macrophages capture nanoparticles. Scavenger receptors absorb bacteria, nanoparticles, and low-density lipoproteins (54).

Nanoparticle delivery to tumours depends on active and passive targeting. Specific targeting involves functionalizing the nanoparticle surface with ligands to target tumoral blood vessels, the extracellular matrix, or intracellular targets.

Nonspecific targeting uses nanoparticle coatings with anti-fouling and stabilising agents. Nanoparticles cross the tumour vascular barrier through intercellular gaps and become trapped in the tumour due to poor lymphatic drainage (called “enhanced permeability and retention” (EPR)) and active targeting (55).

Some mechanisms for tumour nanoparticle extravasation have been described. Transcellular extravasation hypothesis: nanoparticles can enter tumours via transendothelial cells. The EPR effect has been touted for studying nanoparticle transport through intercellular gaps.

Nanoparticles must overcome biological barriers in the tumour microenvironment after crossing the vascular barrier. Nanoparticles interact with tumour stroma components after extravasation from the tumour vasculature.

The high flow of interstitial fluid to the stroma and lymphatic vessels due to increased pressure is strongly correlated with lymphangiogenesis, invasiveness, and metastasis (56).

Protein coronas, microbiome modulation, and the EPR effect play major roles in nanopharmaceutical efficacy. Protein coronas (PCs) occur when proteins are improperly absorbed onto NP surfaces, changing their biological identities.

These identities cause nanoparticle-based immunotherapy to fail, and PC formation causes two types of responses: a nonresponse (immune blinding) caused by the PC's partial or total coverage of the antigens, and an uncontrolled response (immune reactivity) caused by the immune system's hyperresponse to the NP (57).

By changing NP physicochemical properties, immune-blinding can be avoided (58). Uncontrolled immune reactivity is caused by excessive immune activity, which is often linked to proinflammatory cytokines or complement (C3) activation (59). Using biocompatible zwitterionic polymers or hydrophilic nanoparticles can reduce protein adsorption and prevent complement activation (60).

Recently developed cell-membrane coatings permit NP camouflage to avoid immune clearance and activate complement. A cell membrane coating made of RBC membranes or PEG prevents macrophages from absorbing particles, prolonging their circulation and increasing their tumour accumulation (61).

Gut microbiota may modulate immune cell functions, especially Tregs and CD4+ and CD8+ T cells, explaining the heterogeneity of immune response to immune treatment.

Bacteria like *Bifidobacterium longum*, *Bifidobacterium adolescentis*, *Lactobacillus species*, and *Parabacteroides merdae* have been linked to responding to anti-PD-1 treatment by increasing IFN-γ secretion, DC function, and CD8+ tumor-infiltrating T cells.

The enhanced permeability and retention (EPR) effect was first studied on inflammation, and correlates host anatomical and pathophysiological features with solid tumour characteristics (62).

Since tumour cells need blood, they must generate new blood vessels via VEGF or other growth factors to grow rapidly. The newly formed tumour vessels have abnormal fluid transport dynamics, especially for macromolecular drugs. The tumour stroma contains cells that boost EPR-mediated tumour accumulation. Macrophages affect nanomedicine retention, and tumor-associated macrophages (TAMs) can store nanoparticles and release them to nearby tumour cells (63).

I.1.2.4. Types of Nanovectors for Improving Cancer Immunotherapy

FDA-approved biocompatible and biodegradable poly(lactic-co-glycolic acid) can encapsulate many biologically active compounds with low toxicity. PLGA microspheres target MHC class I and class II pathways to mature DCs.

Nonspecifically PLGA nanoparticles are taken up. PLGA nanoparticles transport cytokine agonists, siRNAs, or CpG-coated tumour antigens to increase DC antigen uptake and CTL (CD8+) and Th (CD4+) immune responses (64).

Colzani et al. developed an antibody delivery system that affects cancer cell regulatory signalling pathways and stimulates ADCC using trastuzumab and doxorubicin in poly(lactic-co-glycolic) acid nanoparticles (65). In vitro, PLGA nanoparticles released hD1 10- to 100-fold more efficiently than microparticles, making them better for DC targeting (66).

The highest density of monoclonal antibodies on NPs increases IL-10 production and antitumor response. Thus, PLGA NPs with antigenic peptides can target DCs for vaccine delivery and trigger the cytotoxic T cell immune response, which blocks tumour cell immune escape (66).

Tumour cells alter their genes and epigenetics to avoid immune cell detection and elimination. A study using gold nanoshells and anti-PD-1 peptide (APP)-loaded PLGA nanoparticles intratumorally showed an antitumoral effect at the primary tumour site when combined with photothermal therapy (67).

Widely branched macromolecules with a core and cavities to trap drugs are dendrimers. Drug delivery is possible with dendrimers' well-defined chemical structures, water solubility, and polyvalencies (68). Dendrimers directly interact with immune cells. Poly(phosphorhydrazone)dendrimers selectively increased anticancer natural killer cell proliferation (64).

Solid-lipid nanoparticles, nanoemulsions, lipid nanocapsules, and liposomes are biocompatible lipid nanocarriers with one or more phospholipid bilayers. The cell membrane and liposomes share hydrophobic tails of phospholipids and hydrophilic heads. The hydrophobic and hydrophilic compartments allow compounds to be encapsulated and delivered without affecting their properties, making them an ideal drug-delivery system (69).

Liposomes delivered ovalbumin (OVA) and IFN-encoding pDNA to DCs is an effective treatment. The antitumor effect of OVA and IFN-encoding pDNA is enhanced by CTL activation (70).

Micelles, vesicular particles formed by amphiphilic molecules spontaneously aggregating, are used as cancer carriers. Micelles are biodegradable, nontoxic, and intracytoplasmically delivered, making them easier to synthesise than other nanocarriers. They carry ovalbumin (OVA) or regulate metabolism-related enzymes like IR780, which inhibits IDO (indoleamine 2,3-dioxygenase), activates T lymphocytes, and inhibits distal tumour growth (71).

GNPs and AuNPs can deliver antigenic proteins and gene oligonucleotides to specific sites. AuNP surfaces interact covalently and noncovalently with DNA, peptides, and antibodies (72). Cancer cells' nuclei, subcompartments, and mitochondria were affected by AuNPs.

Light is converted into heat in photothermal therapy, distorting DNA or cells irreversibly. Nanogold particles increase light absorption at a certain wavelength, reducing laser power for photothermal cancer cell removal. When illuminated by GNP-wavelength light, GNP-conjugated antibodies can target cancer cells as monoclonal antibodies (73).

A promising combination of AuNPs and photothermal ablation is being studied in many trials. Gold NPs deliver CgP oligonucleotides to macrophages and DCs, reducing tumour growth. Gold nanoparticles of various sizes and shapes were used to deliver immunotherapeutic adjuvants like OVA or CpG, and 15 nm was found to be the most effective.

Iron oxide nanoparticles deliver vaccines well. They directly polarise immune cells like DCs and macrophages, increasing immune response, or they can be used as a delivery

system with OVA as an immune potentiator (74). The FDA approves ferumoxytol supplementation for mammary cancer due to its intrinsic therapeutic effect (75).

Solid mesoporous silica NPs (MSNs) have a honeycomb-like structure with hundreds of empty mesopores that can absorb large amounts of bioactive molecules (76). Mesoporous silica materials interact with biosystems in many ways, including biodegradation, biodistribution, toxicity, cellular uptake, and, most importantly, immune cell interaction.

A vaccine consisting of mesoporous silica (XLMSNs + OVA + CpG-ODN) successfully induced dendritic cell maturation, CD86 expression, and increased IL-12 and TNF-α secretion. MSNs can transport drugs and siRNAs into the body and induce cytokine secretion (77).

Multiwalled carbon nanotubes (MWNTs) were used to co-deliver OVA and CpG to APCs (78). Single-walled carbon nanotubes also photothermally ablate primary tumours. Photothermal ablation with carbon nanotubes and anti-CTLA-4 antibody therapy prevented metastasis.

2D nanomaterials—graphene (GO), reduced graphene oxide (rGO), graphene quantum dots, and graphene nanoribbons), black phosphorus (BP), layered double hydroxides (LDHs), transition-metal dichalcogenides (TMDs), TMOs, and MXenes are the most popular (79).

Biointeractions between the immune system and nanomaterials, including 2D nanomaterials, affect biological safety, so all affected factors must be identified. Graphene nanoparticles disrupt mitochondrial membrane potential and increase intracellular ROS, activating mitochondrial apoptosis (80). Graphene interactions with cellular genetic material induce DNA intercalation and cleavage.

rGO was approved for chemotherapy and immunotherapy with photothermal therapy. Wang et al. developed a PEGylated rGO-iron oxide platform (81). Yang et al. designed a platform that combined immunotherapy with PTT based on folic acid and a multifunctional IDO inhibitor loaded with reduced graphene oxide (rGO)-based nanosheets (IDOi/rGO nanosheets) to directly kill tumour cells under laser irradiation and induce synergistic antitumor immunity (82).

Inhibition of IDO and PD-L1 blockade led to increased tumour infiltration by lymphocytes, including T and NK cells, while suppressing Tregs and IFN-γ production in CT26 colon cancer cells (83).

Many nanopharmaceuticals for potentiating immunotherapy have reached clinical trials, with promising results.

Bacterial minicells are nanosized (100–300 nm) and originate from bacteria via abnormal cell division (84). Anucleated, nondividing minicells have RNA, ribosomes, peptidoglycan, proteins, and plasmids but no chromosomal DNA.

Minicells can still translate mRNA, synthesise ATP, and transcribe and translate plasmid DNA, but they cannot grow or divide (85). Minicells were engineered to deliver Salmonella (S.) Typhimurium T3SS antigen.

The class I antigen presentation pathway (APC) of T3SS delivers antigens directly into the cytosol, stimulating CD8(+) T cells (86).

Extracellular vesicles (EVs) are a diverse group of small membrane-bound vesicles that mediate many pathophysiological processes and offer many drug and gene delivery and therapeutic benefits (87).

DCs, epithelial cells, neural cells, MSCs, and tumour cells (tumor-derived exosomes) secrete EVs. EVs are used in tumour immunotherapy due to their lower toxicity and more frequent and durable responses.

Tumor-derived exosomes (TEXs) transport synthetic drugs, silencing RNAs, and microRNAs. CD47v inhibits macrophages from consuming tumour cells by binding to SIRPα, acting as a "do not eat me" signal (88). Exosomes with SIRPα variants can enhance tumour phagocytosis and antitumor T cell response by opposing the interaction between CD47 and SIRP.

A phase I trial found that GM-CSF and ascites exosomes enhanced tumor-specific cytotoxic T cells (89). Another phase I trial showed that autologous exosomes from dendritic cells carrying tumour MAGE peptides improved antitumor immunity and disease responses in advanced non-small-cell lung cancer (NSCLC) patients.

In a phase II clinical trial, exosomes loaded with IFN and MHC class I and II proteins improved the NK cell-mediated antitumor immune response in advanced NSCLC patients, prolonging overall survival and progression-free survival in 50% (90). Chimeric antigen (CAR)-T cell-derived exosomes improved clinical responses and immune-related adverse events.

VLPs mimic animal, plant, and bacterial viruses but cannot replicate in human cells. VLPs were developed as empty capsids that can transport other molecules, but their viral nature makes them ideal for nucleic acid transport (91).

VLPs from human pathogens efficiently transfer genes to cancer cells. Immunogenic VLPs can boost immune responses and be engineered as immune cell vaccines. Lizotte et al. used a cowpea mosaic virus-based VLP vaccine as a delivery vehicle and

immunotherapeutic agent. VLPs target TME and tumour cells and can nanocarry tumour antigens and drugs (92).

Oncolytic viruses (OVs) target tumour cell replication to induce immunogenic cell death and host antitumor immunity, regressing tumours. OVs directly oncolyze tumour cells and promote immunogenic cell death, causing CD4+ and CD8+ T cells to react to tumours (93).

OVs can deliver immune-stimulatory transgenes (chemokines, cytokines, ICIs, co-stimulatory ligands, and tumor-associated antigens) to the tumour niche to activate immune cells and transform the immunosuppressive TME (94).

Preclinical studies have shown that engineered OVs can deliver genes that induce immune responses, cytotoxic killing of tumour cells, suppression of tumour neoangiogenesis, radiosensitization, and other strategies (95).

In recent years, many clinical trials using viruses to treat cancer have been published. *Rigvir*, a picornavirus, and *Talimogene laherparepvec*, a herpes simplex virus type 1, are approved for malignant melanoma treatment, and a modified adenovirus H101 combined with cytotoxic chemotherapy is approved for nasopharyngeal carcinoma (96, 97).

Phage display is used in cancer immunotherapy in three ways: 1) peptides that mimic cancer antigens (mimotopes), 2) antigen-carrying phage particles as vaccines, and 3) small-molecule effectors of immune cell functions (98).

Phages can stimulate lymphocytes and APCs or inhibit suppressor cells (Tregs and TAMs) with their peptides. Phages' immunogenicity and low toxicity make them good carriers (99).

This technology faces challenges with peptide stability and delivery, phage immunogenicity, and human immunogenetic diversity (100). TAA mimotopes (CD20, HER2, and EGFR) have been developed to stimulate the production of anti-TAA Abs. These can be given as full-length TAAs, partial proteins with only the antigenic parts, or TAA mimotopes.

In this cancer vaccination, a TAA or mimotope is presented to the immune system to stimulate an immune response. Using mimotopes, this response can target a peptide or one genetically or chemically anchored to the phage surface. Using a phage particle to aggregate a peptide result in a better response and lower immunogenicity than ovalbumin (OVA).

I.1.2.5. Potential Targets for Nanomedicine-Based Cancer Immunotherapy

Nanovectors in cancer aim to improve drug delivery to tumours and metastases and modulate the immune system, which has three main targets: cancer cells, the tumour immune microenvironment (TIME), and the peripheral immune system.

Nanovectors can boost immunogenic cell death. In situ tumour vaccines, nanoparticles designed for ICD, can improve immunotherapy by combining with ICD-inducing modalities. TAAs and danger-associated molecular patterns result from ICD. ICD involves calreticulin (CRT) translocation to the cell surface and ATP and HMGB1 release into the extracellular environment.

These changes alert the immune system, which activates APC and cytotoxic T cells to kill tumours and metastases. Combining Caelyx/Doxil with doxorubicin-loaded liposomes improves immunotherapy (101).

Doxil may promote DC and CD8+ T cell proliferation through ICD. Doxil has higher immunopotentiation than doxorubicine at the same dose. Oxaliplatin-loaded PLGA nanoparticles induce ICD and activate the immune system better than free oxaliplatin (102).

Combined photodynamic therapy–radiotherapy used immunotherapeutic agents for tumor-targeted delivery. When combined with anti-PD-L1, pyrolipid-loaded inorganic nanoparticles increase photodynamic therapy immunoactivation and ICD induction.

Inducing ICD increases proinflammatory cytokines like TNF-α, IL-6, and IFN-γ, improves CD4+ and CD8+ cell infiltration, eliminates primary tumour, and prevents lung metastasis through an abscopal effect.

The European Medicines Agency approved intratumoral injections of NBTXR3 hafnium oxide nanoparticles to enhance radiotherapy's abscopal effect in locally advanced soft-tissue sarcomas (103).

In Tumour Immune Microenvironment (TIME) immunosuppressive mediators and pathways are upregulated due to increased infiltration of TAMs and MDSCs into tumours, as well as increased levels of inhibitors like IDO and TGF-β.

To modify the immune response, tumour acidity and hypoxia are the main targets. Hypoxia negatively regulates T cell activation, increasing CCL22 and CCL28 expression and MDSC and Treg accumulation (104).

Hypoxia leads to increased VEGF and TGF-β secretion, as well as PDL-1 expression on T cells, TIM-3, and CTLA4 on MDSCs, TAMs, and Tregs (105). In albumin-coated MnO2, pH/H2O2 dual-responsive nanoparticles were created. MnO2 reacted with H2O2 and H+ to produce oxygen after tumour penetration, enhancing chemotherapy and photodynamic therapy (106).

CAT@aPDL1-SSL, another immunoliposome, contains catalase (CAT)-encapsulated liposomes and a modified PDL-1 to improve immunotherapeutic effects, enhance T cells in tumour tissues, and block the PD-1/PD-L1 pathway.

To improve cancer immunotherapy, pH-responsive PCL–Hyd–PEG nanovesicles encapsulated immunological adjuvants (CpG ODNs) and endogenous tumour antigens as heat shock protein 70-chaperoned polypeptides (HCP). In the acidic tumour microenvironment, these nanovesicles fragment and release drugs.

It has been shown that DC-endocytosed antigens cross-present to CD8+ cytotoxic cells [242]. Positive results were reported in preclinical and clinical immunotherapy experiments with manipulated DCs using tumor-associated antigens and adjuvants targeting dendritic cells and tumor-specific T cells as therapeutic cancer vaccines (107).

RNA modulation is a nanomedicine DC targeting application. In vaccine clinical trials, low-immunogenicity lipid-based RNA nanoparticles delivered mRNA to DCs. RNA lipoplexes made of cationic lipids (DOTMA, DOTAP, and DOPE) and anionic mRNA deliver DC-targeted mRNA efficiently and precisely without molecular ligands like antibodies (108).

Combination therapy with magnetic nanoparticle-induced hyperthermia, radiotherapy, and a virus-like particle adjuvant was shown to treat dogs with oral melanoma.

NP-based immunotherapy targeting tumor-associated macrophages (TAMs). TAMs, M2-like immune cells in tumours, suppress effector T cell infiltration (109). Ferumoxytol converted M2-like TAMs into M1-like ones and inhibited liver and lung primary and metastatic tumour growth (110).

Secondary lymphoid organs present antigen and generate cytotoxic-T cells in the peripheral immune system, which is outside tumours. Engineering T cells and potentiating antigen presentation can restore peripheral immune system functions.

The subcutaneous or intradermal administration of antigen-containing nanoparticles improves APC processing (111). Local lymph node injections of CpG conjugated with nanoparticles or loaded with peptide antigens in nanodiscs promoted anticancer immunity (112). In addition, imidazoquinoline in nanogels or CpG bound with albumin was injected locally or systemically to reach the lymph nodes. These vaccines show adjuvant tolerability.

An antitumor vaccine was developed using PLGA nanoparticles to deliver antigens to DCs in target lymph nodes, leading to improved immunotherapy and an ex vivo abscopal effect in mice receiving αPD-1 immunotherapy (95).

I.1.2.6. A Possible Mathematical Model for Cellular Communication Mechanisms

Multicellular beings require all cells to communicate for development, adaptation, and functional evolution. In addition to cell-surface receptors, many soluble factors are involved in this communication. RNA interference (RNAi) silences genes with matching sequences in eukaryotic cells when they encounter double-stranded RNA (dsRNA).

The novelty is that in some animals and plants, transporting a silencing signal between cells can silence the same gene in cells that did not encounter the primary dsRNA.

Cell communication in the body and cell microenvironments is crucial to cancer development and growth (113). All cells secrete exosomes, which are involved in intracellular communication, immunological actions, cancer metastasis, and other organ-specific processes.

They are 50–100 nm wide and made of phospholipid double layers. They are important in all cell components, including DNA, miRNA, mRNA, and proteins. Exosomes were first described 50 years ago, but their role as cancer "biomarkers" has been extensively studied in the past decade (114).

To describe these dynamics using differential and non-differential procedures, especially in the expression of fundamental equations that control them, scale resolution for variable expression must be introduced.

Thus, any variable that depends on spatio-temporal coordinates will depend on space, time, and scale resolutions in the new mathematical sense of non-differentiability and non-integrability.

The dynamics of any complex cellular system require new geometric structures and mathematical models. These integrate invariant scaling laws with spatial and temporal transformation-invariant laws of motion.

The authors suggest a structure based on multifractality and a model based on the fractal theory of motion in an arbitrary and constant fractal dimension. Similar dynamics analysis is given in for complex biological systems.

The model assumes continuous and nondifferentiable curves (motion multifractality curves) will describe the dynamics of structural units in complex cellular systems. Their self-similarity at each point can be translated into holography (where each part reflects the whole). Multifractal “regimes” are used to discuss “holographic implementations of the structural unit dynamics of any cellular complex system”.

I.1.2.7. Discussion

Nanopharmaceuticals and bioinspired nanovectors (nanobioparticles) modulate cancer immunotherapy the most.

Two-dimensional (2D) nanomaterials have unique properties due to their structure and morphology. Two-dimensional drug-delivery systems have great potential and could lead to new biomedical applications.

Immune system biointeractions with nanomaterials, including 2D nanomaterials, affect the immune system, so biological safety factors must be identified.

The immune–nanomaterial interface's complexity and heterogeneity still hinder nanopharmaceutical development. Different immune responses result from nanomaterial (NM)-immune cell membrane interactions.

Entropic and nanothermodynamic potentials at immune–nanomaterial interfaces regulate macrophage receptors and stimulate cytokine secretion.

Although nanomaterial-related immunity databases are still developing, they can predict biological responses, the basic mechanisms of nanoimmune interactions, and safe and effective NM screening. Multivariate immune analysis, data integration, and machine learning can also reveal nanomaterial-induced immune responses.

Bioinspired vectors are another nanovector development route with great potential in the coming decades. Future strategies to improve oncolytic virotherapy have been described.

I.1.2.8. Conclusions

The major issues in nanotechnology-based immunotherapy are represented by the optimization of tumor targeting, the control of toxicity, and drug delivery versus clearance.

Additionally, complementing classic checkpoint inhibitors is the promising discovery of new checkpoint co-stimulators, such as OX40/OX40L, which promotes the survival and proliferation of CD4 and CD8 T cells; GITR/GITRL, which exerts a regulatory function on Tregs; and 4-1BB/4-1BBL, which has a co-stimulatory effect on different immune cells (T cells, NK cells, Tregs, and NK T cells).

Checkpoint inhibitors, such as LAG-3, TIGIT, VISTA, and TIM-3, or enhancers of cellular immunity (STING agonists, IDO/TDO, and TRL agonists) are also of interest.

The major direction for developing nanovector technologies to enhance immunotherapy appears to involve nanopharmaceuticals, bioinspired nanoparticles, and combinations of them, which have great potential to be demonstrated in the coming decades.

I.1.3. Nanomedicine to modulate immunotherapy in cutaneous melanoma

I.1.3.1. Introduction

The most aggressive form of skin cancer, cutaneous melanoma, is rising worldwide. Controlling immune system mechanisms with high responses and low side effects is the biggest challenge for immunotherapies' clinical implementation.

This modulation requires the right immunomodulator dose, timing, and localization (115). Cancer vaccines, immune checkpoint inhibitors, and nano-immunostrategies that reprogram the tumour microenvironment improve immunotherapy.

I.1.3.2. Immune system in cancer

Macrophages, NKs, and DCs form the first barrier against non-selfs in innate immunity. DCs and macrophages cause inflammation and innate and adaptive cell alerting. Tumor-infiltrating lymphocytes (TILs) from TME are important for tumour initiation and progression and have protumoral and antitumoral properties (116).

Typically, CD4+ T helper 1 (Th1), Th2 (Th2), CD8+ T, and NK T cells produce IFN-γ to inhibit tumour growth, activating macrophages for cancer cell phagocytosis. Macrophages synthesise IL-2, which promotes Th1 cell differentiation (117).

The antitumor immune response depends on Th1-Th2 balance. Th1 cells produce IL-2 and IFN-γ, promoting cellular immunity and tumour removal, while Th2 cells induce tumour necrosis and humoral immunity (118). To promote tumour cell lysis, IFN-γ stimulates antigen-presenting cells (APC) to activate cytotoxic CD8+ T cells that recognise peptide antigens from MHC class I molecules.

Most tumours are MHC class I positive and MHC class II negative. Th2 release IL-10, IL-13, IL-5, and IL-4, which enable Treg cells to inhibit CD4+ and CD8+ synthesis (119, 120). Immature myelomonocytic cells are myeloid-derived suppressive cells (MDSCs) that boost T cell immunosuppression. MDSCs produce arginase-1 (ARG-1) and indoleamine 2,3 dioxygenase (IDO), contributing to inefficient T-cell receptor complex expression on Ag-activated T cells and suppressing anti-tumoral immunity through IL-10, TGFβ, and nitric oxide expression (121, 122).

Other major players in cancer progression are macrophages, which are activated by various signals: i) Classical macrophage activation (M1), which produces

proinflammatory cytokines that cause reactive oxygen species to cytolyze cancer cells, and ii) Alternative activation (M2), which produces anti-inflammatory cytokines that promote tissue repair and angiogenesis, favouring tumour progression (123, 124).

I.1.3.3. Immunotherapy in melanoma

The therapy classification includes active and passive immunotherapy (125). Active immunotherapy boosts antigen-specific immunity. This category includes vaccines and checkpoint inhibitors. These are immune-active and work closely with the host immune system.

Passive immunotherapy stimulates the immune system with molecules like antibodies and cytokines. Monoclonal therapeutic antibodies and adoptive cell transfer therapy are passive immunotherapies (126).

Active or passive cancer immunotherapies are classified in three ways. Nanoparticles (NPs) are delivery systems for stimulating molecules or antigens. Nano-vaccines migrate into lymph nodes (LNs) to trigger T lymphocytes and generate a tumor-specific cytotoxic response (127). Specific nanoparticles can also target tumour microenvironment dendritic cells by presenting antigens to stimulate cytotoxic T cells.

The second method, adoptive cell transfer therapy, involves collecting, training, and reinfusing immune cells from the patient (128). Therapeutic delivery to the immune tumour microenvironment is the third promising melanoma treatment strategy.

Therapeutics can target cancer cells and immune system components in the tumour microenvironment, such as DCs, tumor-associated macrophages, cytokines (IFNs, TGF-β, IL-2), and enzymes involved in cancer metabolism. Last decades' biologic devices as viral therapies opened new ways to modulate the immune system against tumour cells (Figure I.1).

The main medical immunotherapies for melanoma are tumour vaccines, gene therapy, checkpoint inhibition immunotherapies, T-cell-directed therapies, and non-specific approaches like cytotoxic chemotherapy, photodynamic therapy, photothermal therapy, and radiotherapy, recommended only in carefully selected patients (20).

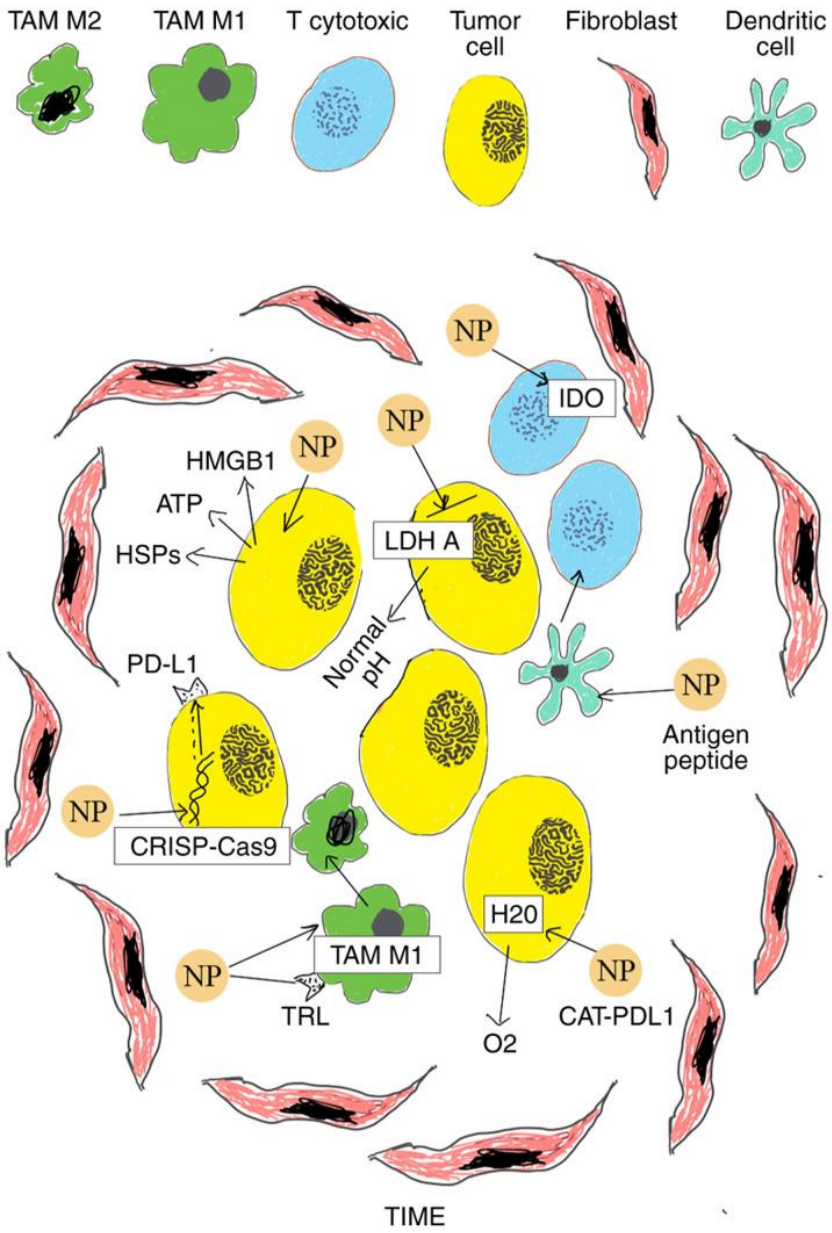

Figure I.1. Schematic of various nanomedicines applied in cancer immunotherapy of cutaneous melanoma. i) Multifunctional CAT-PDL1 liposomes includes CAT that decreases tumor hypoxia decomposing H2O2 into O2 and PDL1 which improves immunotherapeutic effects, promoting CD4+and CD8+ T cells; ii) PLGA NPs deliver antigenic peptides that target dendritic cells to promote cytotoxic T lymphocyte responses; iii) NPs inhibit IDO and block tryptophan metabolism of cancer cells; iv) NPs block LDH A in tumor cells leading to normal pH; v) NPs cause the translocation of calrecutin and lead to the release of ATP, HMGB1 and HSPs in extracellular environment, inducing ICD of cancer cells; vi) co-polymer NPs aPBAE knock down Cdk5 and cause PD-L1 downregulation via CRISPR-Cas9 genome editing; vii) aCD47@CaCO3 NPs increase the macrophage polarization to M1 phenotype and block the 'don't eat me' signal in cancer cells. NPs, nanoparticles; PLGA, poly-lactic-co-glycolic acid; TIME, Tumor Immune Microenvironment; IDO, indoleamine 2,3-dioxygenase; CAT, encapsulated catalase; ICD, Immunogenic cell death; ATP, adenosine triphosphate; HMGB1, high mobility group box 1 protein; HSPc, heat shock proteins.

I.1.3.4. Classification of nanotechnologies for cancer immunotherapy

Polymeric nanoparticles, lipid nanocarriers, metal nanoparticles, inorganic non-metallic nanoparticles, exosomes, and engineered viruses are used to improve cancer immunotherapy (78, 129, 130).

Many drug delivery systems use polymeric NPs like PLGA, dendrimers, and micelles. Polymeric nanoparticles have size, morphology, therapeutic drug loading, and surface functionalization advantages. Synthesis of proinflammatory molecules and inconstant degradation and inactivation of the therapeutic pay load during preparation are drawbacks.

FDA-approved PLGA is the most widely used biocompatible, biodegradable, and low-toxicity polymer. PLGA microspheres activate MHC class I and II pathways and mature DCs (131).

Dendrimers, branched macromolecules with a core and cavities to entrap drugs, are suitable for modified drug delivery due to their water solubility, polyvalency, and well-defined chemical structure, interacting directly with immune cells. Dendrimers have many functional groups on their surfaces (68).

Liposomes, solid-lipid NPs, and phospholipid micelles are lipid nanocarriers. Highly biocompatible liposomes contain synthetic or natural phospholipids and a cell membrane-like structure with hydrophobic tails and hydrophilic heads. Hydrophilic and hydrophobic compartments allow compound mechanisms to encapsulate and release without intracellular mechanisms (132).

Micelles, vesicular particles formed by spontaneous aggregation of amphiphilic molecules, carry imaging, radiotherapy, chemotherapy, and immunotherapy in cancer treatment. Micelles can transport Ovalbumin (OVA) and metabolism-related enzymes like IR780 for IDO metabolism (133).

Gold nanoparticles Metal AuNPs transport antigenic proteins and gene oligonucleotides to specific sites. Peptides, DNA, and antibodies on Au NPs interact covalently and non-covalently (133). Cancer cell survival, growth, proliferation, and death are linked to AuNPs' interactions with tumour cell subcellular organelles.

Iron oxide nanoparticles can deliver vaccines, polarise immune cells like DCs and macrophages, and boost immune response. They can also carry immune-boosting adjuvants like OVA (134).

Mesoporous silica NPs (MSNs) are honeycomb-like porous structures with hundreds of empty mesopores that absorb bioactive molecules (76). Larger mesoporous silica particles

and higher concentrations are more effective on monocyte-derived dendritic cells (MDDC) than small particles in low concentrations, suggesting its use in cancer vaccines (77).

Cylindrical multi-walled carbon nanotubes (MWNTs) can transport ovalbumin (OVA) and cytosine-phosphate-guanine oligodeoxynucleotide (CpG) to antigen presenting cells (APCs) as tumour antigen nanocarriers (78).

Exosomes (EXOs) transport lipids, proteins, and nucleic acids between cells and organs and play different roles in physiological and pathological immune system processes**.** Plasma membrane invagination generates endosomes, which migrate to the cell centre and form multivesicular bodies (MVBs) that carry DNA, mRNA, and non-coding RNA or protein. Lymphoid and myeloid lineages produce exosomes, but many other cells involving TME and cancer cells secrete tumor-derived exosomes with growth factors and microRNAs (89, 135). Chemical drugs delivered by exosomes avoid macrophage phagocytosis, inhibiting tumours. The use of exosomes to promote melanoma immunotherapy for strong and lasting responses is under investigation.

Virus-like particles Virus-like particles (VLPs) are artificial nanostructures 20–100 nm in size that cannot replicate. VLPs are immunogenic and target immune cells as engineered vaccines.

Engineered oncolytic viruses selectively infect and kill tumour cells. The goal during delivery is to generate systemic and local immune response against tumour cells with minimal collateral effects on normal cells. To accomplish this, oncolytic viruses are designed to target tumour cells. Lysis, release of antigens, damage-associated molecular patterns, and cytokines after viral replication promote the immunogenic reaction and model the antitumor immune system (136).

I.1.3.5. Factors that modulate the efficacy of nanoparticles

Gut microbiota regulates the immune system, suggesting that many microorganisms can affect immune cells, especially Tregs, CD4+, and CD8+ T cells. Human commensal *Bacteroides fragilis* boosts CD4+ naive T cell transformation into Treg and anti-inflammatory cytokine production (137). The colon's thymus-derived Tregs recognise *Clostridiales, Lactobacillus,* and *Bacteroides* antigenic materials and can maintain tolerance. Colonic Tregs can be reduced by antibiotics that reduce gut microbiota Clostridium family members (138). In a ‘love-hate’ relationship, commensals like *Escherichia coli* can boost pro-inflammatory gut immunity (139, 140).

Bacteria like *Bifidobacterium longum, Bifidobacterium adolescentis, Enterococcus faecium, Klebsiella pneumoniae, Collinsella aerofaciens, Parabacteroides merdae, Veillonella parvula, and Lactobacillus species* are linked to anti-PD-1 treatment response by increasing IFN-γ secretion, DCs, and CD8+ tumor-infiltrating T cells.

The unique EPR effect in solid tumours is strongly correlated with anatomical and physiological characteristics. The inadequate vessel architecture, large branches among endothelial cells in blood vessels, excess vascular mediators, and defective lymphatic drainage lead to plasma and nanomedicine extravasation (141).

Different tumours or areas of the same tumour had different EPR effects, especially large tumours. The EPR effect is also dynamic, involving pathophysiological factors, biological events, tumour growth, and inflammation (142, 143). Molecular targeting and tumour microenvironment modulation can improve the EPR effect (144).

Proteins are inappropriately absorbed on NP surfaces, forming protein corona (PC) and a different biological identity than normal NPs. PC has two biomolecular recognition roles. In "immune-blinding," the PC covers the surface of NPs to hide their antigen or biomolecule from their receptor. Second, some PC proteins can bind to immune cell receptors, causing unwanted immune responses.

Nanoparticle-based immunotherapy can fail due to PC formation, causing non-responses and uncontrolled responses. Covering the antigens or stimulating molecules on nanoparticles can promote the immune-blinding response (non-response), which retards specific stimulation and prevents the immune response. PC formed on NPs can also have an altered structure that binds to monocyte and macrophage scavenger receptors and induces phagocytosis. This prevents NPs' stimulating molecules from being recognised. In uncontrolled responses, NP aggregation causes toxic effects via immune system strange-body recognition (57, 145, 146).

I.1.3.6. Nanomedicine to enhance the immunotherapy in melanoma

Cancer vaccines are neoantigen, dendritic cell, nucleic acid, and whole tumour cell (147, 148). Presenting antigens to dendritic cells is a challenge in promoting T-cell responses to eradicate tumour cells after vaccination. A polyamidoamine dendrimer modified with guanidinobenzoic acid (DGBA) efficiently transported antigen and adjuvant proteins like ovalbumin (OVA) and unmethylated cytosine-guanine dinucleotides (CpG), which DCs cross-presented.

DGBA-OVA-CpG nano-vaccine promotes powerful antigen-specific cellular immunities and prevents B16-OVA melanoma. The percentage of tumor-infiltrating CD3+CD8+ and CD3+CD4+ T-cells increased with anti-PD-1 treatment and DGBA-OVA-CpG nano-vaccine. In contrast, DGBA-OVACpG or anti-PD-1 vaccination results in low CD8+ infiltration (147).

It is well known that tumours with higher tumour mutational burden (TMB), such as cutaneous melanoma, produce more neoantigen to activate the immune system to recognise tumours. Non-synonymous mutations in tumour cell genome antigens produce non-autologous neoantigens. Due to their strong and specific immunogenicity, higher affinity for MHC, and lack of expression in normal tissues, they can virtually eliminate off-target side effects while boosting the immune response to cancer cells (148).

TAA is present in tumour and normal tissues, but it is highly enhanced in tumour cells expressing HER2, MART-1, MUC1, and MAGE. Neoantigens have higher immunogenicity and MHC affinity than TAAs and are immune to central immunological tolerance.

The first step in neoantigen identification is a quick DNA comparison of tumour and normal cells. Neoantigens activate T cells and produce highly active T cells with strong affinity for MHC-neoantigen-peptide complexes, evading central immune system recognition (149). Neoantigen vaccination can boost pre-existing neoantigen-specific T-cell populations and expand new T-cell specificities in cancer patients, improving tumour control. Melanoma tumour antigens with four peptide sequence epitopes, similar to the pathogen and more easily recognised by T cells, have sustained clinical responses to immunosuppressive agents (150).

Anti-tumor therapy is complicated, involving a neoantigen vaccine that T cells recognise. In a recent study, aPD-L1@HC/PM NPs were prepared using Chlorin e6 (Ce6)-conjugated hyaluronic acid (HC), dextro-1-methyl tryptophan (1-mt)-conjugated polylysine (PM), and anti-PD-L1 monoclonal antibodies (aPD-L1). In melanoma mice model radiotherapy, tumour volume was reduced, but in mice treated with aPD-L1@HC/PM NPs, it disappeared almost completely (151).

Despite being optimal targets for an anti-tumor immune response, neoantigens were only discovered and evaluated by using parallel sequencing and machine learning to detect tumour mutations and predict mutated peptides with high affinity that bind autologous HLA molecules.

Personalised vaccines with 20 peptide fragments containing neoantigen and PolyIC:LC as the immune adjuvant were tested on six advanced melanoma patients (152).

60% of the peptides developed a T-cell immune response in patients, and four of six treated patients had stable disease 25 months after vaccination and two had recurrence treated with PD-1 antibody with complete remission.

A vaccine with a PD-1 inhibitor was developed to increase the therapeutic effect and efficacy of the inhibitor. Antigen-specific vaccines stimulate the immune system to produce PD-1-positive T-cells that work with PD-1 inhibitor to attack the tumour twice. This personalised vaccine accelerates the immune response and removes PD-1 inhibitors, reducing metastasis (153). Nucleic acid vaccines deliver neoantigen-encoding mRNA or DNA to intracellular or intranuclear APCs (154).

T-lymphocytes destroy tumour cells expressing epitope-matched antigens. RNA vaccines avoid host cell genome integration. Due to delivery barriers and immunogenicity, many DNA and RNA vaccine clinical trials have failed, but recent promising studies are underway (90). An intravenous liposomal RNA vaccine (FixVac) targeting four non-mutated, tumor-associated antigens could boost immune check-point blockade by boosting the antitumor immune response. The IFNγ-ELISpot assay revealed immune responses in over 75% of 50 patients in a phase I dose-escalation trial of FixVac alone or with anti-PD-1 in stage IIIB, IIIC, or IV melanoma (Lipo-MERIT trial, ClinicalTrials.gov identifier NCT 02410733). In 42 patients with stage IV melanoma, FixVac monotherapy produced 12% partial responses and 28% stable disease, while FixVac with check-point inhibitors produced 35% partial responses in 17 patients (155).

Autologous and allogeneic tumour cell lysate-derived vaccines are also used in cancer immunotherapies. Autologous vaccines use patient-derived tumour cell lysate, while allogeneic vaccines use another species. MHC molecules present tumour cell lysates to trigger immune responses. It is well known that 25% of melanoma patients express NY-ESO-1 cancer/testis antigen. In a study on 11 melanoma patients, tumours expressing NY-ESO-1 that received autologous TCR-transduced T cells plus interleukin-2 showed objective clinical responses in five patients, the first successful treatment of a non-melanoma tumour (156).

Encapsulated GM-CSF and CpG ODN, a specific toll-like receptor (TLR) agonist that activates DCs, were added to sponge-like macroporous cryogels to create a biomaterial-based vaccination system. Subcutaneously administering cryogels to mice in a melanoma model delivered immunomodulatory factors (GM-CSF and CpG ODN) in a controlled manner. This vaccine caused local DC infiltrates that induced a potent, durable, and specific

anti-tumor T-cell response, suggesting cryogels could be used to vaccinate cancer cells (157).

Cancer stem cells are another immune therapy target for melanoma. CSCs are found in melanoma, where their proliferation causes metastasis and recurrence, but targeting and eliminating them in vivo is difficult. Novel synthetic high-density lipoprotein nanodiscs reduce ALDH, a marker for CSC isolation. This vaccine increases antigen trafficking to lymph nodes and generates strong ALDH-specific T-cell responses against ALDH-enriched CSCs (158).

A CSC-DC vaccine targeting ALDH highly enriched CSCs targeting dendritic cells and anti-PD-L1 and anti-CTLA-4 was designed to manipulate T-cell functions and induce T cell activation and proliferation in a B16-F10 murine melanoma tumour model (159).

Targeting immune checkpoint inhibitors to improve immunotherapy. A meta-analysis of 46 studies including 12,808 cancer patients treated with PD1/PD-L1 inhibitors found a global incidence of 26.8% (all grades) of adverse events (AEs) in melanoma patients treated with this treatment. Escalating checkpoint inhibitor doses can improve efficacy, but Aes are an emerging issue in cancer immunotherapy (160).

Biomaterial delivery systems like hydrogels, nanoparticles (NPs), and microneedle patch-assisted delivery were tested. A B16-F10 melanoma model received celecoxib and PD-1mAb locally via an alginate hydrogel system. Alginate hydrogel delivery significantly increased the antitumor activities of celecoxib (CXB), PD-1mAb, or both. The hydrogel system synergistically increased tumour CT4+ and CD8+ T cell accumulation (161). A self-degradable microneedle patch with biocompatible hyaluronic acid and dextran nanoparticles encapsulating aPD1 and glucose oxidase delivered an anti-PD1 antibody. A single intratumoral microneedle patch injection in a B16F10 mouse melanoma induced strong immune responses (162).

Encapsulated PLGA nanoparticles (anti-PD-1 NPs) were also used to deliver anti-PD-1 antibodies into the spleen in a B16-F10 murine melanoma model, enhancing their antitumor effect. Due to T cell hyperexpression, high doses of anti-PD-1 NPs can cause higher mortality than free antibodies. In contrast, anti-PD-1 NPs reduced mortality in splenectomized mice and showed the role of secondary lymphoid tissues in anti-PD-1 antibody toxicity.

Anti-PD-1 NPs also stimulate spleen DC internalisation, T cell maturation, and activation (163). (CTLA-4)-siRNA (NPsiCTLA-4) is another platform biomaterial-based

cytotoxic lymphocyte-associated molecule-4 used in a mouse model with B16 melanoma to increase CD4+ and CD8+ T cell activation and proliferation in vitro (164).

Oxaliplatin and doxorubicin can induce immunogenic cell death (ICD) in cancer cells by releasing ATP, CXCL10, calreticulin (CALR), and HMGB1 and stimulating the immune system. Combining chemotherapy and checkpoint inhibitors is another cancer treatment paradigm. In a recent study, anti-CTLA-4 was combined with liposomal doxorubicin in a PEGylated liposome to improve treatment efficiency and reduce SEs. Liposomal anti-CTLA-4 reduced tumour size and increased survival in B16 mouse melanoma models (165).

Tumor-infiltrating cytotoxic T lymphocytes control tumour development. Nano-immunostrategies to reprogram the tumour microenvironment targeting tumour acidity may improve T cell-associated immunotherapy.

RNAi nanoparticles reversed tumour acidity and activated T cells for checkpoint blockade therapy. Following this idea, an optimised vesicular cationic lipid-assisted nanoparticle was used in melanoma tumour models to block LDH A in tumour cells. The treatment reduced lactate production, neutralised tumour pH, and increased CD8+ T and NK cell infiltration, slowing tumour growth. The PD-1 antibody inhibited checkpoints after tumour pH was restored (166).

Hypoxia, a major component of the tumor-suppressive microenvironment, inhibits T cell activation. A multifunctional immunoliposome, CAT@aPDL1-SSL, was developed with modified aPDL1s on the surface to improve tumour immunotherapy and an encapsulated catalase. It was suggested that CAT-encapsulated liposomes reduced tumour hypoxia by decomposing endogenous H2O2 into O2. Immunoliposomes also increased CD4+ and CD8+ T cell infiltration in tumour tissues and blocked the PD-1/PD-L1 pathway (167).

Immunogenic cell death (ICD) includes apoptosis, necroptosis, and immunogenic apoptosis. Damage-associated molecular patterns (DAMPs), cytokines, and chemokines are produced during ICD, triggering enhanced anti-tumor immune responses. Radiotherapy, chemotherapy (oxaliplatin, cyclophosphamide), magnetic fluid hyperthermia, photodynamic therapy, and other stimuli can cause ICD.

New experimental data suggest that biomaterials, or "in situ tumour vaccines," can boost the immunogenicity of dying cancer cells, making immunotherapy more effective by combining with ICD-inducing modalities (168). Calreticulin (CRT) translocation on the cell surface releases ATP, HMGB1, and HSPs into the extracellular environment during ICD. The immune system activates APCs and cytotoxic T cells to eliminate tumours and

metastases. ATP recruits APCs by chemo-attraction, and CRT sends a ‘eat-me’ signal to stimulate APCs to capture dying tumour cells and debris. HMGB-1 and HSPs boost T cell antigen presentation (169).

ICD also triggers the release of pro-inflammatory cytokines like TNF-α, IL-6, and IL-1β, transforming immunosuppressive TIME into immunogenic TIME (170). AC-NPs were designed to capture and present TAAs to APCs. AC-NPs increased CD8+ and CD8+ cytotoxic T cell proliferation, improving anti-PD-1 treatment on the B16F10 melanoma model with a 20% cure rate compared to 0% without them (171).

Another study showed that low-dose paclitaxel and imiquimod in a co-delivery system for B16F10 melanoma worked together (172). The researchers found 2500% DC proliferation, pro-inflammatory and Th1 cytokine secretion, and tumour growth inhibition, resulting in 70% survival at day 41 compared to 0% survival for individual components. Cationic copolymer aPBAE for CRISPR-Cas9 genome editing inhibits tumour cell PD-L1 expression in vivo. In murine melanoma, knocking out cyclin-dependent kinase 5 (Cdk5) reduced tumour cell PD-L1 expression and inhibited tumour growth. PBAE/Cas9-Cdk5 treatment increases CD8 T cells and decreases Tregs in tumour microenvironment thanks to strong T cell-mediated immune responses (173).

A biodegradable nanoparticle delivery platform that genetically reprograms cancer cells and their microenvironment in situ was also developed. The reprogrammed cancer cells express IL-12 and 4-1BBL to mimic tumor-associated antigen-presenting cells (tAPCs). Nanoparticles and checkpoint blockade significantly slowed B16-F10 melanoma growth. Locally delivered tAPC-reprogramming nanoparticles enhanced cell-mediated cytotoxic immune response with systemic effects in vitro and in vivo (174).

In another study, pH-dependent dual-rebound nanoparticles (shPD-L1@NPs) containing plasmid DNA expressing small hairpin RNA of PD-L1 silenced the gene and reduced T cell-tumor PD-L1/PD-1 interactions. Hyaluronidase (HAase) degraded overexpressed hyaluronic acid (HA) in tumour tissues' extracellular matrix (ECM) to increase shPD-L1-loaded nanoparticle penetration. Combining HAase and shPD-L1@NPs increased tumour inhibition in a malignant melanoma mouse tumour model (175).

In a study that vaccinated mice with melanoma B16 tumours with PLGA nanoparticles (NPs) containing encapsulated poorly immunogenic melanoma antigen, TRP2 and TLR ligand covered by TLR4 agonist (7-acyl-lipidA) were evaluated. Interferon-gamma production in lymph nodes and spleens of vaccinated mice induces therapeutic anti-tumor effects, and cytokines are higher than in the control group (176).

Another poly(d,l-lactide-co-glycolide) nanoparticle (PLGA-NP) delivered antigenic peptides to induce cytotoxic T-lymphocyte responses against tumor-associated self-antigens in C57BL/6 melanoma mouse models. Vaccinating subcutaneously inoculated B16 melanoma cells with PLGA-NP containing TRP2180-188 and monophosphoryl lipid A slowed cell growth. Combining the peptide-loaded DC vaccine with IFN-γ to suppress tumour escape enhanced its anti-tumor potential (177).

In a recent study, cyclodextrin nanoparticles targeted a small molecule toll-like receptor 7/8 agonist to TIME macrophages, stimulating M2 to M1 polarisation and improving checkpoint-inhibiting immunotherapy in anti-PD-1 unresponsive tumours (178). CaCO3 nanoparticles and anti-CD47 antibodies increase macrophage polarisation towards M1, improving checkpoint blockade therapy. CaCO3 nanoparticles were administered as hydrogel during tumour surgery and interacted with TIME protons. The embedded anti-CD47 antibodies block tumour cells' "don't eat me" signal, increasing macrophage phagocytosis (179).

Statins can be more effective against tumours with tumor-targeted delivery systems. Antitumor activity of LCL-SIM versus free SIM in B16.F10 murine melanoma-bearing mice was compared. Previously, LCL-SIM inhibited B16.F10 melanoma growth by 85%, while free SIM has no antitumor activity. The efficacy of LC-SIM was linked to reducing TAM-mediated oxidative stress and HIF-1 α production in tumours, indicating that the liposome formulation's tumor-targeting property is linked to TAM presence in tumour tissue (180).

M2-like TAM dual-targeting nanoparticles are other carriers. The survival signal of M2-like TAMs was blocked by loading anti-CSF-1R siRNA on M2NPs in a molecular-targeted immunotherapeutic approach to reduce them from melanoma tumours. Administration to tumor-bearing mice eliminated 52% of M2-like TAMs, reduced tumour size 87%, and prolonged survival. The M2NP-based siRNA delivery system reduced IL-10 and TGF-β production, increased IL-12 and IFN-γ expression, and increased CD8+ T-cell infiltration in the TME, while reducing PD-1 and Tim-3 expression on infiltrating T cells, restoring T-cell immune function (181).

IDO1, a cytosolic enzyme with a heme prosthetic group secreted by DCs, converts tryptophan (Trp) from the tumour microenvironment to kynurenine (Kyn). IDO1 is overexpressed in over 50% of tumours that use its mechanisms to spread and survive (182). In the ‘elimination’ phase, the TME produces low levels of IDO1, which inhibits tumour growth. Tolerogenic dendritic cells (DCs) become immunogenic when IDO1 degrades (183). In the ‘equilibrium’ phase, surviving tumour cells are ‘edited’ by the immune system

and acquire mutations. Tumour and tolerogenic immune cells (DCs, MDSCs, TAMs) produce high IDO1 levels during the "escape" phase. Trp depletion and Kyn accumulation switch DCs to regulatory T cells and inhibit effector and NK cell functions (184). Preclinical and clinical trials tested nanomedicine formulations with small IDO inhibitor molecules (185).

A three-in-one immunotherapy nanoplatform for cancer immunity cycle elimination, equilibrium, and escape was reported. APD-L1@HC/PM NPs (Ce6-conjugated hyaluronic acid, dextro-1-methyl tryptophan-conjugated polylysine and aPD-L1) platform was designed to prevent tumour metastasis relapses and postsurgical regrowth. We also created a bilateral mouse tumour model of B16F10 melanoma to test aPD-L1@HC/PM NPs' abscopal effect. To improve immune response and memory, the enhancing tumour antigen for DC maturation and lymphocyte activation (elimination), the suppression of the IDO pathway (equilibrium), and the blocking of the PD-1/PD-L1 pathway for tumour elimination (escape) worked together (88).

Peptide-based nanoparticles also inhibit IDO by blocking tryptophan metabolism and block PD-L1. This NP promotes cytotoxic T lymphocyte survival and activation, inhibiting melanoma growth in mice by stimulating anticancer immunity (186). An embedded immunotherapeutic nanocapsule microneedle-based transcutaneous delivery strategy targets the immunoinhibitory receptor programmed cell death protein 1 (PD1) and immunosuppressive enzyme indoleamine 2,3-dioxygenase (IDO) into the TIME to treat melanoma (187).

Targeting TGF-β, a pleiotropic cytokine, promotes tumour evasion from the immune response in the tumour microenvironment. TGF-β signalling is crucial for immune suppression in tumour microenvironments, but blocking it can cause inflammation, autoimmune disease, and cardiac toxicity in animal models (188).

Current nanoparticle designs accumulate in tumours inefficiently after systemic administration due to slow passage through tumour vascular barriers and rapid reticuloendothelial particle clearance. To maintain T-cell proliferation and cytotoxicity in B16F10 melanoma tumours, a PEGylated liposomal antibody targeting TGF-βI inhibits signalling in primary T-cells. T-cells pre-loaded with liposomes targeting CD45-infiltrated tumours were found to be more effective than those targeting CD90 (Thy1) (189).

Nanoparticles with T-cell membranes (TCMNPs) were created. Due to T-cell membrane-derived proteins, TCMNPs can eliminate tumours. In addition, TCMNPs can release anticancer drugs and activate suppressed CTLs by inhibiting TGF-β1 and PD-L1.

TCMNP, when combined with dacarbazine, reduced tumour growth in B16F10 melanoma models and increased CD8+ Granzyme B+ and CD8+ IFN-γ+ T cell counts. Since they are made from T-cell lines and synthetic polymers in two days, TCMNPs may be cheaper and faster than adoptive T-cell transfer therapy in cancer immunotherapies (190).

In recent years, nanomedicine has focused on peripheral immune system compartments outside tumours. The peripheral immune system's lymph nodes and spleen present antigens and generate cytotoxic T-cells. These compartments often affect cancer occurrence and progression. Engineering T-cells to restore peripheral immune system functions can boost antigen presentation (191).

A previous study found that tumor-draining lymph nodes (TDLN)-targeting NPs containing tumor-associated antigen TRP-2 or CpG oligonucleotide induce strong cytotoxic lymphocyte (CTL) responses in B16-F10 melanoma cancer models. This strategy has been shown to slow immunosuppressive cells and boost antitumor immune cells in TDLN. The antigen-adjuvant combination in NPs could deliver TLDN to DCs and induce anti-tumor T-cell responses (192).

Oncolytic viruses induce host anti-tumor immunity and selectively replicate and lyse cancer cells. Talimogene Laherparepvec (T-VEC) is a genetically modified type I herpes simplex virus (HSV-1) that preferentially replicates in tumour cells and induces systemic antitumor immunity that can eradicate tumours remotely.

T-VEC was created by deleting neurovirulence genes that cause fever and a viral gene that blocks antigen presentation. T-VEC was modified to improve antigen presentation and T-cell priming by deleting the ICP47 viral gene and adding human GM-CSF (193). T-VEC selectively replicates in tumour cells by disrupting the PKR pathway oncogenically. T-VEC releases interferons, chemokines, PAMP, and DAMP factors locally in an immunosuppressive tumour microenvironment. Toll-like receptor agonists restore the tumour milieu to a pro-immunogenic state that boosts anti-tumor immune responses.

T-VEC-induced local GM-CSF expression enhances dendritic cell migration and maturation, which form phagocyte-soluble tumour antigens and apoptotic tumour cells. The T-VEC generates a higher immune response in injected tumours than distant metastases due to inadequate effector T-cell expansion and/or inability of circulating effectors to defeat the immunosuppressive tumour microenvironment at distant sites. This is why TVEC and immune checkpoint blockade are used together to slow melanoma progression (194).

T-VEC, the first viral oncolytic immunotherapy, was FDA-approved in 2015 to treat unresectable, cutaneous, subcutaneous, and nodal lesions in melanoma patients recurrent

after surgery based on OPTiM, a randomised phase III open-label trial. T-VEC had a 4.4-month longer median overall survival (OS) than GM-CSF in the OPTiM trial, with estimated 5-year survival of 33.4%, reaching 48.9% in patients with early metastatic melanoma (stage IIIB-IVM1a) and acceptable safety (97).

In melanoma, T-VEC plus checkpoint inhibitors is more effective than CPIs alone. MASTERKEY 265 (NCT02263508) is a phase III trial of T-VEC/placebo plus pembrolizumab in unresectable stage IIIB-IVM1c melanoma. Standard dose TVEC with ipilimumab was tolerable in 19 advanced melanoma patients in a phase IB trial (NCT01740297) (195).

A phase II randomised trial compared immediate surgical resection to 12 weeks of neoadjuvant intratumoral TVEC followed by surgery in 150 resectable stage III B/C or IV melanoma patients (NCT02211131). Latest interim 1-year analysis of recurrence-free survival results showed that T-VEC treatment group patients were more likely to remain recurrence-free (33.5 vs. 21.9%, P=0.05) and had higher overall survival after 1 year (95.9 vs. 85.8%) (196).

I.1.3.7. Conclusions and future directions

Current immunotherapy for melanoma has reached a limit of clinical responses. New methods are needed to increase the effectiveness of the treatments. One of the major ways to improve clinical responses is represented by nanomedicine modalities to manipulate the immune responses. The major challenge for nanomedicine-based immunotherapy remains the optimization of tumor targeting, drug delivery vs. clearance and control of toxicity.

In order to achieve a sustained and efficient anti-tumor immune response, a controlled release of immunostimulating substances, together with antineoplastic drugs combined with specific targeting are needed. In addition to classical well-known check-point inhibitors PD-1, PD-L1 and CRLA-4, other potential molecular targets in immunomodulatory therapy of melanoma can be represented by newly identified small-molecule immune checkpoint co-stimulators (GITR, OX40 with their ligands), inhibitors (VISTA, LAG-3, TIM-3, TIGIT) (143-145).

The immune system can also be modulated by small molecules that enhance cellular immunity, such as IDO/TDO, STING agonists, TLR agonists, GSK-3 inhibitors. The tumor microenvironment modulators including CSF-1R inhibitors, TGF-β or CXCR antagonists and epigenetic regulators of immune response as HDAC inhibitors, BET, EZH2 inhibitors are also promising for the enhancement of immunotherapy.

I.1.4. Theoretical model for the diclofenac release from PEGylated chitosan hydrogels

I.1.4.1. Introduction

Controlled drug delivery attracts researchers due to its health benefits. Systemic administration, the most common route, has indiscriminate side effects because it affects the entire body, but controlled drug release targets the affected sites, increasing drug bioavailability and limiting side effects (197). Drugs with high cytotoxicity are crucial for cancer treatment (198, 199).

Encapsulating drugs in an injectable matrix ensures their administration and prolonged release directly into tumors. Due to their porosity, hydrophilicity, biocompatibility, and similarity to biological tissues, hydrogels are the best matrix for this purpose (200). Chitosan-based ones are special because of their compositional and mechanical similarity to the extracellular matrix (201). Based on these premises, chitosan-based hydrogels are extensively studied as a matrix for controlled drug delivery systems, and new biocompatible formulations are developed to meet in vivo requirements.

In recent years, our group developed a new method for making biocompatible chitosan-based hydrogels using natural monoaldehydes as physico-chemical crosslinkers. Chitosan polyamine reacts with monoaldehydes to form dynamic polyimines, which self-assemble into three-dimensional networks and form hydrogels through imination, transamination, and hydrophilic/hydrophobic segregation. This method successfully converted chitosan into materials with tailored properties by selecting the right aldehydes. The hydrogels prepared this way were able to anchor and release drugs stably. Instead of chitosan, PEGylated chitosan was considered to improve matrix properties. PEG hydrophilicity and safety made it a good candidate for drug delivery applications that passed clinical trials.

New biocompatible hydrogels were made by grafting poly(ethylene glycol) and citral onto chitosan. They showed improved hydrophilicity and thixotropic properties due to PEG, making them a promising matrix for local drug injection to tumor sites (202). PEGylated chitosan hydrogels were used to encapsulate diclofenac sodium salt to test their ability to prolong drug release. DCF was chosen as a model drug because of its anti-inflammatory and anticancer properties on many tumor cell lines (203). This activity was due to electron-withdrawing halogens, like many other antitumor drugs, making it a model (204, 205).

Initial testing of these drug delivery systems showed in vivo biocompatibility, prolonged drug release, and slow matrix biodegradation (206). This encouraged us to study

the drug delivery mechanism to understand drug release phenomena and develop formulations. A Multifractal Theory of Motion-based mathematical model was created for this. Kink, soliton, antisoliton, breather, and other model solutions induced by the SL(2R) invariance groups are correlated with drug release mechanisms.

I.1.4.2. Materials and methods

Citral (95%), low molecular weight chitosan (217 kDa, DA: 85%), O-[2-(6-Oxocaproylamino)ethyl]Sigma Aldrich supplied -O′-methylpolyethylene glycol 2000, phosphate buffer saline (pH = 7.4), DCF, and ethanol, which were used as received.

The acid condensation reaction of the free amino groups of two hydrolytically stable PEGylated chitosan with citral's aldehyde group in DCF produced drug delivery systems. According to Ailincai, Mititelu-Tartau, et al. (206), the two PEGylated chitosan derivatives were synthesized by acid condensation reaction of chitosan with PEG-aldehyde in the amine/aldehyde molar ratio of 40/1 and 50/1, followed by reductive amination. The acid condensation of two PEGylated chitosan derivatives with citral and DCF produced four drug delivery systems. The DCF amount was kept constant while the crosslinking density was changed by modifying the molar ratio between amine and aldehyde functionalities to create drug delivery systems with different PEG content. Figure 1 shows formulation codes and component counts. This in situ encapsulation method encapsulated all drug (Figure I.1). Drug delivery somatic pain testing on mice using tail-flick assay showed that encapsulating the drug in these hydrogels preserved its activity.

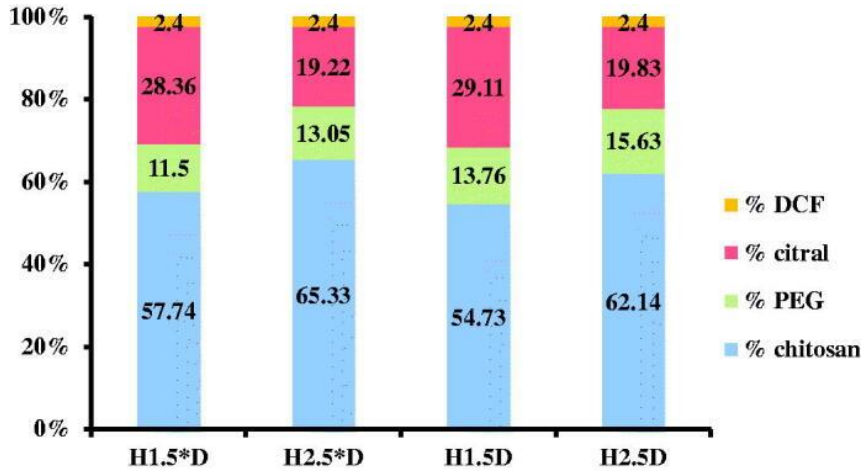

Figure I.1. Intrastenotic blood flow velocity at ICA bifurcation.

The PEGylated chitosan derivatives and the drug delivery systems have been obtained by freezing them in liquid nitrogen and further lyophilization using a LABCONCO Free Zone Freeze Dry System equipment, in working conditions −54 °C and 1.510 mbar, for 24 h.

ATR-FTIR spectra of the drug delivery systems (H1.5D; H2.5D; H1.5*D; H2.5*D) were recorded using an FTIR Bruker Vertex 70 Spectrophotometer equipped with a ZnSe single reflection ATR accessory.

Wide-angle X-ray diffraction (WAXD) was performed on a Bruker D8 Advance diffractometer at 36 kV and 30 mA, using Ni filtered Cu-Ka radiation ($\lambda = 0.1541$ nm). The diffractograms were recorded in the 2°–40° range, at room temperature, on pellets obtained by pressing a certain amount of sample using a hydraulic press (5 N/m^2).The investigations of the supramolecular architecture of the systems were realized by polarized optical microscopy (POM), using a Leica DM 2500 microscope.

The morphology of the samples was evaluated with a field emission scanning electron microscope (Scanning Electron Microscope SEM EDAX – Quanta 200) at an accelerated electron energy of 10 eV.

The monitoring of the *in vitro* release kinetics was performed in phosphate buffer saline (PBS) (pH = 7.4), at human body temperature, 37 °C. The obtained drug delivery systems (H1.5D; H2.5D; H1.5*D; H2.5*D) were used for the *in vitro* release experiments, following a previously used experimental procedure (203, 206). Pieces of xerogels with a mass of 62 mg, containing 1.5 mg of DCF drug were immersed into 10 mL of PBS. After different time intervals, 2 mL of supernatant were withdrawn and replaced with fresh PBS, to keep the same sink conditions. The concentration of the drug in the removed supernatant was determined by UV-vis spectroscopy, by measuring the absorbance of the characteristic absorption band of DCF at 275 nm and fitting on a calibration curve. The calibration curve was previously drawn by measuring the absorbance for different solutions of DCF with well-known concentrations and by the graphical representation of the absorbance as a function of concentration. The cumulative drug release was calculated using the following mathematical equation:

$$\% \text{ DCF} = [(10Cn + 2\Sigma Cn - 1)/m0] \times 100$$

where C_n and C_{n-1} are the concentrations of the drug in the supernatant after n and $n-1$ withdrawing steps, respectively, while $m_0 = 1.5$ mg, corresponding to the amount of DCF loaded in the samples. The experiments were done in triplicate and the

values are given as the mean value of three independent measurements. The absorbance of the DCF drug was measured using a Perkin Elmer Lambda 35 UV-Vis spectrophotometer.

In the past years, a wide range of theoretical models aiming at describing drug release mechanisms has been developed. The first type of models are empirical and semi-empirical models. The most used ones are the zero-order model, Higuchi model, Hixson–Crowell model, Korsmeyer–Peppas model, first-order model, etc (207-210). There are also kinetic models, based on the usual conservation laws, developed on spaces with integer dimensions or kinetic models, based on the conservation laws, developed on spaces with a non-integer dimension, explicitly written through fractional derivatives (209, 211, 212).

Recently, a new generation of theoretical models has arisen, based on Scale Relativity, either in the monofractal dynamics as in the case of Nottale, or in the multifractal dynamics as is the case for the Multifractal Theory of Motion (213-215). In such a context, supposing that, from both structural and functional perspectives, the polymer–drug complex system is assimilated to a multifractal system (216, 217) the wide ranges of drug release dynamics can be described through the movement of the so-called polymer-drug complex system structural units on multifractal curves. Accepting multifractality as a fundamental property in drug release dynamics (and since multifractality is induced through stochasticity, the drug release dynamics can be associated to various flow regimes of a stochastic fluid at various scale resolutions (multifractal fluid) (218).

Then, for a large temporal scale resolution, with respect to the inverse of the highest Lyapunov exponent, the deterministic trajectories of the polymer–drug system structural units can be replaced by a collection of potential trajectories (virtual trajectories), while the concept of definite trajectories can be replaced by that of probability density (218). In such a context, a multifractal probability density conservation law will become functional for the drug release dynamics, in the form of a diffusion-type equation at various scale resolutions (multifractal diffusion equations) (216):

$$\partial t\rho=2\lambda(dt)[2f(\alpha)]-1\partial l\partial l\rho \quad (1)$$

where

$$\partial t=\partial\partial t,\ \partial l=\partial\partial Xl,\ \partial l\partial l=\partial\partial Xl(\partial\partial Xl) \quad (2)$$

In the above relation, ρ is the multifractal probability density, Xl with l=1, 2, 3 are the multifractal spatial coordinates, t is a non-multifractal temporal coordinate having the affine parameter role on the movement curves, dt is the scale resolution, λ is a coefficient associated to the multifractal to non-multifractal transition, $f(\alpha)$ is the singularity spectrum of order α and α is the singularity index through which the fractal dimension D_F is specified

(for D_F we can use any definitions – Kolmogorov fractal dimension, Hausdorff–Besikovich fractal dimension, etc (219); it is regularly found that $D_F < 2$ for correlative processes and $D_F > 2$ for non-correlative processes). From such a perspective, through $f(\alpha)$ it is possible to identify not only the drug release volumes that are characterized by a certain fractal dimension (i.e. the case of mono-fractal drug release dynamics) but also the drug release quantity for which the fractal dimension is situated in an interval of values (i.e. the case of multifractal drug release dynamics). More than that, for the same $f(\alpha)$, it is possible to identify classes of universality in the drug release dynamics laws, even when regular or strange attractors have various aspects (218).

In a recent paper, operating with Equation (1), it has been shown that specific mechanisms of the release dynamics of the polymer–drug complex system (i.e. Fickian-type diffusion, non-Fickian-type diffusion, degradation of matrix, dissolution of matrix, etc.), can be 'mimed' as multifractal fluid diffusion modes (at various scalar resolutions) (216).

Then, $\rho(t)/\rho\infty$ was assimilated to the fraction of dissolved drug, that is, $M(t)/M\infty \equiv \rho(t)/\rho\infty$, where $M(t)$ is the amount of drug dissolved in time t and $M\infty$ is the total amount of drug dissolved, when the pharmaceutical dosage form is released.

Now, new data regarding release dynamics, complementary to the class of solutions associated with Equation (1) (generated through initial and boundary conditions), can also be given on the base of the transformation groups (which leave invariant the Equation (1)) (214, 220). These transformation groups constitute, in the most general case of the one-dimensional drug release dynamics, a realization of the Lie group $SL(2R)$, through the action (221):

$$t' \rightarrow \alpha t + \beta\gamma t + \delta,\ X' \rightarrow X\gamma t + \delta \quad (3)$$

where α, β, γ and δ are real elements.

Let us consider that, in accordance with general mathematical procedures (222), the release dynamics may be generally described with the help of a 2×2 matrix, with real elements. In a polymer–drug type system, it is obvious that the problem revolves around a family of such matrices, each of them describing the dynamics of a complex system entity (structural unit). The interactions between the complex system entities can then be expressed through relations between the representative matrices. These relations must contain certain parameters that characterize the structure of the polymer–drug complex system, adequate to the description of the drug release dynamics.

Therefore the matrix which generates an unharmonic curve (222), is a 2 × 2 matrix with real elements, written in the form:

$$M\hat{}=(\alpha\gamma\beta\delta) \quad (4)$$

The elements of this matrix contain, in an unspecified form, both the physical parameters of the complex system of polymer–drug type implying release dynamics and the possible initial conditions of the release dynamics. More precisely, the elements of the matrix in Equation (4) depend on the scale resolution in the sense of the Multifractal Theory of Motion (the release curves are continuous and non-differentiable, that is, multifractal curves) (221). In such a conjecture, the results to be obtained will also be in a sense of the previously-mentioned theory.

A set of such matrices, with variable elements, may be admitted as relevant for the release dynamics, for example by means of a fundamental spinor set, given by 2 × 2 matrices which describe the release dynamics. This description is analogous with the spinor description of space–time (223).

In such a situation, any 2 × 2 matrix of form in Equation (4) can be written as a linear combination with real coefficients, which implies two special matrices, specifically the unity matrix $U\hat{}$ and a null-trace matrix $I\hat{}$(from involution), meaning:

$$M\hat{}=\lambda U\hat{}+\mu I\hat{} \quad (5)$$

The involution $I\hat{}$ has some important properties, such as its squared form is a multiple of $U\hat{}$ and the fixed points of its homographic action are the ones of matrix $M\hat{}$.

In Equation (5), there exists the liberty to choose a parameterization in which the squared form of $U\hat{}$ can be the unity matrix, up to a sign.

In this case the elements of $I\hat{}$ maybe expressed with the help of only two parameters, which represent the asymptotic directions of matrix $M\hat{}$. If the asymptotic directions are complex, being of the form $u\pm iv$, the representation of the matrix $I\hat{}$ through asymptotic directions is of a spherical type. Then, satisfying the afore-mentioned properties (a) and (b) implies, for the matrix $I\hat{}$, the form:

$$I\hat{}=1v(-u1-u2-v2u),\ I\hat{}=-U\hat{} \quad (6)$$

Such a representation of the release dynamics has an important advantage. When analyzing the physics of the problem, the model allows an explicit differential description of the release dynamics, through matrix geometry, identic to the metric geometry of space at a certain moment, the hyperbolic geometry of the second type (in a Barbilian sense (224, 225)).

The representation of release dynamics through 2 × 2 matrices leads to a natural matrix of the matrices' space, for example, the Killing–Cartan metric of $SL(2R)$-type algebra of these matrices (222, 226). The basic co-vectors of such geometry are, in the general case of matrix in Equation (4), given by the external differential forms as follows:

$$\omega 1=\alpha d\beta-\beta d\alpha\Delta,\ \omega 2=\alpha d\gamma-\gamma d\alpha\Delta,\ \omega 3=\beta d\gamma-\gamma d\beta\Delta\Delta=\alpha\gamma-\beta 2 \quad (7)$$

In the parameterization given through Equations (5) and (6), Equation (7) becomes:

$$\omega 1=1vd\Phi+\sin 2\Phi duv2-\sin\Phi\cos\Phi dvv2\omega 2=2uvd\Phi+2\sin 2\Phi udu+vdvv2+2\sin\Phi\cos\Phi vdu-udvv2\omega 3=u2+v2vd\Phi+\sin 2\Phi(u2-v2)du+2uvdvv2+\sin\Phi\cos\Phi 2uvdu-(u2-v2)dvv \quad (8)$$

where:

$$\tan\Phi=\mu\lambda \quad (9)$$

Related to these co-vectors, the metric is given by the squared form as follows:

$$ds2=\omega 1\omega 3-(\omega 22)2=d\Phi 2-\sin 2\Phi du2+dv2v2 \quad (10)$$

As such, for as long as the polymer–drug complex system is represented defined by the core property that physics admits as being essential – which is the release dynamic – its description mode is a metric geometry.

In this case, the metric is given through (10), where Φ is an arbitrary 'phase,' and u and v are 'coordinates' obtained from the (local) dynamic of the polymer–drug complex system, in the way previously described.

Such a metric approach for the release dynamics can be certainly delegated to harmonic maps, from the polymer–drug complex system to space. As soon as the mapping mode of the polymer–drug complex system on the space available its disposal is solved, the quantities Φ, u, and v – and, the elements of the matrix family which represent the polymer–drug complex-system – are obtained. In principle, a 'position' function will be sufficient to correctly define a specific quantity of the polymer–drug complex system.

The difficulty of representing the polymer–drug complex system in this form is overcome through the harmonic map $X=(X1,X2,X3)\rightarrow\xi=(\xi 1,\xi 2,\xi 3)$ which can provide a set of quantities as functions of spatial coordinates. Let it be considered the function corresponding to the harmonic mapping principle (227):

$$J=12\iiint d3X|h|\overline{}\sqrt{}\ hil(X)\partial\xi\mu\partial\xi\nu\partial Xi\partial Xlg\mu\nu(\xi) \quad (11)$$

where h is the space metric and g is the associated metric of the polymer–drug complex system.

Canceling the first-degree variation of this functional, in relation to the spatial coordinates, gives the sought harmonic map. Taking into account the fact that space is Euclidean and using Equation (9) for the metric tensor associated with the polymer–drug complex system, for the integrand of Equation (11) the expression will be as follows:

$$|h|\overline{}\sqrt{}\, hil(X)\partial\xi\mu\partial\xi v\partial Xi\partial Xlg\mu v(\xi)\equiv\partial l\Phi\partial l\Phi-(\sin\Phi v)2[\partial lu\partial lu+\partial lv\partial lv] \quad (12)$$

where the usual notation ∂l denotes the gradient. The Euler equations corresponding to the functional Equation (12) are as follows:

$$\partial l\partial l\Phi+\sin\Phi\cos\Phi\partial lu\partial lu+\partial lv\partial lvv2=0\partial i(\partial luv2)=0,\ \partial i(\partial lvv2)+\partial lu\partial lu+\partial lv\partial lvv2=0 \quad (13)$$

The last two equalities of Equation (13) represent a harmonic map from the Euclidean space to the hyperbolic plane (Lobacevsky plane), in the Beltrami–Poincaré representation. As a consequence of these equalities, there will be:

$$\partial i(\partial lu\partial lu+\partial lv\partial lvv2)=0 \quad (14)$$

This means that the scalar quantity under the gradient ∂i is constant in space, but at the same time positive, being a sum of two squares of a real quantity. Let this quantity be denoted as $m2$, where m is real. The first equality in (13) becomes 3-dimensional Sine–Gordon type equation (in a multifractal sense):

$$\partial l\partial l\Phi+m2\sin\Phi\cos\Phi=0 \quad (15)$$

It extension on a space–time manifold (in a multifractal sense) through a generalized mapping principle of Equation (11) type implies the functionality of a 4-dimensional Sine–Gordon type equation (in a multifractal sense):

$$\Box\Phi+m2\sin\Phi\cos\Phi=0 \quad (16)$$

where □ is the d'Alembert-type operator (in a multifractal sense). For the standard Sine–Gordon equation, see Jackson and Cristescu (218, 228).

A solution of the equation (13) can be given relatively simply, if it is assumed that the quantities depend on the 'localization' on the space–time manifold by means of the linear form (the ansatz in a multifractal sense (222, 229)):

$$\xi=a1X1+a2X2+a3X3+a4X4=V0t \quad (17)$$

where $X1$, $X2$, $X3$ are the spatial coordinates and, $X4$ is the time. As such, Equation (16) becomes:

$$d2\Phi d\xi2+m2a2\sin\Phi\cos\Phi=0 \quad (18)$$

where:

$$a2=a21+a22+a23+a24 \quad (19)$$

Further on, Equation (18) is multiplied by $d\Phi d\xi$, after which it can be integrated and leads to the following expression:

$$(d\Phi d\xi)2+m2a2\sin2\Phi=b2$$

where b is an integration constant which is assumed to be real. As such, ξ is an elliptic integral of the first kind (230):

$$b\left(\xi-\xi0\right)=\pm\int arcsinZ0dc(1-z2)(1-s2z2)\sqrt{} \quad (20)$$

of modulus:

$$s2=m2b2a2,\ 0\leq s\leq 1 \quad (21)$$

where $z=\sin\Phi$, $\xi0$ is an integration constant assumed to be real, while Φ becomes the *sn* Jacobi elliptic function of the same modulus (Equation (21)),

$$\Phi=sn[b(\xi-\xi0);s] \quad (22)$$

The elliptic Equation (22) degenerates both in the limit $s\rightarrow0$, the situation in which it implies the periodic mode (in a multifractal sense):

$$\Phi\rightarrow\sin[b(\xi-\xi0);s\rightarrow0], \quad (23)$$

as well as in the limit $s\rightarrow1$, the situation in which it implies the kink mode (in a multifractal sense):

$$\Phi\rightarrow\tanh[b(\xi-\xi0);s\rightarrow1] \quad (24)$$

Finally, admitting that Φ is a measure of a drug release degree though Equation (19), (i.e. the usual $M(t)/M\infty$ in normalized coordinates) it results that the release process in a complex drug–polymer system can be dictated by release modes (i.e. those described through Jacobi elliptical function).

I.1.4.3. Results

A deep investigation by FTIR, X-ray diffraction, polarized light microscopy, and scanning electron microscopy was performed in order to reveal the structural and supramolecular particularities of the formulations.

FTIR spectra confirmed that the hydrogelation process was the result of the formation of the imine units and their supramolecular ordering, by the occurrence of the specific vibration band of the imine units at 1645 cm−1 and of the vibration band characteristic to the intra- and inter-molecular H-bonds around 3400 cm−1. Besides, the presence of the drug into formulations was confirmed by the presence of characteristic vibrations bands of the diclofenac (206).

With the aim to investigate the supramolecular architecture of the drug delivery systems and also to evaluate the form in which the drug was encapsulated into the polymeric matrix, X-ray diffraction has been performed.

As it could be observed in Figure I.2, all the diffractograms displayed broad diffraction peaks with a maximum around 21°, which was attributed based on the literature data to the semicrystalline state of the matrix (231, 232).

No reflection corresponding to the drug was clearly observed, suggesting that the drug crystallization into this matrix did not occur. This can be explained by taking into consideration the strong interactions which may establish between the matrix and the drug, which in this case seems to be stronger than the drug–drug interactions. Consequently, it was estimated that matrix-drug fractal entities were formed during the hydrogelation process.

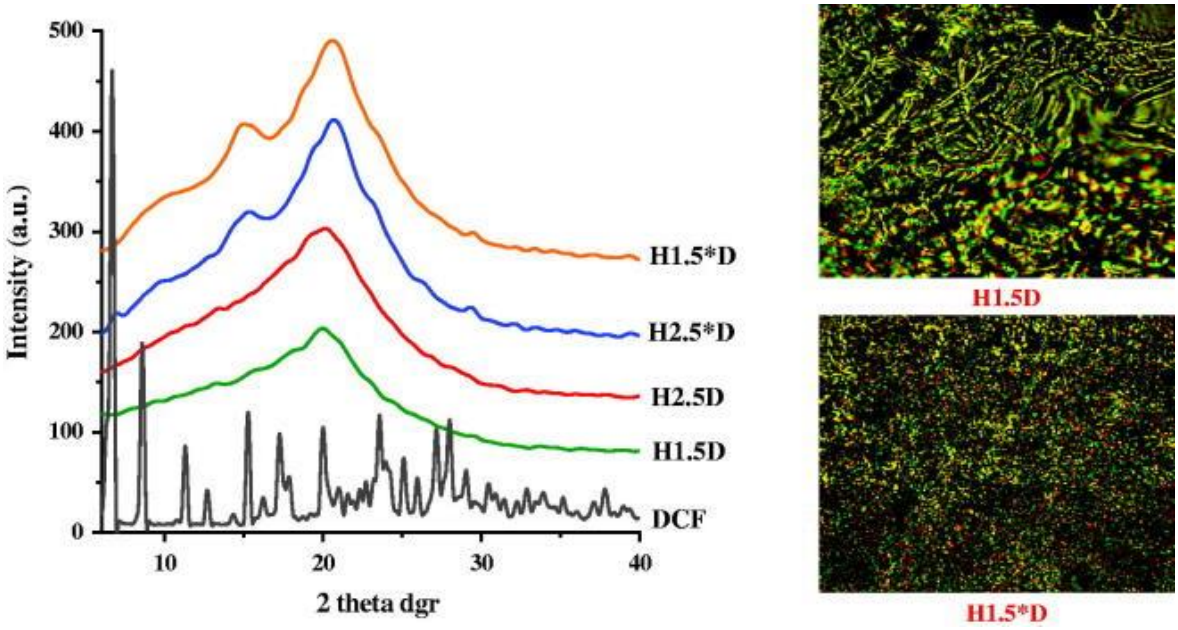

Figure I.2. XRD diffractograms of the drug delivery systems and DCF drug model and POM images (magnification: 200×) of representative drug delivery systems.

Polarized optical microscopy images of the formulation confirmed the X-ray diffraction data. All the samples presented birefringence, the signature of an ordering degree characteristic to the semicrystalline state (Figure I.2).

The continuous birefringence allowed us to conclude that the supramolecular matrix-drug fractal entities were dispersed into the samples in a quite uniform manner, leading to the appearance of a continuous texture due to their superposing across the sample (205).

SEM images displayed a porous microstructure forming interconnected micrometric pores with thick walls (Figure I.3). The microstructure of the samples was quite homogenous in the entire mass, with no obvious drug crystals in the pores. This indicated that the encapsulation of the drug occurred mainly inside the pores' walls, at the nanometric level.

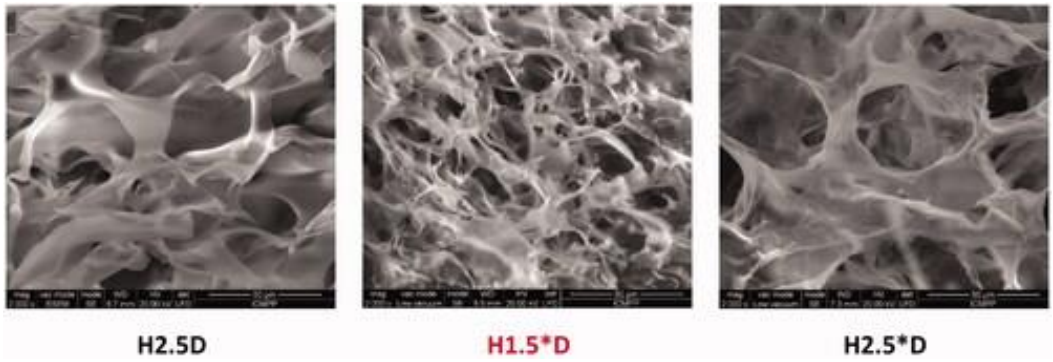

Figure I.3. SEM microphotographs of representative drug delivery systems.

These data allowed us to conclude that:

(i) DFC was dispersed into the hydrogel matrix as submicrometric crystals, eventually, as molecules, anchored by H-bonds, probably forming matrix-drug fractal entities;

(ii) the formulations have microporous morphology;

(iii) the drug was uniformly dispersed into the hydrogel matrix, more exactly into the hydrogel walls.

The investigation of the in vitro drug delivery behavior showed that the composition of the formulations and their morphologic particularities significantly influenced the drug release, especially in the first stage.

Thus, the sample with a higher content of PEG and lower crosslinking density (H2.5D) showed the most abrupt burst release effect (release of ~65%), while the sample with the lower PEG content and the higher crosslinking degree (H1.5*D) displayed the lowest burst release effect (release of ~30%).

The different release rate appeared to be related to the hydrophilicity of the systems; the systems containing a higher content of PEG were more hydrophilic and prompted a faster erosion by dissolution favoring a more rapid drug release (Figure I.4).

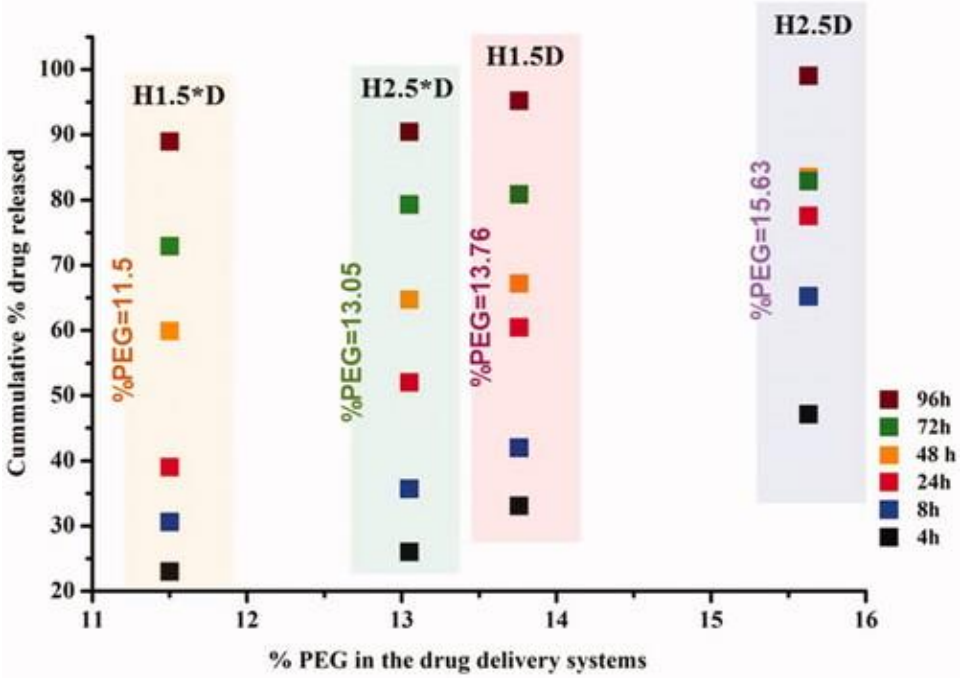

Figure I.4. The graphical representation of the PEG percent of samples versus the cumulative drug release, measured in an environmental mimicking physiologic conditions (pH = 7.4, 37 °C).

The fitting of the release data on five traditional mathematical models (Zero order, First order, Korsmeyer–Peppas, Higuchi, and Hixson–Crowell) gave excellent correlation coefficients (R^2 = 0.97−0.99) (see supporting information) indicating a complex drug delivery mechanism governed by the matrix particularities and drug encapsulation peculiarities, but not a clear conclusion could be drawn. Consequently, a new theoretical mathematical model based on the Fractal Theory of Motion was developed in order to investigate the drug release from a series of four formulations based on DCF dispersed into a hydrogel matrix of PEGylated chitosan crosslinked with citral.

The complexity of the release processes (i.e. drug diffusion, erosion of polymer matrix, drug solubility, etc.) can be expressed through non-linear behaviors of the release dynamic in the complex system drug–polymer, the explicit presentation of these non-linearities is a parabola through the modulus *s* if the elliptical functions *sn*.

Therefore, the linear behaviors of the release process (induced by weak type interactions between the composing components of the polymer–drug system) can be expressed through periodic type release modes (Equation (23)) while the nonlinear behaviors induced by strong interactions between the components of the system can be expressed through kin-type release modes (Equation (24)). The latter fits well with the empirical data and with the usual dependences reported in the literature. The solution (Equations (19)–(21))

represents release modes that contain multifractal behavior of the release dynamics in a global sense.

Without giving up of the ansatz in a multifractal sense, the Sine–Gordon type equation (in a multifractal sense), both through separation and intervention of some normalized coordinates (in the sense $\eta=a1X1\leftrightarrows$, $\tau=a4X4$), all of these based on specific operational procedures (214, 220). also implies the following special solutions:

i. soliton (+) and antisoliton (−) modes (in a multifractal sense):

$$\Phi 1(\eta,\tau,\alpha)=4arctan[\exp(\pm\tau-\alpha\eta 1-\alpha 2\overline{\quad}\sqrt{})],\ 0\leq\alpha<1 \quad (25)$$

ii. breather modes – localized oscillating modes (in a multifractal sense):

$$\Phi 2(\eta,\tau,q)=4arctan\{q1-q\overline{\quad}\sqrt{}[\sin(1-q\overline{\quad}\sqrt{}\tau)\cosh(q\eta)]\},\ 0<q<1 \quad (26)$$

These can be assimilated to a soliton–antisoliton oscillating pairs (in a multifractal sense). In Equations (25) and (26) a_1 and a_4 are characteristic parameters of the release process (for instance, a_1 is a specific wavenumber and a_4 is a specific velocity), while through constants α and q are detailed the local release processes.

The special solution (Equations (25) and (26)) are presenting an explicit manner the local behaviors in a multifractal sense, of the release dynamics of the complex system polymer–drug.

These solitons and antisolitons (in a multifractal sense) release mode (Equation (25)) describe local un-localized behavior of the release dynamics, while the breather type release modes (in a multifractal sense) (Equation (26)) describe localized behaviors.

In figure I.5 we have represented the 3D representations of soliton modes (left side) and breather modes (right side). We can see that these to depict two types of localized behavior that the model predicts will be found in drug-release related scenarios. The soliton mode is in line with the classical approach and we can see that it follows well the global behavior of the investigated conditions. This means that the release is controlled and increases over time both locally and globally.

A peculiar scenario can be seen for the breather modes. There is a periodic burst type release localized around the release surfaces. Globally these should not be seen as it does not completely affect the general behavior of the polymer–drug matrix. However, we do see in figure I.6 that the data presents some waves in the time span of 10–70 h.

This means that although the steep increase and the saturated regions are still seen as in our previous reports the transitions here seem to be described better by a combination of the two modes predicted by our model with the contribution ratio from each mode strongly depending on the fractality degree of the system.

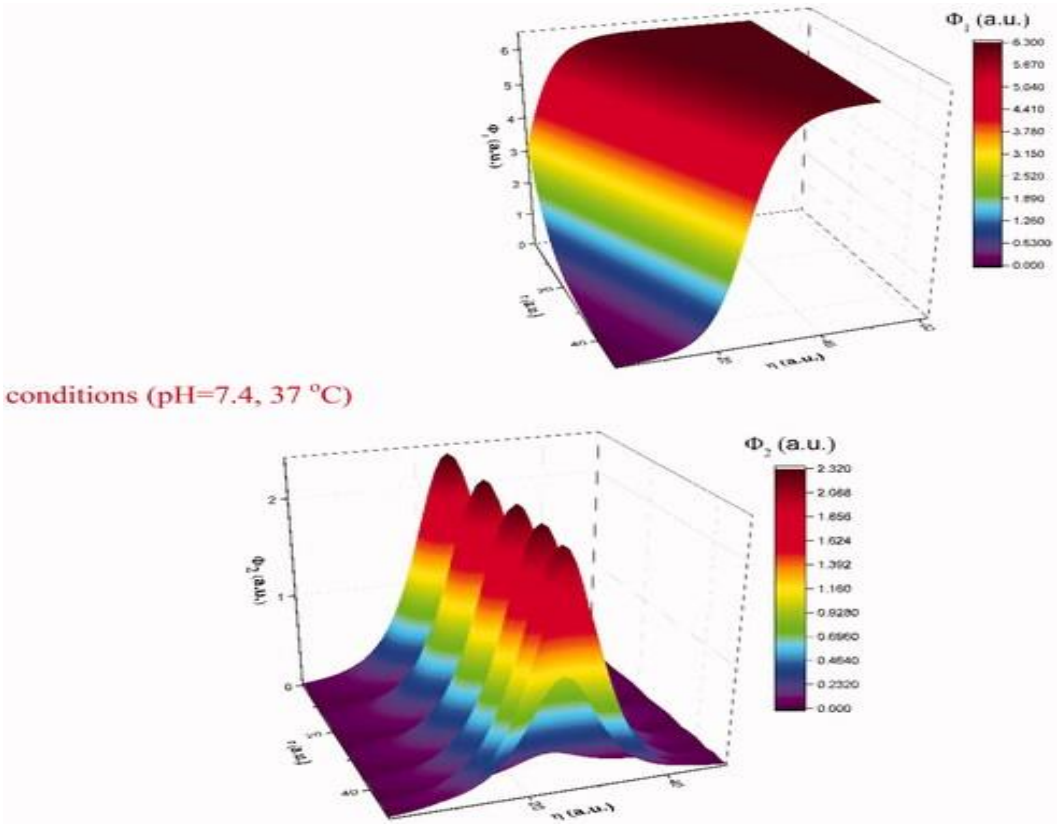

Figure I.5. 3D representations of soliton modes (Equation (22)) (left side) and breather modes (Equation (23)) (right side).

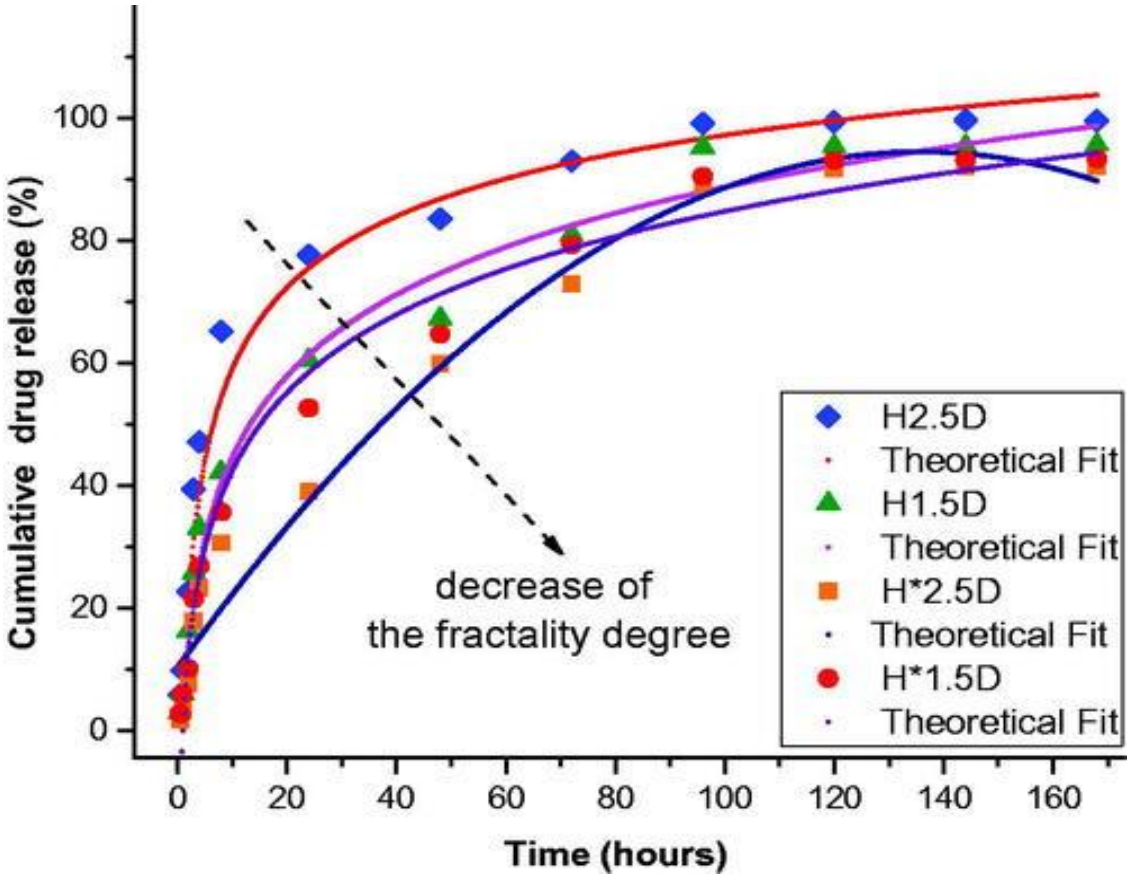

Figure I.6. Theoretical fit of the empirical data using the multifractal mathematical model.

In order to confirm the predictions made by our multifractal model, we used Equation (24) to fit the empirical data. Each theoretical fit leads to an R2 > 97%, which validates our model for long-time release dynamics. The results are presented in Figure I.6.

We can observe that the fractality degree, extracted from the fit, decreases with the decrease of PEG concentration. This is in good agreement as a faster release would indeed assume a high density of interaction between the released drug molecules and the environment. Therefore now, by contrasting the empirical data with an understanding of the fractality degree we can now say that the fractality degree can accurately describe the changes in hydrophilicity of the polymer.

A lower fractality degree as we can see (green) will also be more susceptive to a breather periodic burst type release, while a higher fractality leads to a release pattern defined mainly by the soliton mode.

Based on the existent literature (233, 234), the burst effect in the first release stage can be attributed to the faster dissolution of the bigger drug crystals.

In this time-span breather-type solution more accurately depicts the drug release process. We stated that for low fractality systems (Figure I.4 – H*2.5D and H*1.5D) breather-type of release is dominant as the existence of a low density of large drug crystals will generate a fast release with limited interactions with the medium.

With the increase of the hydrophilicity and thus of the fractality degree in the same time-span the drug release scenario it is depicted better by the steep increase (Figure I.4 – H2.5D and H1.5D). The steep increase defined by a soliton-type solution and the inhibition of the breather modes could also be a sign for the increase in larger crystals density in the matrix.

For longer time-scales the progressive release of the second stage is attributed to the slower dissolution of the drug encapsulated as nanocrystals or even as single molecules, which were stronger anchored in the hydrogel matrix. The transition is seen faster for high fractality systems that are described by soliton-type release where the presence of multiple large release sources mediates the whole process transitioning to the quasi-stationary regime.

I.1.4.4. Discussions and conclusions

Based on the notion that the fractal theory of motion is invariant to the homographic transformations, the release dynamics were described through 2×2 matrices with real

elements. Using the 2 × 2 matrix properties and the Killing–Cartan formalism for obtaining the SL(2R) invariant metrics through a harmonic mapping procedure we showed that the release dynamics can be described by a multifractal Sine–Gordon type equation. The solution of the equation, in its most general form, specifies the fact that the release modes are of elliptic type.

The degeneration of the elliptic solution leads to the Kink type release mode, which described the global drug-release behavior. The particular solution of soliton–antisoliton and breather type describe the local drug release behaviors. Therefore, the solition–antisoliton solution corresponds to the nonlocalized drug-release mechanism while the breather solution corresponds to the localized mechanism.

This multifractal mathematical model was developed in order to stimulate the release of DCF from a PEGylated chitosan matrix for a better understanding of the rules governing this process and thus to further improve it for *in vivo* applications.

The mathematical model has been applied for a series of drug delivery systems prepared by *in situ* dispersion of the drug into a PEGylated chitosan matrix. The systems proved the formation of the drug/matrix fractals and an *in vitro* drug release rate in dependence to the hydrophilicity degree. The mathematical model demonstrated a good correlation supporting the influence of the matrix hydrophilicity on the drug release rate.

Chapter 2: Prognostic and predictive factors in colorectal and non-small cell lung cancers

I.2.1. State of art

According to the GLOBOCAN predictions for the year 2020, lung cancer accounted for 11.4% of the total 19.3 million reported cases, making it the predominant form of cancer. Furthermore, it retained its status as the primary cause of cancer-related mortality, resulting in 1.8 million fatalities (4).

The two main types of lung cancer are non-small cell lung cancer (NSCLC), which represents around 80-85% of cases, and small cell lung cancer (SCLC). While tobacco use is widely recognized as the primary risk factor for the development of lung cancer, it is important to note that a significant proportion of individuals, ranging from 10-15% in Caucasians to as high as 40% in Asians, who are diagnosed with this disease are non-smokers. The precise determinants and underlying causes of diseases in those who do not smoke are still largely unexplored. Non-small cell lung cancer (NSCLC) is typically not detected until the disease has progressed to an advanced stage (235).

The examination of stage distribution at the time of diagnosis throughout the period of 2014-2018 revealed that around one-fourth, one-fourth, and half of the patients exhibited localized, regional, and distant stage disease, respectively. Patients diagnosed with metastatic cancer at the time of diagnosis continue to account for 46% of the patient population. However, there has been a notable increase in the number of cases discovered at a localized stage, rising from 17% in the mid-2000s to 28% in 2018. This improvement can be attributed to the implementation of cancer screening and preventive initiatives (236).

The process of carcinogenesis is associated with the existence of somatic molecular changes in particular oncogenic drivers, a subset of which can be targeted by therapeutic interventions. Modifications in the RAS/MAP kinases pathway have resulted in the emergence of distinct pharmaceutical interventions that aim to address EGFR mutations, MET exon14 skipping, ALK/RET/ROS1/NTRKs fusions, and more recently, the KRAS G12C mutation hotspot. Consequently, lung adenocarcinoma stands as the solid tumour with the most extensively verified targeted therapeutic approaches. As such, it serves as a genomic paradigm for mutation-based cancer therapy in the context of metastatic disease (237).

Furthermore, ICI has demonstrated favourable outcomes in the context of non-small cell lung cancer (NSCLC), particularly among patients lacking driver alterations. As a result,

it has received approval for utilization as a first-line treatment in conjunction with platinum-based chemotherapy for the management of stage IV illness. Nevertheless, with the exception of rare instances where patients exhibit complete long-term pathology responses, there is currently no therapeutic aim for metastatic illness. In contrast, the primary objective in managing individuals diagnosed with early-stage lung cancer is to achieve a cure by the implementation of a complete surgical resection (238).

Nevertheless, it is worth noting that a significant proportion, ranging from 30% to 50%, of patients may experience a recurrence of their condition following a full resection with R0 status. The current consensus guidelines advocate for the use of adjuvant or neoadjuvant chemotherapy in cases where tumours have a higher likelihood of recurrence (239).

Therefore, risk stratification plays a critical role in identifying individuals who will derive significant benefits from adjuvant treatment. Nevertheless, there is a limited number of prognostic variables that have been confirmed for localized non-small cell lung cancer (NSCLC), and the current categorization primarily relies on the assessment of the disease stage through pathological examination.

These patients are subjected to the adverse effects of cisplatin-based chemotherapy, including nephrotoxicity, anaphylaxis, cytopenia, hepatotoxicity, ototoxicity, cardiotoxicity, nausea and vomiting, diarrhea, mucositis, stomatitis, pain, alopecia, anorexia, cachexia, and asthenia, which may not be necessary. In addition, the application of genomic-alteration-driven adjuvant treatment, which is based on the promising outcomes observed in metastatic illnesses, has emerged as a prominent area of research in the context of localized non-small cell lung cancer (NSCLC).

Two phase 3 trials were conducted to evaluate the efficacy of nivolumab, an antibody that inhibits the programmed death 1 (PD-1) immune checkpoint, in patients with metastatic non-small cell lung cancer (NSCLC) who experienced disease progression while receiving or following platinum-based chemotherapy (240, 241). The results of both trials demonstrated a statistically significant increase in overall survival when compared to docetaxel. The observed benefit was evident irrespective of the amount of PD-1 ligand 1 (PD-L1) expression, but it was more pronounced in patients with nonsquamous non-small cell lung cancer (NSCLC) as PD-L1 expression increased.

Colorectal cancer (CRC) is a prevalent malignancy, with its incidence and mortality rates ranking fourth and second, respectively (4). Moreover, the incidence and mortality rate of colorectal cancer (CRC) continue to increase in numerous nations, posing a significant

threat to the health of individuals (242). Consequently, it is imperative to ascertain the factors that impact prognosis.

Currently, the tumour node metastasis (TNM) staging system, established by the International Union Against Cancer, is extensively employed for prognostic prediction and therapeutic guidance. Patients who are classified under the same stage in the TNM staging system are expected to have comparable outcomes. Nevertheless, clinical practice frequently yields varying outcomes for individuals, particularly those diagnosed with stage II colorectal cancer (CRC).

While the prognosis for stage II patients is generally favourable, a subset of individuals may experience local recurrence or distant metastasis during a five-year period following radical surgery. This occurrence is considered the primary factor contributing to a diminished prognosis and mortality associated with cancer.

Currently, despite the utilization of certain conventional clinicopathologic markers to differentiate these individuals at high risk, relying solely on these parameters does not result in an improved classification of such patients. Hence, the task of identifying risk variables and accurately classifying these patients remains a difficult task. In addition to traditional clinicopathological criteria, there has been an increasing focus on the investigation of molecular markers. The utilization of molecular markers has the potential to enhance prognostic stratification.

Claudins, which are the primary components of intercellular tight junctions, have an important role in the preservation of the paracellular barrier (243). Nevertheless, the dysregulation of claudins has been implicated in the pathogenesis of numerous illnesses (244). At present, the claudin family comprises a total of 27 members (245).

Among these members, claudin 7 has garnered significant attention due to its importance. According to reports, there is aberrant expression of claudin 7 observed in several tumour types, and this dysregulation is associated with the promotion of cancer invasion and metastasis (246, 247).

Furthermore, it has been observed that the atypical manifestation of claudin 7 is associated with the prognosis of various types of cancer, including breast carcinoma, lung cancer, nasopharyngeal carcinoma, oral and oropharyngeal squamous cell cancer, hepatocellular cance, ovarian cancer, laryngeal carcinoma, gastric carcinoma, and clear cell renal cell carcinoma (248).

Nevertheless, the existing body of research on colorectal cancer (CRC) is very scarce, and thus far, no studies have been conducted to investigate the relevance of claudin 7 as a predictor for the recurrence and metastasis of CRC.

Personal contributions:

1. Săftescu S, Negru Ș, Volovăț S, Popovici D, Chercota V, Stanca S, Feier H, Malita D, Dragomir R, **Volovăț C**. Predictors of the response to nivolumab immunotherapy in the second or subsequent lines for metastatic non-small cell lung cancers. Exp Ther Med. 2021 Jun;21(6):605. doi: 10.3892/etm.2021.10037. Epub 2021 Apr 14. PMID: 33936262; PMCID: PMC8082661.
2. Ianole V, Danciu M, **Volovat C**, Stefanescu C, Herghelegiu PC, Leon F, Iftene A, Cusmuliuc CG, Toma B, Drug V, Ciobanu Apostol DG. Is High Expression of Claudin-7 in Advanced Colorectal Carcinoma Associated with a Poor Survival Rate? A Comparative Statistical and Artificial Intelligence Study. Cancers (Basel). 2022 Jun 13;14(12):2915. doi: 10.3390/cancers14122915. PMID: 35740581; PMCID: PMC9221359.

I.2.2. Predictors of the response to nivolumab immunotherapy in the second or subsequent lines for metastatic non-small cell lung cancers

I.2.2.1. Introduction

PD-1/PD-L1 inactivation is one of the best-documented mechanisms of cancer cell immune evasion (249). PD-1, a membrane immunoglobulin on T and pro-B lymphocytes, suppresses T cell proliferation and activation after binding to PD-L1. Ig4 monoclonal antibody nivolumab blocks PD-1/PD-L1 signaling by binding to PD-1, disinhibiting the antigen-dependent antitumor immune response. Nivolumab was approved by the FDA in 2014 for metastatic melanoma and in 2015 for NSCLC and kidney cell cancer (250-252)

Nivolumab stimulates T cell reactivity at 1.5 ng/ml in the presence of antigenic stimuli for T cell receptors (253). Compared to chemotherapy, the wide therapeutic range of anti-PD-1 molecules has allowed the escalation of nivolumab doses, although it is also effective at one-tenth of current doses (254).

Nivolumab has no maximum tolerated dose and toxicity profiles are similar from 0.1 to 10 mg/kg q2w, but a dose-effect relationship is seen for NSCLC up to 3 mg/kg q2w (255). Recent studies have shown that dose reduction (20 and 100 mg, fixed doses every 3 weeks,

respectively) does not affect progression-free survival (PFS) or overall survival (OS) in NSCLC patients compared to 3 mg/kg q2w (256).

Nivolumab clearance is increased with ipilimumab and decreases inversely with BMI and albuminemia (257). Tumor type does not affect clearance. Sarcopenia, a symptom of cachexia, is a negative predictor of immunotherapy (IT) response in NSCLC. Note that albumin deficiency can cause hypocalcemia (258).

Sarcopenia and cachexia are linked to low creatinine levels, which indicate mediocre immunotherapy response. It is interesting that nivolumab serum levels at 14, 45, and 60 days after treatment correlate with plasma 25-hydroxycholecalciferol (259).

I.2.2.2. Materials and methods

The present study was approved by the Oncohelp Clinic Ethics Committee; all 78 patients included in the study voluntarily agreed to participate and provided written consent. We screened 692 admission charts/medical files (from January 1, 2019 to August 31, 2020) and created a MySQL database with anthropometric (sex, age, height, BMI), imagistic (metastases topography), hematological (red and white blood cell count), biochemical [creatinine, calcium, alanine aminotransferase (ALT), aspartate aminotransferase (AST)] and therapeutic (the use of opioids) variables.

The statistical analysis of the association between the overall time on treatment with the anthropometric, imagistic, hematological, biochemical and therapeutic variables was performed using the Cox Proportional Hazards Survival Regression (CPHSR) test available at https://statpages.info/prophaz.html) and included both past and ongoing immunotherapy cases.

I.2.2.3. Results

There were no statistically significant differences found between the age and duration of immunotherapy in our study group, analysed by gender (28.2% women) (table II.1).

Table II.1. Age and duration of treatment by sex.

Variables	Males and females	Males	Females	P-value
Age (years), average ± SD	63.6±8.4	64.3±7.5	62.0±10.3	0.509
Duration of immunotherapy (days), average ± SD	130.5±140.7	129.8±144.0	132.9±132.3	0.689

Legend: SD- standard deviation.

In terms of age group distribution, we found no significant differences between males and females (table II.2).

Table II.2. Age group distribution of the patients by sex.

Age group, years	**40-49**	**50-59**	**60-69**	**70-79**	**≥80**
Males and females (%)	9.0	20.5	43.6	24.4	2.5
Females (%)	18.2	18.2	40.9	18.2	4.5
Males (%)	5.4	21.4	44.6	26.8	1.8
z-test (males vs. females)	0.075	0.748	0.764	0.423	0.496

Analysis of anthropometric variables showed a statistically significant difference between height of the males and females, but not body mass index (BMI) (table II.3).

Table II.3. Height and BMI of patients by sex.

Sex distribution	**Height (cm)**	**BMI (kg/m2)**
Males and females	169.7±9.2	25.2±5.9
Females	174.0±6.4	26.2±6.0
Males	159.3±6.0	24.6±5.9
P-value (males vs females)	<0.00001	0.453

Legend: BMI, body mass index.

Most of the patients included in the study exhibited a good biological status, all with Eastern Cooperative Oncology Group Performance Score (ECOG PS) <3 at the time of immunotherapy initiation (table II.4).

Table II.4. Patient distribution by ECOG and sex.

Sex distribution	ECOG PS 0	ECOG PS 1	ECOG PS 2
Males and females (%)	38.5	50.0	11.5
Females (%)	39.3	50.0	10.7
Males (%)	36.4	50.0	13.6
z-test (males vs. females)	0.81	1.00	0.72

Legend: ECOG PS, Eastern Cooperative Oncology Group Performance Score.

In contrast with the female patients, more male patients (76.9 vs. 55%) showed various degrees of anemia (grade 1 and 2, P=0.067) (table II.5).

Table II.5. Hematological parameters at immunotherapy initiation.

Parameters	Males and females (%)	Males (%)	Females (%)	P-value (males vs. females)
Hemoglobin (Hb)				
Grade 2 anemia	15.3	15.4	15.0	0.97
Grade 1 anemia	55.6	61.5	40.0	0.10
Normal Hb level	29.1	23.1	40.9	0.13
ALC ($x10^9$/l)				
<1	25.0	25.0	25.0	1
1-4.8	73.6	73.1	75.0	0.87
≥4.8	1.2	1.9	0.0	0.52
ANC ($x10^9$/l)				

<2	1.4	0	5.0	0.11
2-9.9	87.5	86.5	90.0	0.69
≥10	11.1	13.5	5.0	0.30

Legend: ALC, absolute lymphocyte count; ANC, absolute neutrophil count. Grade 3 anemia <8 g/dl; Grade 2 anemia: 8-9.9 g/dl; Grade 1 anemia: 10-11.2 for female patients, 10-13.6 for male patients. Normal hemoglobin value: ≥13.7 for male, ≥11.3 g/dl for female.

On average, the hemoglobin (Hb) level did not change significantly at 6 weeks upon therapy (the average change was +0.09 g/dl) (Table II.6).

However, we noted wide individual variations [standard deviation (SD)=1.30 g/dl for Hb variation]. Of note, there were no statistically significant differences between Hb levels at initiation and the fourth cycle of immunotherapy (P=0,6891, Mann Whitney test).

Table II.6. Percent distribution of cases by hemoglobin at 6 weeks.

Males and females (%)	**Males (%)**	**Females (%)**	**P-value (males vs. females)**
Grade 3 Anemia	1.9	2.6	0.45
Grade 2 Anemia	9.4	7.9	13.3
Grade 1 Anemia	66	71.1	53.3
Normal Hb level	22.6	18.4	33.3

Legend: Hb- hemoglobin.

Almost 26% of the patients showed an abnormal number of lymphocytes at baseline, while in the case of neutrophils, the percentage of anomalies was much lower (12.5%).

Similarly, to the Hb variable, there were minimal global variations (on average +0.06x109/l) for absolute lymphocyte count (ALC) (Figure II.1) and absolute neutrophil count (ANC) (on average +0.16x109/l) at six weeks of immunotherapy, with wide individual variations (SD=0.55x109/l for ALC variation and SD=4.06 for ANC variation).

Neutropenic cases were absent at 6 weeks and neutrophilia was present in 7.5% of cases (maximum value=39x109/l). Of note, there were few cases of status reversals (e.g. neutrophilia turned to normal range neutrophils).

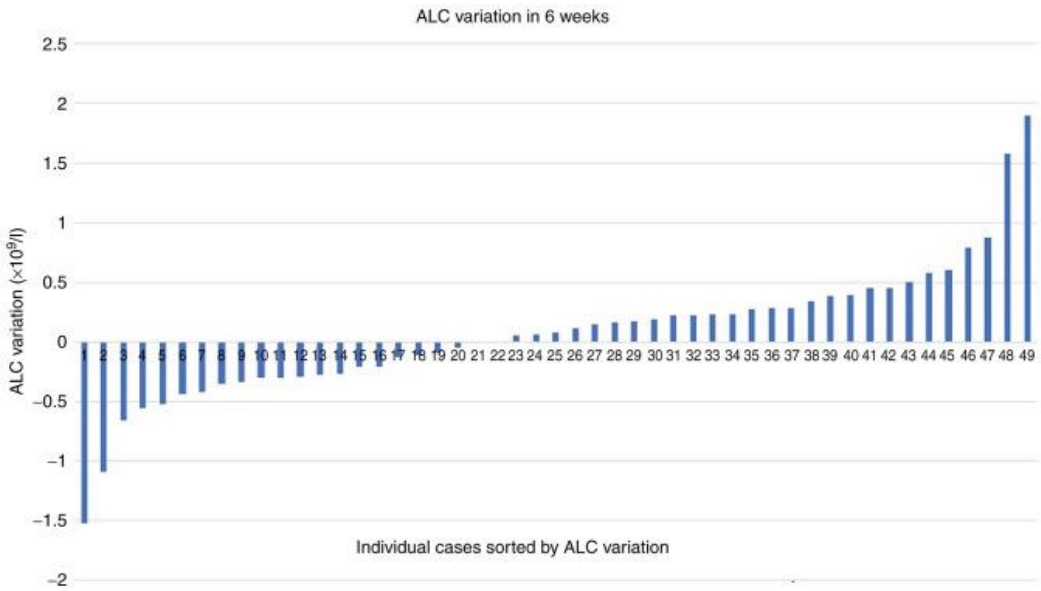

Figure II.1. Individual variations in ALC at 6 weeks of treatment. ALC, absolute lymphocyte count.

Leukocyte count and platelet (PLT) count showed significant differences in regards to sex distribution at initiation (Table II.7).

Table II.7. Other hematological parameters at immunotherapy initiation.

Parameters	**Males and females (average ± SD)**	**Males (average ± SD)**	**Females (average ± SD)**	**P-value (males vs. females)**
MCV (fL)	91.7±7.2	91.6±6.8	91.5±8.0	0.180
Leukocyte count (x109/l)	9.1±4.0	9.9±4.3	7.1±2.1	0.0214
PLT count (x109/l)	313.9±123.3	332.5±126.0	265.4±100.9	0.020

Legend: SD, standard deviation; MCV, mean corpuscular volume; PLT, platelet.

Creatinine, total calcium, ALT and AST showed no significant sex differences at initiation (Table II.8). There was a slight (statistically not significant) decrease in both creatinine (5.4%) and calcium (1.7%) levels during the first six weeks of therapy.

Table II.8. Other hematological parameters at immunotherapy initiation.

Parameters	**Males and females (mean ± SD)**	**Males (mean ± SD)**	**Females (mean ± SD)**	**P-value (males vs. females)**
Creatinine (mg/dl)	0.91±0.44	0.92±0.45	0.90±0.42	0.872
Calcium (total) (mg/dl)	9.63±0.89	9.64±1.0	9.6±0.5	0.441
ALT (IU/l)	21.6±29.6	22.1±33.3	20.6±17.5	0.880
AST (IU/l)	27.5±31.4	28.8±36.7	24.3±8.3	0.342

Legend: SD, standard deviation; ALT, alanine aminotransferase; AST, aspartate aminotransferase.

Next, we evaluated the overall number and the topography of metastases and found statistically significant differences in males vs. females, with female predilection towards brain and lung metastases.

In regard to brain metastases, the frequency in patients <60 years was significantly higher than in patients ≥60 years (P=0.00032).

In addition, liver metastases were more frequent in patients <60 years of age (P=0.048). Moreover, there was a clear predilection of both the 40-49 and 50-59 age groups for brain metastasis.

Interestingly, in our cohort, more males than females had no metastasis among evaluated sites (brain, lungs, liver, adrenal and bones), while females tend to be overrepresented in the 2 metastatic site subgroup.

Evaluation of the immunotherapy status at 20 months showed that 15.7% of the patients underwent a single administration of nivolumab and the treatment was discontinued immediately.

A total of 14.1% of the patients were treated for at least 2 cycles, but for less than 2 months and discontinued. A total of 21.8% of patients underwent at least 6 months of treatment (and from these patients, 14.1% are still in treatment) (figure II.2).

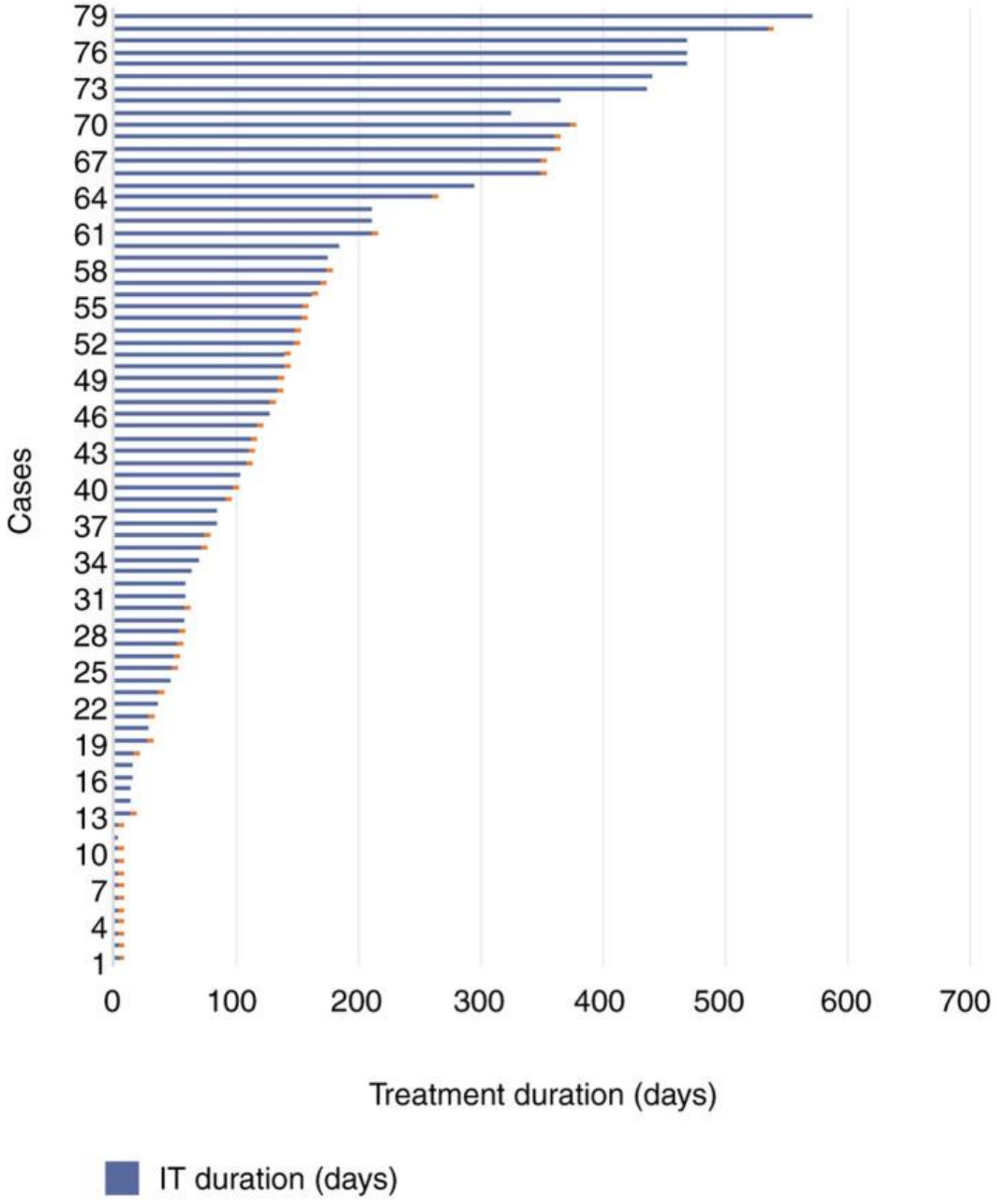

Figure II.2. Nivolumab immunotherapy treatment duration and actual status. Ended treatments indicated in orange.

The results of our CPHSR analysis are summarized [risk ratios (RR), 95% CI intervals, P-values] (table II.9), with a focus on initiation and at six weeks of immunotherapy time points (figure II.3).

Table II.9. Other hematological parameters at immunotherapy initiation.

Parameter	**Baseline parameters**			**Parameter variation after 6 weeks of nivolumab treatment**		
	RR (95% CI)	**P-value**	**No. of cases**	**RR (95% CI)**	**P-value**	**No. of cases**
Number of organs with metastases (BRA+PUL+HEP+SR+OSS) (values from 0 to 5, average 1.01)	1.5569 (1.156-2.095)	0.0035	76	NA	-	-
Hepatic metastases present (0/1, average 0.14)	2.6651 (1.268-5.599)	0.0097	76	NA	-	-
Adrenal metastases present, males <65 years (0/1, average 0.24)	3.5232 (1.165-10.629)	0.0257	25	NA	-	-
ANC >8 (x10^9/l) (0/1, average 0.18)	2.3863 (1.100-5.176)	0.0277	72	2.2495 (0.972-5.201)	0.0580	53
ALC (x10^9/l) (average 1.61)	0.9261 (0.61-1.41)	0.7202	72	2.5236 (1.046-6.087)	0.0394	49
ANC (x10^9/l) (average 6.37)	1.1003 (1.004-1.205)	0.0406	72	1.0169 (0.99-1.22)	0.0569	49
Brain metastases present at initiation (0/1, average 0.22)	1.9332 (1.017-3.671)	0.0440	76	NA	-	-
Lung metastases present at initiation (0/1, average 0.26)	1.7943 (0.98-3.26)	0.0562	76	NA	-	-
Leukocyte count (± x10^9/l) (average 9.13)	1.066 (0.996-1.140)	0.0637	72	1.0877 (0.89-1.31)	0.3920	49

Calcium total <9 mg/dl at initiation	2.1237 (0.80-5.58)	0.1267	67	NA	-	-
Male sex	1.6421 (0.81-3.30)	0.1647	76	1.6421 (0.81-3.30)	0.1647	76
AST IU/l at initiation	1.0052 (0.99-1.01)	0.21	70	NA	-	-
Hb at initiation (g/dl)	1.0108 (0.85-1.21)	0.9053	72	0.803 (0.56-1.14)	0.2212	49
ALT IU/l at initiation	1.0053 (0.996-1.014)	0.2447	70	NA	-	-
Opioid usage at initiation	1.604 (0.62-4.09)	0.3233	76	1.1406 (0.267-4.873)	0.8591	53
Adrenal metastases present at initiation	1.4187 (0.69-2.88)	0.3332	76	NA	-	-
MCV (fL) at initiation	1.0165 (0.97-1.05)	0.3864	72	1.0036 (0.94-1.06)	0.906	49
PLT count ($x10^9$/l) at initiation	1.001 (0.998-1.003)	0.4456	72	1.0032 (0.998-1.008)	0.2157	49
Creatinine (mg/dl) at initiation	0.7559 (0.36-1.55)	0.4473	71	0.6269 (0.08-4.54)	0.644	49
Height, male patients (cm)	0.9874 (0.93-1.04)	0.6353	52	0.9874 (0.93-1.04)	0.6353	52
Bone metastases present at initiation	0.848 (0.37-1.90)	0.6892	76	NA	-	-

ECOG PS (0-4) at initiation	0.9133 (0.58-1.42)	0.6895	76	NA	-	-
Age (years)	0.994 (0.95-1.03)	0.7360	76	0.994 (0.95-1.03)	0.7360	76
Calcium total at initiation (mg/dl)	1.0713 (0.71-1.62)	0.7445	67	NA	-	-
BMI at initiation (kg/m^2)	0.9917 (0.93-1.04)	0.7621	70	NA	-	-

Legend: RR, risk ratio; CI, confidence interval; BRA, brain; PUL, pulmonary; HEP, hepatic; ADR, adrenal; OSS, osseous; ANC, absolute neutrophil count; ALC, absolute leucocyte count; ALT, alanine aminotransferase; AST, aspartate aminotransferase; Hb, hemoglobin; MCV, mean corpuscular volume; PLT, platelets; ECOG PS, Eastern Cooperative Oncology Group performance status; BMI, body mass index; NA, not applicable.

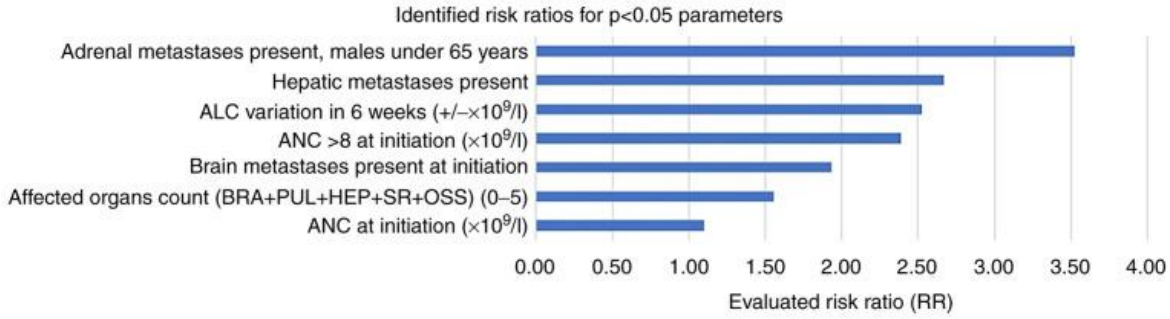

Figure II.3. RR for parameters with P<0.05. RR, risk ratio; ALC, absolute lymphocyte count; BRA, brain; PUL, pulmonary; HEP, hepatic; ADR, adrenal; OSS, osseous; ANC, absolute neutrophil count.

I.2.2.4. Discussions and conclusions

Following international incidence data on lung cancer (260), our cohort was mostly men (71.8%). There were no significant differences between male and female patients in age and age group distribution (except for the 40-49 group, where females predominated, P=0.075). There were no significant differences in BMIs between male and female patients, but males were significantly taller (P<0.00001). Most of our patients (88.5%) had ECOG PS below 2 and were in good biological health (P=0.741). Male and female patients had similar ECOG PS.

Men had a higher percentage of anemia than women (which may be due to a wider grade I anemia interval in men), and their leukocyte and platelet counts were significantly higher. At baseline, male and female biochemical parameters were similar.

The mean variation in hemoglobinemia (Hb) showed that only some patients recovered from toxic chemotherapeutic effects on hematopoiesis.

Female patients had double and more than double lung and brain metastases, respectively, while male patients had 5-times higher adrenal metastases (P=0.0394). Differences reached statistical significance for brain metastases (P=0.0104) and were close to the limit for lung metastases (P=0.0523). Most women (72.7%) had 1 or 2 metastatic sites, compared to 51.8% of men.

CPHSR analysis showed that each baseline metastatic site (aggregated brain, lung, liver, adrenal, bone topography) increased treatment exit risk by 56% (P=0.0035). Hepatic metastasis at baseline raised the risk ratio (RR) to 2.67 (P=0.0097), a significant negative predictive value.

Baseline adrenal metastasis was a significant negative predictor only in the <65-year-old male subgroup, with a 3.52 RR (P=0.0257), consistent with published data indicating a decrease in median overall survival (OS) (261). In our cohort, adrenal metastasis was almost double in the 40-49/50-59 age groups.

As expected, cerebral metastasis delays treatment (RR=1.93, P=0.044). Nivolumab therapy led to a 39% disease control rate and a median OS of 8.6 months in NSCLC patients, according to Crinò et al. (262).

A baseline neutrophil count over 8x109/l and an ALC variation of +1x109/l at six weeks on therapy were negative predictive factors, with RR=2.39 (P=0.027) and 2.52 (P=0.0394), respectively. Note that baseline ANC alone was a weaker negative predictor (RR=1.10, P=0.0406).

Our data showing ALC variation as a negative predictor may be surprising since previous studies show a positive correlation between ALC (at baseline and 6 weeks on treatment) and OS with nivolumab (263). The absolute change in ALC between baseline and 6-week time point was emphasized in our approach, unlike Karantanos et al. Why a positive ALC variation at 6 weeks of therapy decreases treatment time needs to be investigated in larger patient cohorts.

Other authors examined 50 disease-specific survival predictors during NSCLC nivolumab treatment. ECOG PS, size of the largest brain metastasis, number of metastatic

sites, toxicity, and malignant pleural effusion correlated with disease-specific survival and time to treatment failure (264).

Patients were screened for ocular changes and treatment options because lung and breast cancers metastasize to the eye and metastatic choroid tumors, though rare, are the most common intraocular malignancy.

The duration of nivolumab immunotherapy may be negatively correlated with total calcium levels below 9 mg/dl (hypocalcemia). Hypoalbuminemia is associated with poor immunotherapy results (possibly by increasing antibody degradation) and lower total calcium values; serum calcium values should be corrected in hypoalbuminemia.

Research shows that 17% of NSCLC patients have hypoalbuminemia and 37% have lost more than 5% of their weight in the past six months before starting nivolumab. PFS and OS are strongly influenced by albumin levels, with hypo- vs. normal albuminemia differences of 5.2 vs. 8.5 months for PFS and 6.9 vs. 18.5 months for OS (265).

In addition to the limitations of a retrospective study, the low number of probands in the subgroups caused uncomfortably wide confidence intervals for many variables.

The presence of adrenal metastases (in men under 65), liver metastases, neutrophilia at the start of treatment (expressed both as ANC and as a value exceeding 8x109/l), absolute variation (increase) of lymphocytes at 6 weeks of treatment, brain metastases, and the number of metastatic affected organs were negative predictive factors for nivolumab treatment duration.

Early evolutive parameters that predict nivolumab treatment duration, as shown for circulating lymphocyte variation in the first 6 weeks, should be reported.

I.2.3. Is High Expression of Claudin-7 in Advanced Colorectal Carcinoma Associated with a Poor Survival Rate? A Comparative Statistical and Artificial Intelligence Study

I.2.3.1. Introduction

As a result of their tumours' faster proliferation, greater propensity for invasion and metastasis, and heterogeneity in treatment response, patients with advanced stages of colorectal carcinoma (CRC) are at a significant risk of recurrence (266-269). One of the most significant members of the claudin family and a tight junction component called claudin-7 has 211 amino acid residues.

It is essential for maintaining the integrity of epithelial mucosa, epithelial cell polarity, and tight junction integrity. According to recent reports, Claudin-7 is also engaged in non-

tight junction-related processes such the start of an infection and several stages of tumour growth (270).

According to reports, abnormal Claudin-7 expression has been linked to carcinogenesis, progression, and metastasis in a number of malignancies, including those of the ovary, breast, prostate, oesophagus, stomach, colon, and lung (271, 272). Claudin-7 has been found to be up-regulated, down-regulated, or even deleted in CRC, and these changes are crucial for carcinogenesis, invasion, epithelial-to-mesenchymal transition (EMT), metastasis, and even tumour suppression (273-275).

The literature contains conflicting and sparse data, despite the fact that Claudin-7 is involved in the pathogenesis of CRC through a variety of different mechanisms (276-278). Therefore, the current study's goal was to look into Claudin-7 expression and its potential prognostic significance in later stages of CRC. Despite being a well-established area of study, artificial intelligence (AI) has recently seen significant application in the medical industry, primarily through the use of its subdomains, machine learning and deep learning.

AI algorithms are frequently applied in medicine to provide treatment predictions, identify patterns in data, and identify specific illnesses. In relation to CRC, AI algorithms were employed to detect the disease at an early stage or predict how the disease would progress or how a CRC treatment would turn out. More precisely, RNA molecular biology, biopsies, and colonoscopy were used along with AI algorithms to diagnose CRC (279-281). Additionally, chemotherapy or CRC surgery both frequently employed AI (282). We are unaware of any previous research employing AI algorithms to examine the function of Claudin-7 expression in CRC.

I.2.3.2. Materials and methods

In Iasi, Romania's "Sf. Spiridon" Emergency County Hospital, 84 patients with advanced stage CRC (stage IV) diagnosed between 2008 and 2020 were included in the study. All participants provided written informed consent for this study, which was authorised by the ethics committee of the "Sf. Spiridon" Emergency County Hospital in Iasi.

Frequently, paraffin embedding and fixation in neutral buffered formalin 10% were used to handle tumour sample. Two punches (4 mm in diameter) from each patient, one from the invading tumour front and the other from the tumour core, were used to create tissue microarrays (TMAs).

Twenty samples of normal colonic mucosa resection margins that were taken from tumours that were at least 10 cm in diameter made up the control group. Anti-Claudin-7

monoclonal antibody (rabbit anti-human, 1:1500, ab207300, Abcam, Cambridge, UK) immunohistochemical tests were conducted after pretreatment with a particular epitope retrieval solution (pH 9) at 96 °C, for 25 min. ThermoFisher Scientific, Fremont, California, USA, provided the UltraVision LP Detection System and 3,3′-Diaminobenzidine chromogen (DAB) for the detection of the immunoreaction. By deleting the primary antibody and substituting non-immunized serum at the same dilution (negative control) for each TMA, the specificity of the immunoreactivity was examined. Two replicates from each TMA were used in the immunohistochemical assays.

Two separate researchers evaluated the expression of Claudin-7 in a blind fashion. Membranous staining in tumour cells was used to determine Claudin-7 expression. The percentage of stained tumour cells per core was calculated using a semi-quantitative four-tiered scoring method as follows: 0 = 5% positive tumour cells; 1 = 5-30%; 2 = 30-60%; and 3 = >60%.

A four-tiered scale was used to assess the strength of the immunoreaction: 0 indicates a negative reaction, 1 indicates a weak reaction, 2 indicates a moderate reaction, and 3 indicates a strong reaction. The invasive front and tumour core were both assessed. In order to reach agreement, the panel reevaluated cases where there was disagreement.

Microsoft Office Excel and IBM Statistical Package for the Social Sciences (SPSS) version 26 were used to analyse the data. The 8th edition of the AJCC Cancer Staging Manual, 2017 and the 5th Edition of the WHO Classification of Tumours: Digestive System Tumours, 2019: age, sex, T stage, N stage, grading, tumour location, venous invasion, lymphovascular invasion, perineural invasion, tumour growth pattern, tumour deposits, tumour budding, leukocyte) were used to determine the relationship between Claudin-7 expression and clinicopathological parameters.

The period of time from the date of diagnosis and the start of treatment, to the date of death or the last follow-up, was referred to as survival. The Kaplan-Meier method and scatter plots were used to estimate the overall survival (OS) for univariate survival, and the log-rank test was employed to analyse the data. Multivariate survival analysis was performed using Cox multiple regression. Statistical significance was defined as a p-value 0.05.

Only 6 Claudin-7 attributes were initially chosen from the dataset as inputs: Cldn7 (Front) P, Cldn7 (Front) I, and Cldn7 (Front) membranous staining pattern: discontinuous vs. continuous are Cldn7 (Front) P, Cldn7 (Front) intensity, and Cldn7 (Core) membranous staining pattern variables.

The output, in two separate forms—a classification issue and a regression problem—was the survival rate. The data were preprocessed to determine the number of years between the Visit Date and the Death Date (where applicable).

Then, three values for the Survival class were created: "2" for differences of less than 2 years, "5" for differences of between 2 and 5 years, and "T" (10) for differences of more than 10 years. The output was the real difference in years when the issue was looked at in its regression form.

It is helpful to get an overall visual picture of the distribution of the data before using the machine learning techniques. Although it is an oversimplifying assumption, the way each attribute is treated in this section in relation to the output can give some first insight into the issue.

There is no discernible pattern in this representation, as the class values are evenly distributed across the range of input values. For the classification task (Cldn7—Claudin-7; P—percentage, I—intensity, D—membranous staining pattern: discontinuous vs. continuous).

Three different circumstances were used in the experiments:

- to gauge whether an algorithm can even learn the data from the entire training set;
- using 10-fold cross-validation, the de facto method for comparing and evaluating the generalisation potential of various algorithms;
- when there are only a few training examples (in our case, 84 patients), the leave-one-out method is helpful.

Using Weka software, the following algorithms were implemented:

- K-nearest neighbour (kNN), which has k neighbours and a distance weighting function, is the next-closest neighbour.
- generalised examples that are not nested (NNGE);
- decision-tree C4.5;
- Rough forest;
- Linear models for classification and regression;
- Support vector machine (SVM) classification and regression, with a chosen kernel, such as the radial basis function (RBF).

Information gain was used to assess the same one-to-one relationship between clinicopathological factors (as inputs) and Claudin-7 expression (as outputs). This approach evaluates an attribute's usefulness in addressing a categorization issue. More specifically, if

an attribute's values can fully separate class values when tested, then that attribute can resolve the classification issue on its own.

In this ideal scenario, every attribute value relates to a subset of the dataset where all of the instances have the same class value. The entropy gap between the original dataset and the partitioned dataset is at its maximum since the resulting partitions have zero entropy. More homogeneous partitions are still desirable when the attribute values cannot properly partition the dataset, and entropy can still be employed as a homogeneity metric.

This rise in entropy is specified as follows for a class C and an attribute A:

InfoGain(C,A)=H(C)H(C|A)(1) where H is the entropy

$$H(C)=-\sum i=1cp(i|C)log2p(i|C) \quad (2)$$

The fraction of cases with a class value of i allows for the straightforward computation of the probabilities p from the data. The conditional entropy is calculated using the same method for each attribute value Aj. A bigger information gain essentially indicates that an attribute is more pertinent for the categorization issue.Every 10 years, we used discretized classes with ages ranging from 20 to 90 for the information gain algorithm.

The next AI study we conducted tries to choose a subset of inputs (same clinicopathological factors as before) with the greatest relevance to the outputs (Claudin-7 expression). A classification algorithm is used in a wrapper feature selection approach to evaluate the impact of progressively bigger subsets of input attributes on the output.

This method, which is greedy, adds additional inputs one at a time while measuring the classification accuracy as a result. With a medium to large number of inputs, the greedy technique presupposes that there is no backtracking and no exhaustive attempt to evaluate all conceivable attribute combinations.

I.2.3.3. Results

In this retrospective study, the immunohistochemical assessment of Claudin-7 expression was performed on 84 tumor samples, with histologically confirmed advanced stage CRC (stage IV). At the time of the last clinical follow-up, 64 patients (76.2%) out of the total group had died. Expression of Claudin-7 was defined as the presence of membranous staining in tumor cells.

As shown in Table II.10, the proportion of stained tumor cells was graded 3 for almost all cases, both in the core and invasive front. However, Claudin-7 staining intensity showed a larger variation in the scoring system, both in the core and invasive front. In the control

group samples, represented by normal colonic mucosa, the intensity and the proportion of the Claudin-7 immunoexpression were both graded as 3.

Table II.10. Comparison of Cldn7 expression between tumor core and invasive front.

	n	Min	Max	Mean
Cldn7 (Core) P	84	2	3	2.99
Cldn7 (Core) I	84	1	3	2.42
Cldn7 (Front) P	84	1	3	2.90
Cldn7 (Front) I	84	1	3	1.81
Control group	20	0	3	3.00

Legend: Cldn7, Claudin-7; Cldn7 (Core) P, the proportion of Claudin-7 stained tumor cells in the tumor core; Cldn7 (Core) I, the intensity of Claudin-7 immunoreaction in the tumor core; Cldn7 (Front) P, the proportion of Claudin-7 stained tumor cells in invasive front; Cldn7 (Front) I, the intensity of Claudin-7 immunoreaction in invasive front.

A discontinuous membranous staining pattern of Claudin-7 was observed mostly in the tumor invasion front (table II.11).

Table II.11. Comparison of Cldn7 staining pattern between tumor core and invasive front.

Staining Pattern	Cldn7 (Core) n	Cldn7 (Core) %	Cldn7 (Front) n	Cldn7 (Front) %
Continuous	62	73.8	15	17.9
Discontinuous	22	26.2	69	82.1
Total	84	100.0	84	100.0

Legend: Abbreviations: Cldn7, Claudin-7.

Claudin-7 immunoexpression in the normal colonic mucosa, staining intensity variations according to the scoring system and different Claudin-7 staining patterns (discontinuous vs. continuous) are shown in figure II.4.

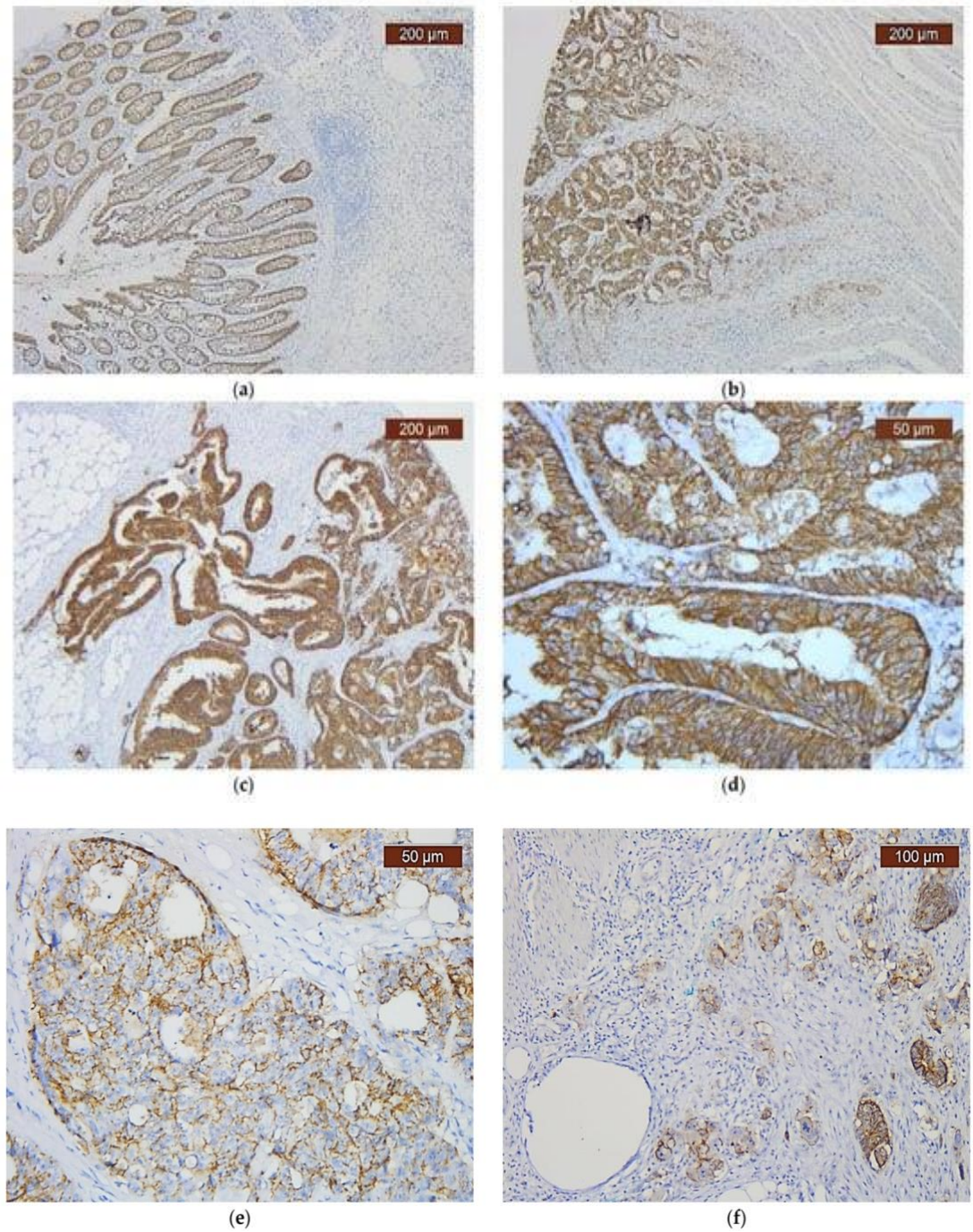

Figure II.4. Immunohistochemical profile of Claudin-7 (IHC, anti-Claudin-7 monoclonal antibody) in: (a) normal colonic mucosa (magnification ×50); (b) CRC, intensity decreasing from core to invasive front (magnification ×50); (c) CRC, continuous membranous staining pattern in the tumor core and invasive front (magnification ×50); (d) CRC, continuous membranous staining pattern in the tumor core (magnification ×200); (e) CRC, discontinuous membranous staining pattern in the tumor core (magnification ×200);

(f) CRC, discontinuous membranous staining pattern in invasive front (magnification ×100).

In order to evaluate the relation between Claudin-7 expression (in the tumor core, respectively in the tumor invasive front) and clinicopathological parameters, correlations were made using Chi-squared and Fisher's exact test (Table II.12). A significant correlation ($p = 0.033$) was identified between Claudin-7 invasive front intensity and tumor leukocyte infiltrate, implying that a decrease in Claudin-7 intensity in the tumor invasive front is associated with an increase in leukocyte infiltrate. However, Claudin-7 expression regarding the proportion and intensity was not correlated with age, sex, T stage, N stage, grading, tumor location, venous invasion, lympho-vascular invasion, perineural invasion, growth pattern, tumor deposits and tumor budding ($p > 0.05$).

Table II.12. Univariate analysis of Claudin-7 and clinicopathological parameters.

Clinicopathological Parameters	**Cldn7 (Core) P**	**p-Value**	**Cldn7 (Core) I**	**p-Value**	**Cldn7 (Front) P**	**p-Value**	**Cldn7 (Front) I**	**p-Value**
Age								
21–30	0	0.310	0	0.655	0	0.227	0	0.647
31–40	0	0.000	1	1.000	0	0.206	1	0.523
41–50	1	0.190	2	0.821	1	0.744	4	0.389
51–60	0	0.298	2	0.906	0	0.677	2	0.438
61–70	0		2		0		7	
71–80	0		1		1		0	
81–90	0		0		0		0	
Sex								

F	1	0.429	3	1.000	1	0.523	13	0.953
M	0		3		2		7	
T stage								
T2	1		2		3		1	
T3	0		3		17		7	
T4a	0	0.190	1	0.206	1	0.744	4	0.389
T4b	0		0		0		0	
N stage								
N0	0		0		1		1	
N1a	0		1		1		0	
N1b	0		1		1		1	
N1c	0	0.298	1	0.613	0	0.677	1	0.438
N2a	1		1		2		1	
N2b	0		2		1		7	
Grading								
High Grade	0		1		1		4	
Low Grade	1	0.821	5	0.906	1	1.000	8	0.278
Tumor Location								

LeftColon	1		4		1		3	
Rectum	0	1.000	0	0.625	0	0.312	2	0.053
RightColon	0		2		0		6	
Venous Invasion								
V0	0		0		1		2	
V1	1	0.762	1	0.168	1	1.000	7	0.255
Lymphovascular Invasion								
L0	0		0		1		0	
L1	1	0.893	1	0.122	1	0.562	12	0.553
Perineural Invasion								
Pn0	0		2		1		3	
Pn1	1	0.762	4	0.352	1	1.000	9	0.640
Tumour Growth Pattern								
Expansive	0		1		1		2	
Infiltrative	1	0.881	5	0.882	1	0.603	10	0.651
Tumor Deposits								
Absent	1		4		2		5	
Present	0	0.512	2	0.244	4	0.427	7	0.832

Tumor Budding								
Bd1	0		0		1		0	
Bd2	0	1.000	1	0.354	2	0.438	3	0.743
Bd3	1		5		4		9	
Leukocyte Infiltrate								
3	0		1		0		1	
5	0		1		2		3	
10	0		3		2		2	
15	1		2		1		2	
20	0		0		2		3	
25	0	0.143	0	0.366	1	0.876	0	0.033
30	0		0		0		1	
50	0		0		1		1	

Legend: Cldn7, Claudin-7; Cldn7 (Core) P, the proportion of Claudin-7 stained tumor cells in the tumor core; Cldn7 (Core) I, the intensity of Claudin-7 immunoreaction in the tumor core; Cldn7 (Front) P, the proportion of Claudin-7 stained tumor cells in invasive front; Cldn7 (Front) I, the intensity of Claudin-7 immunoreaction in invasive front.

As previously mentioned, survival was defined as the time elapsed between the date of diagnosis and therapy initiation, to the date of death or of the last follow-up.

The Kaplan–Meier univariate survival analysis using the log-rank test showed a significant correlation between survival and Claudin-7 intensity in the invasive front ($p = 0.00$), with a higher expression (score 3) being associated with a worse prognosis. This decrease in survival occurred independently of Claudin-7 intensity in the tumor core, which

had no impact on survival. In addition, scatter plots were also used for the statistical analysis of survival data (Figure II.5).

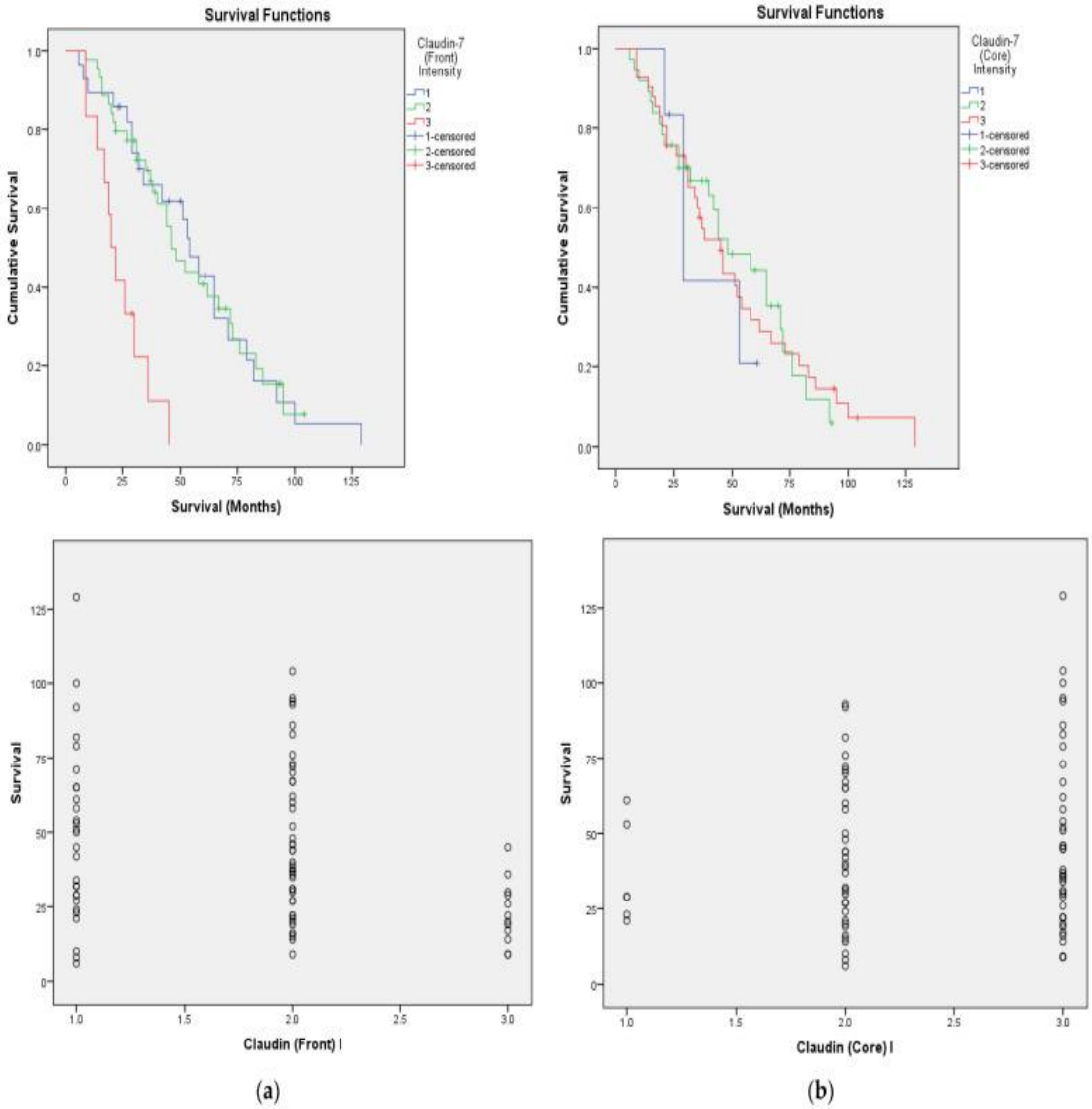

Figure II.5. Prognostic significance of Claudin-7 intensity (I) expression regarding overall survival as calculated by Kaplan–Meier analysis and scatter plots: (a) invasive front; (b) tumor core. The intensity of immunoreaction: 1—weak, 2—moderate, 3—strong.

Table II.13 and Table II.14 present the results of the algorithms mentioned in the Materials and Methods section for the two considered problems (classification and regression, respectively), in terms of accuracy for classification and coefficient of determination for regression.

The algorithms in table II.13 and table II.14 are different because some algorithms cannot be applied for both types of problems.

Table II.13. The results of different algorithms for the classification problem.

Algorithm	Training	Cross Validation	Leave One Out
NN	60.7143%	36.9048%	40.4762%
kNN, k = 10, w = 1/d	60.7143%	38.0952%	42.8571%
NNGE	48.8095%	45.2381%	42.8571%
C4.5	51.1905%	40.4762%	38.0952%
Random Forest, 100 trees	60.7143%	39.2857%	45.2381%
SVM, RBF kernel	60.7143%	34.5238%	39.2857%
Linear model	59.5238%	45.2381%	47.619%

Table II.14. The results of different algorithms for the classification problem.

Algorithm	Training	Cross Validation	Leave One Out
NN	0.5803	0.3225	0.2759
kNN, k = 10, w = 1/d	0.5801	0.2981	0.2524
Random Forest, 100 trees	0.5715	0.3069	0.2843
SVR, RBF kernel	0.55	0.156	0.1066

Linear regression	0.498	0.3268	0.2529

For our case study, table II.15 shows the InfoGain measure for each combination of inputs and outputs.

Table II.15. The information gain values.

Clinicopathological Parameters	**O1**	**O2**	**O3**	**O4**
Cldn7 (Core) P	0.01328	0.02698	0.03564	0.07025
Cldn7 (Core) I	0.00389	0.00277	0.00406	0.02741
Cldn7 (Front) P	0.03746	0.14349	0.03254	0.05841
Cldn7 (Front) I	0.04147	0.10628	0.06594	0.10709
Tumor Location (I1)	0.00492	0.04001	0.00640	0.01225
Grading (I2)	0.00241	0.05595	0.00358	0.03046
T-stage (I3)	0.00525	0.02838	0.00738	0.00748
Leukocyte Infiltrate (I8)	0.04120	0.13327	0.06169	0.17204
Tumor Deposits (I9)	0.01328	0.04099	0.01975	0.01006
Tumor Budding (I10)	0.00389	0.05448	0.01788	0.01834
Tumor Growth Pattern (I11)	0.00274	0.00181	0.00324	0.01211
Sex (I12)	0.01600	0.00256	0.01735	0.00179
Age Group (I13)	0.03936	0.10040	0.06750	0.12619

Legend: Cldn7—Claudin-7; P—percentage; I—intensity.

In the following experiments, we use the order of attributes found by information gain and use the C4.5 decision tree algorithm, which naturally uses information gain for node splits. The full training set is used for these case studies. The results of this technique are presented in figure II.6.

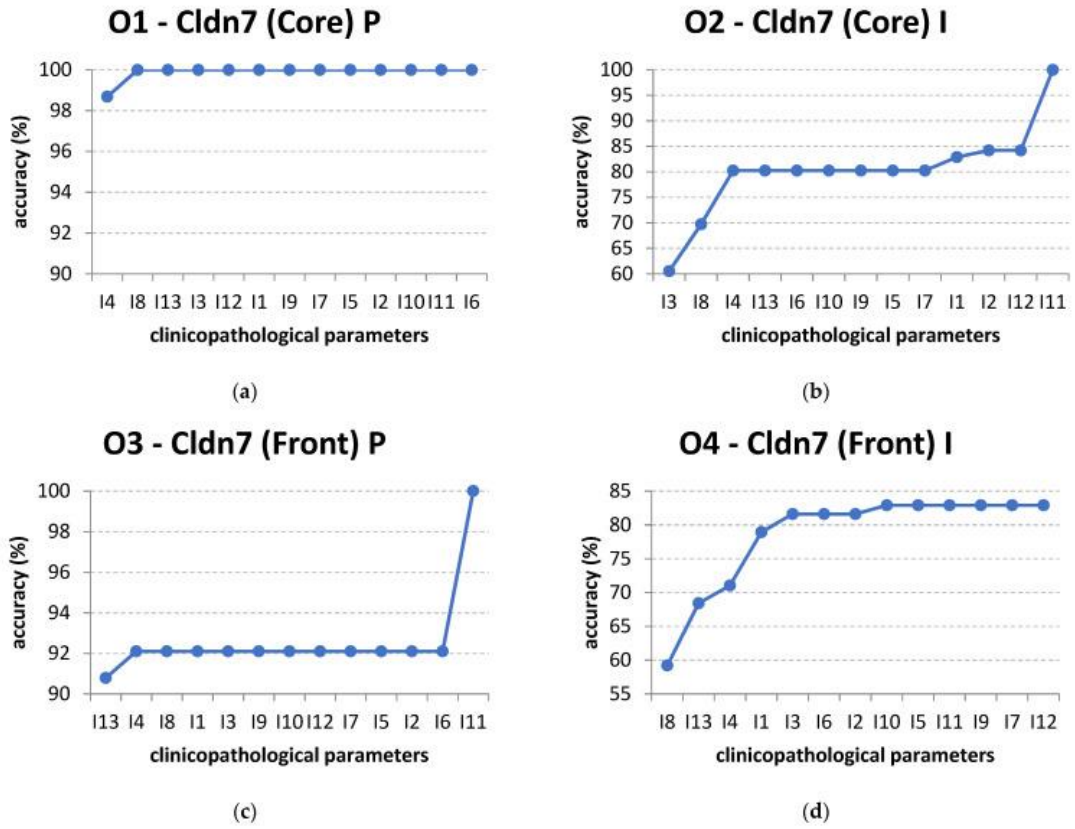

Figure II.6. The increase of classification accuracy for each output by adding input attributes in the order specified by information gain: (a) output O1; (b) output O2; (c) output O3; (d) output O4.

For output O1, only I4 and I8 are enough to correctly classify the instances (Figure II.6). This is not the case for the other outputs, which require all the inputs for maximum accuracy. For example, in the case of output O2, Cldn7 (Core) I, if only input I3, T-stage, is used, the decision tree has an accuracy of 60.5263%. If input I8, Leukocyte Infiltrate, is added, i.e., only the attributes I3 and I8 are used, the classification has a larger accuracy of 69.7368%.

When I3, I8, and I4 are used, the accuracy becomes 80.2632%. Adding more inputs no longer increases the accuracy until the final attribute I11 is added, which leads to a 100% classification accuracy. The other subfigures in Figure II.6 present the increase in accuracy

for different orders of inputs corresponding to their respective outputs, as found by the information gain method.

I.2.3.4. Discussions

This retrospective study was designed to investigate the immunohistochemical expression of Claudin-7 and the potential prognostic significance in advanced CRCs. Furthermore, we aimed to draw a parallel between classical statistical algorithms and those used in AI.

Since its first discovery, a variety of studies suggested a link between Claudin-7 low expression and CRCs development and progression (283-285). However, other studies obtained opposing results (286).

The present study identified a significant correlation between Claudin-7 intensity in the tumor invasive front and tumor leukocyte infiltrate ($p = 0.033$), implying that a decrease in Claudin-7 intensity in the tumor invasive front is associated with an increase in leukocyte infiltrate.

To our knowledge, this is the first study to investigate the correlation of Claudin-7 immunohistochemical expression with inflammatory infiltrate in CRCs in humans. Consistent with our findings, but in animal models, Wang et al. reported that loss of Claudin-7 increases colonic infiltration of leukocytes during experimental colitis and demonstrated the promotion of colitis and associated CRC colitis in a Claudin-7 knockout mouse model (287).

We found that, in almost all cases (98.8% in the tumor core and 91.66% in the tumor invasive front), more than 60% of the tumor cells (grade 3) showed a high expression of Claudin-7.

Similar results were reported by Kuhn et al. and Darido et al. where a low expression of Claudin-7 was found in normal colonic crypts, while in CRCs the expression was high. They identified the Claudin-7-EpCAM-CO-029-CDn44v6 complex and its upregulation also in hepatic metastasis of patients with CRC and a significant correlation was found between this complex and the clinical diversity, apoptosis resistance, and disease-free survival (274, 286).

On the other hand, in contradiction to our results and also to the above-mentioned studies, Bornholdt et al. found an intense immunohistochemical reaction of Claudin-7 in normal colonic tissue, but a decreased or absent reaction in dysplastic and CRC tissue. These

observations were sustained by the Claudin-7 mRNA levels, suggesting an early change in CRC carcinogenesis (284).

Moreover, Xu et al. proved that the positivity rate of Claudin-7 expression was significantly lower in CRC tissues than in peritumoral normal tissue and Claudin-7 expression was correlated with the grade of differentiation, being downregulated in well-differentiated adenocarcinomas, further downregulated in moderately differentiated adenocarcinomas, and significantly downregulated in poorly differentiated adenocarcinoma (288).

When analyzing the relationship between Claudin-7 expression and the morphological manifestations of EMT (tumor budding) we found no significant correlation. However, in contrast to our results Philip et al., Bhat et al. and Wang et al. concluded that Claudin-7 low expression or downregulation induced EMT, which plays a major role in CRC invasion, progression and metastasis process (283-285).

Furthermore, Xu et al. analyzed the effects of Claudin-7 knockdown in CRC stem cells through cell proliferation assay, migration assay, apoptosis assay and reported changes in cell characteristics such as promotion of cell proliferation, migration, and inhibition of cell apoptosis and the presence of EMT (288).

The present study found that when using a statistical approach, except for the leukocyte inflammatory infiltrate, Claudin-7 expression was not correlated with other clinicopathological parameters: age, sex, T stage, N stage, grading, tumor location, venous invasion, lympho-vascular invasion, perineural invasion, growth pattern, tumor deposits and tumor budding ($p > 0.05$), nor in the tumor core, neither in the tumor invasive front).

Consistent with our results, Hou et al. who conducted a study to explore the role of Claudin-7, a p53 regulated gene, in tumorigenesis and progression of CRC through quantitative real-time PCR, Western blot, a luciferase reporter assay, and immunohistochemistry, found no correlation between clinicopathological parameters (tumor size, invasion depth, lymphatic metastasis, stage III/IV) and Claudin-7 high expression. In addition, Claudin-7's high expression was significantly correlated with a favorable prognosis (289).

However, in contrast with these findings, in our study, the Kaplan–Meier univariate survival analysis, by using the log-rank test and the scatter plots, showed a significant correlation between survival and Claudin-7 intensity in the invasive front ($p = 0.00$), where a higher expression was associated with a worse prognosis.

Whenever conducting multivariate analysis, such as with the Cox regression method, one of the major pitfalls is having an insufficient number of outcome events (such as death) relative to the number of variables analyzed in the model.

This proportion has been termed EPV (events per variable), and a small value of the EPV affects the accuracy (risk estimates) and precision (95% confidence intervals) of odds or hazard ratios of the variables included, which may render misleading results (290).

An adequate minimum value of the EPV is 10–20 (at the very least 10 outcome events per variable analyzed) (291). In keeping with this rule, we found multivariate analysis unsuitable for our study (84 cases, 64 events, 15 variables). Taken together, our study advocates for the potential prognostic and therapeutic role of Claudin-7 in advanced CRCs.

Concerning the study of AI, in this paper, we presented various analyses based on machine learning methods.

In concordance with the findings of the statistical approach, we found that none of the applied algorithms can properly predict the survival rate based on the Claudin-7 inputs, therefore it is likely that there is no correlation between these inputs and outputs. We have considered the input data both in discrete and continuous forms.

When considering the influence of clinicopathological parameters on Claudin-7 expression based on information gain, by analyzing the inputs on the rows in Table 6, one can identify the most relevant inputs for all the outputs.

The applied information gain algorithm found that the most relevant single inputs are Leukocyte Infiltrate and N-stage. Age was found to be relevant for the Cldn7 (Core) P, Cldn7 (Front) P and Cldn7 (Front) I.

T-stage was found to be relevant only for the Cldn7 (Core) I expression. These findings are consistent only with the correlation found by statistical means between Leukocyte Infiltrate and Claudin-7 intensity in the tumor invasive front.

The analysis based on subsets of input attributes shows that no single attribute can lead to a high accuracy classification. The actual accuracy values depend on the base classification algorithm wrapped for feature selection. For the multivariate approach using AI algorithms, we used C4.5 decision trees and information gain algorithms, which generally provide good results for the analyzed issue.

We found that two or three attributes from the set of Leukocyte Infiltrate, T-stage, N-stage, and Age increase the accuracy to more than 75% for each of the four outputs (Cldn7 (Core) P, Cldn7 (Core) I, Cldn7 (Front) P, and Cldn7 (Front) I). For Cldn7 (Core) P and Cldn7 (Front) P, the results are very good, with accuracies of 100% and 92%, respectively.

However, with the exception of Cldn7 (Core) P, all input attributes are necessary to obtain maximum accuracy.

I.2.3.5. Conclusions

Given the fact that the patients' database is reduced (under 100 patients), classical machine learning methods seem to be a reasonable choice. With various error rates, all the applied algorithms support the finding that the survival rate cannot be predicted based only on Claudin-7 expression, yet there are correlations between clinicopathological parameters and Claudin-7, e.g., Leukocyte Infiltrate.

Different outcomes might result from applying more complex deep learning techniques, but they may require a larger database of patients, since less data may result in overfitting and thus unreliable results. However, classical statistical algorithms have once again proven their crucial role in this research field.

By contrast, from a statistical point of view, the study showed that immunohistochemical intensity overexpression of Claudin-7 in the tumor invasive front may represent a poor prognostic factor in the advanced stages of CRCs.

Chapter 3: Efficacy of growth factors for patients who received chemotherapy of non-small cell lung cancers and breast carcinoma

I.3.1. State of art

Neutropenia is a prevalent adverse effect observed in cancer patients undergoing myelosuppressive chemotherapy. Individuals who experience neutropenia are more susceptible to developing infections accompanied by fever (292). Febrile neutropenia (FN) frequently necessitates hospitalization and the administration of intravenous antibiotics. It may also lead to the need for adjustments or delays in chemotherapy doses and can result in mortality rates ranging from 8.0% to 14.3%, depending on the specific form of malignancy (293, 294).

Severe neutropenia is frequently observed during the early rounds of chemotherapy, and a longer persistence of neutropenia is correlated with a higher susceptibility to infection (295). The clinical objective of ensuring sufficient and effective prophylactic neutrophil support is crucial due to the varying prevalence of febrile neutropenia (FN) observed in different cancer types treated with regularly utilized chemotherapy regimens, which ranges from 5% to 44% (296).

The clinical efficacy of granulocyte colony-stimulating factor (G-CSF) products has been observed in patients who are at risk of developing neutropenia due to chemotherapy. These medicines stimulate the proliferation and enhance the activity of neutrophils, hence providing therapeutic benefits. Therefore, it is standard practice to advocate the regular use of G-CSF products as a preventive measure to maintain absolute neutrophil counts (ANC) in patients undergoing chemotherapy regimens with a risk of febrile neutropenia (FN) that is equal to or more than 20% (297).

Filgrastim is a recombinant formulation of granulocyte colony-stimulating factor (G-CSF) generated from Escherichia coli. It has a relatively brief elimination half-life (t1/2) and necessitates subcutaneous injections on a daily basis (298). The conjugation of a polyethylene glycol moiety to filgrastim, resulting in pegfilgrastim, serves to prolong its elimination half-life, so enabling administration once per treatment cycle.

Lipegfilgrastim, marketed as Lonquex by Teva Pharmaceuticals Ltd., is a recombinant form of human G-CSF that undergoes glycopegylation in a site-specific manner. This modification leads to enhanced structural uniformity and yields pharmacological characteristics that exhibit small variations compared to pegfilgrastim when administered to individuals without underlying health conditions. In a comparative analysis, it was observed

that lipegfilgrastim exhibited a prolonged elevation in ANC as compared to pegfilgrastim at a similar dosage, while not causing an escalation in peak ANC levels (299).

A novel approach was employed to create balugrastim (also known as Egranli [CG-10639]), a recombinant protein consisting of human serum albumin and human G-CSF. This technology, developed by Teva Pharmaceutical Industries in Netanya, Israel, involved the use of recombinant DNA technology in Saccharomyces cereviseae, as an alternative to pegylation (300). The inclusion of the albumin domain in balugrastim extends its duration in the bloodstream, resulting in a longer circulation half-life compared to granulocyte colony-stimulating factors (G-CSFs). This enables the administration of balugrastim through subcutaneous injection once per treatment cycle at a set dosage.

A recent phase III noninferiority assessed the effectiveness and safety of balugrastim at doses of 40 mg and 50 mg, in comparison to a 6 mg dose of pegfilgrastim for the prevention of neutropenia generated by chemotherapy, and demonstrated that once-per-cycle balugrastim is not inferior to pegfilgrastim in reducing cycle 1 DSN in breast cancer patients receiving chemotherapy; both drugs have comparable safety profiles (301).

Personal contributions:

1. **Volovat C,** Bondarenko I, Gladkov O, Buchner A, Lammerich A, Müller U, Bias P. Efficacy and safety of lipegfilgrastim compared with placebo in patients with non-small cell lung cancer receiving chemotherapy: post hoc analysis of elderly versus younger patients. Support Care Cancer. 2016 Dec;24(12):4913-4920. doi: 10.1007/s00520-016-3347-3. Epub 2016 Aug 8. PMID: 27501966.
2. **Volovat C**, Bondarenko IM, Gladkov OA, Elsässer R, Buchner A, Bias P, Müller U. Phase III, randomized, double-blind, placebo-controlled, multicenter study of lipegfilgrastim in patients with non-small cell lung cancer receiving myelosuppressive therapy. Springerplus. 2015 Jul 3;4:316. doi: 10.1186/s40064-015-1067-7. PMID: 26155455; PMCID: PMC4489970.
3. **Volovat C**, Gladkov OA, Bondarenko IM, Barash S, Buchner A, Bias P, Adar L, Avisar N. Efficacy and safety of balugrastim compared with pegfilgrastim in patients with breast cancer receiving chemotherapy. Clin Breast Cancer. 2014 Apr;14(2):101-8. doi: 10.1016/j.clbc.2013.10.001. Epub 2013 Oct 25. PMID: 24485296.

I.3.2. Efficacy and safety of lipegfilgrastim compared with placebo in patients with non-small cell lung cancer receiving chemotherapy: post hoc analysis of elderly versus younger patients

I.3.2.1. Introduction

According to estimates, individuals over 65 account for 60% of all malignancies, and as the population ages and life expectancy rises, there will be more old cancer patients (302) In the USA, older persons (those over 65) are likely to see a 67% increase in the incidence of all malignancies, and the proportion of all cancers diagnosed in senior adults is anticipated to rise from 61 to 70% by 2030 (303).

Patients receiving myelosuppressive chemotherapy for cancer may experience neutropenia or febrile neutropenia (FN) without prophylactic therapy, which is indicated when the patient has an absolute neutrophil count (ANC) of 0.5 109/L (grade 4 neutropenia) and fever, which is typically indicated by an oral body temperature of 38.3 or 38.0 °C for at least 1 h at the same time as the low ANC level (304, 305).

Neutropenia is a significant dose-limiting complication for many chemotherapy regimens, and increases the risk of serious or life-threatening infections. Patients over 65 are more likely than younger patients to have comorbid conditions and use more drugs, which puts them at a higher risk of developing myelosuppression and neutropenia, the duration of which may shorten survival. In addition, whether or whether they have neutropenia, elderly people are more susceptible to infections.

Recombinant G-CSFs (granulocyte colony-stimulating factors) encourage neutrophil proliferation and differentiation in myelosuppressive chemotherapy patients who are at risk for FN. Treatment recommendations call for G-CSFs as prophylactic to shorten the severity of severe neutropenia (DSN) in individuals with a 20% or lower chance of developing FN (306). G-CSFs have been demonstrated to lessen FN and other myelosuppressive chemotherapy-related toxicities in elderly adults (307).

The European Medicines Agency has licenced lipegfilgrastim, a glycoPEGylated G-CSF, for lowering the incidence of FN and the length of neutropenia in individuals receiving cytotoxic chemotherapy for cancer (apart from chronic myeloid leukaemia and myelodysplastic syndromes). Lipegfilgrastim's effectiveness and safety have been proven in clinical trials with patients who have non-small cell lung cancer (NSCLC) [12] and breast cancer (308). In a phase 3 trial involving NSCLC patients, there was no significant difference in the primary end point of FN incidence between lipegfilgrastim and placebo during cycle 1 (2.4% for lipegfilgrastim vs 5.6% for placebo; $p = 0.1151$); however, lipegfilgrastim was

associated with significant advantages in terms of severe neutropenia, including a lower incidence (41.4 vs 80.0%, respectively; p 0.0001).

All patients in this trial received cisplatin plus etoposide, an effective combination chemotherapy regimen for NSCLC known to produce only mild to moderate myelotoxicity and not necessarily requiring primary G-CSF prophylaxis in accordance with best practice guidelines (309).

This was done to provide an experimental setting that would ethically allow for a placebo control arm. By grouping patients by age (65 and >65 years), the following post hoc analysis sought to assess the efficacy and safety of lipegfilgrastim in an elderly subgroup from this phase 3 trial.

I.3.2.2. Materials and methods

This was an age-based, post hoc, subgroup analysis of patients who had participated in a phase 3 multicenter, multinational, double-blind, randomized, and placebo-controlled trial (controlled-trials.com identifier ISRCTN55761467). Full details of the study design and the primary results have been reported elsewhere (309). In brief, eligible patients were adults (aged ≥18 years) who were scheduled to receive 4 cycles of cisplatin/etoposide as first-line therapy for stage IIIb/IV NSCLC and had an Eastern Cooperative Oncology Group performance status ≤2, ANC of ≥1.5 × 109/L, platelet count ≥100 × 109/L, and adequate hepatic, renal, and cardiac function. Patients with an individual high risk of FN according to the assessment of the investigator (with consideration of risk factors such as age >65 years, low performance status, poor nutritional status, and liver, renal, or cardiovascular disease) were to be excluded from this placebo-controlled study because of ethical considerations. Within 6 months prior to randomization, patients must have had no exposure to G-CSF products (including filgrastim, pegfilgrastim, lenograstim, or investigational agents).

Patients were randomized 2:1 to receive a once-per-cycle single subcutaneous fixed dose injection of lipegfilgrastim 6 mg or placebo [12]. Patients received intravenous (IV) cisplatin 80 mg/m2 (over at least 1 h) on day 1 and IV etoposide 120 mg/m2 (over at least 1 h) on days 1 to 3 every 3 weeks, for a maximum of 4 cycles. Study medication was injected subcutaneously on day 4 of each chemotherapy cycle (approximately 24 h after the last chemotherapy infusion).

Prior to each subsequent cycle, patients were required to have an ANC of ≥1.5 × 109/L and a platelet count of ≥100 × 109/L, or the next cycle was to be postponed. Dose delays of up to 2 weeks were allowed, after which time patients were required to withdraw from the

study. Patients experiencing FN were to receive prophylactic open-label treatment with lipegfilgrastim during further chemotherapy cycles (irrespective of double-blind assignment) and were not to be withdrawn from the study unless deemed necessary by the investigator. Other G-CSF products were not allowed during study participation, and the randomized treatment was not to be unblinded in these patients with documented FN.

Safety was evaluated via assessment for adverse events (AEs) until 3 weeks after the last dose of study medication. Blood samples for hematology and clinical chemistry testing were obtained on day 15 of each cycle.

The primary efficacy end point was the incidence of FN in cycle 1 of cisplatin/etoposide chemotherapy; FN was defined as ANC <0.5 × 109/L with oral body temperature of >38.5 °C on ≥2 consecutive measurements ≥60 min apart, or neutropenic sepsis, or serious or life-threatening neutropenic infection. Severe neutropenia was defined as grade 4 neutropenia with ANC <0.5 × 109/L, and the time to ANC recovery was defined as the time from any post-chemotherapy day with ANC <2 × 109/L to the first day with ANC ≥2 × 109/L. Data were analyzed and are reported herein for the intent-to-treat (ITT) population, defined as all patients who were randomized at the baseline visit (including those with major protocol violations). P values of FN in the lipegfilgrastim 6 mg and placebo groups were calculated for patients ≤65 and >65 years of age. P values and estimates served an informational role only.

Independent ethics committees reviewed and approved the study protocol, and the study was conducted in accordance with the principles of the Declaration of Helsinki and the International Council for Harmonization Good Clinical Practice guidelines. Written informed consent was obtained from all patients before the start of any study-related procedures.

I.3.2.3. Results

Overall, 427 patients were screened at 72 centers in 8 European countries (Belarus, Bosnia-Herzegovina, Bulgaria, Poland, Romania, Russia, Serbia, and Ukraine). Of these, 376 (88.1 %) patients were randomized (1 randomized erroneously). The ITT population comprised 375 patients (n = 250 lipegfilgrastim; n = 125 placebo). A total of 57 patients (22.8 %) in the lipegfilgrastim group and 31 patients (24.8 %) in the placebo group were >65 years old. The safety population comprised 248 patients who had received lipegfilgrastim and 125 patients who had received placebo under double-blind conditions (309).

Patient demographics and baseline disease characteristics, as summarized in table III.1, were similar between the treatment groups for patients aged ≤65 years (n = 292) and >65 years (n = 83).

Over 80 % of patients were male in each treatment group and in each age group. In the overall patient population, 60.8 % of patients in each treatment group had stage IV NSCLC. In the group of patients >65 years old, 57 patients (68.7 %) were aged 66 to 70 years, 22 patients (26.5 %) were aged 71 to 75 years, and 4 patients (4.8 %) were aged >75 years.

Table III.1. Patient demographics and baseline characteristics (ITT population).

Variable	**≤65-year population**		**>65-year population**	
	Placebo n = 95	**Lipegfilgrastim n = 197**	**Placebo n = 30**	**Lipegfilgrastim n = 53**
Age				
Mean (SD), year	55.3 (6.7)	55.2 (6.9)	69.4 (2.9)	69.4 (2.8)
Sex, n (%)				
Female	15 (15.8)	24 (12.2)	5 (16.7)	6 (11.3)
Male	80 (84.2)	173 (87.8)	25 (83.3)	47 (88.7)
Weight				
Mean (SD), kg	70.7 (13.0)	70.2 (13.3)	69.5 (14.7)	64.6 (10.3)
≤60 kg, n (%)	24 (25.3)	49 (24.9)	10 (33.3)	21 (39.6)
>60–≤75 kg, n (%)	42 (44.2)	82 (41.6)	11 (36.7)	24 (45.3)
>75 kg, n (%)	29 (30.5)	66 (33.5)	9 (30.0)	8 (15.1)

NSCLC stage at enrollment				
Stage IIIB	31 (32.6)	75 (38.1)	18 (60.0)	22 (41.5)
Stage IV	64 (67.4)	122 (61.9)	12 (40.0)	30 (56.6)
Unknown	0	0	0	1 (1.9)
Time since diagnosis				
Mean (SD), months	2.8 (6.9)	2.2 (6.1)	5.4 (14.1)	2.8 (6.4)
ECOG performance status				
0	15 (15.8)	22 (11.2)	4 (13.3)	6 (11.3)
1	75 (78.9)	157 (79.7)	21 (70.0)	37 (69.8)
2	5 (5.3)	18 (9.1)	5 (16.7)	10 (18.9)
Reason for chemotherapy				
Adjuvant therapy	14 (14.7)	25 (12.7)	7 (23.3)	10 (18.9)
Metastatic disease	81 (85.3)	172 (87.3)	23 (76.7)	43 (81.1)
Lung cancer surgery				
No	73 (76.8)	170 (86.3)	25 (83.3)	45 (84.9)
Yes	22 (23.2)	27 (13.7)	5 (16.7)	8 (15.1)

Legend: ECOG Eastern Cooperative Oncology Group, ITT intent-to-treat, NSCLC non-small cell lung cancer, SD standard deviation.

In the overall ITT population, 250 patients (66.7 %) completed the study (169 [67.6 %] lipegfilgrastim patients; 81 [32.4 %] placebo patients). When stratified by age,

approximately half of the patients >65 years of age received all 4 chemotherapy cycles (Table III.2).

Dose delays were more frequent in the placebo group versus the lipegfilgrastim group in both age groups, but dose reductions and omissions were infrequent in both treatment groups, irrespective of age.

Table III.2. Chemotherapy cycles administered by treatment group.

Variable	**≤65-year population**		**>65-year population**	
	Placebo	Lipegfilgrastim	Placebo	Lipegfilgrastim
Patients completing chemotherapy cycles				
1	95	95 (100.0)	197	197 (100.0)
2	95	85 (89.5)	197	172 (87.3)
3	95	73 (76.8)	197	147 (74.6)
4	95	64 (67.4)	197	140 (71.1)
Patients with chemotherapy delays				
Cycle 2	85	54 (63.5)	172	49 (28.5)
Cycle 3	73	45 (61.6)	147	62 (42.2)
Cycle 4	64	46 (71.9)	140	61 (43.6)

Patients with chemotherapy dose reductions/omissions				
Cycle 2	85	0	172	2 (1.2)
Cycle 3	73	2 (2.7)	147	1 (0.7)
Cycle 4	64	1 (1.6)	140	4 (2.9)

Among patients aged ≤65 years, there was no difference in the incidence of FN during cycle 1 in the lipegfilgrastim group compared with the placebo group (3.0 vs 3.2 %, respectively; Table III.3).

Fewer patients aged >65 years receiving lipegfilgrastim 6 mg (0/53; 0 %) had FN during cycle 1 compared with placebo (4/30; 13.3 %) (Table III.3).

In patients aged ≤65 years, the incidence of severe neutropenia during cycle 1 was higher in the placebo group than in the lipegfilgrastim group (56.8 vs 27.6 %, respectively).

In patients aged >65 years, there was a smaller difference in the incidence of severe neutropenia during cycle 1 relative to that observed in patients aged ≤65 years: 66.7 % with placebo compared with 49.1 % with lipegfilgrastim.

In patients aged ≤65 years, the mean DSN during cycle 1 in the lipegfilgrastim group was 0.6 days compared with 2.1 days in the placebo group.

Similarly, in patients aged >65 years, mean DSN during cycle 1 in patients receiving lipegfilgrastim was shorter (1.0 days) than DSN in patients receiving placebo (3.0 days).

In patients aged ≤65 years, the mean time to ANC recovery during cycle 1 in the lipegfilgrastim group was 6.8 days compared with 13.3 days in the placebo group (Table III.3).

These findings were similar to those in patients aged >65 years, in whom time to ANC recovery during cycle 1 was shorter in those receiving lipegfilgrastim 6 mg (6.5 days) compared with those receiving placebo (12.2 days).

The mean depth of the ANC nadir during cycle 1 in the lipegfilgrastim group was higher (1.6 × 109/L) than that in the placebo group (0.7 × 109/L) in patients aged ≤65 years, as well as in patients aged >65 years (1.5 × 109/L and 0.5 × 109/L, respectively).

Table III.3. Efficacy outcomes (ITT population).

	≤65-year population								**>65-year population**							
	Placebo *n* = 95				**Lipegfilgrastim *n* = 197**				**Placebo *n* = 30**				**Lipegfilgrastim *n* = 53**			
Chemotherapy cycle	**1**	**2**	**3**	**4**	**1**	**2**	**3**	**4**	**1**	**2**	**3**	**4**	**1**	**2**	**3**	**4**
Incidence of febrile neutropenia, *n* (%)	3 (3.2)	0	1 (1.4)	2 (3.1)	6 (3.0)	0	0	2 (1.4)	4 (13.3)	0	0	0	0	1 (2.1)	1 (2.4)	0
Incidence of severe neutropenia, *n* (%)	54 (56.8)	40 (48.2)	34 (46.6)	35 (54.7)	54 (27.6)	22 (13.2)	19 (13.0)	24 (17.4)	20 (66.7)	15 (68.2)	13 (68.4)	10 (58.8)	26 (49.1)	14 (29.2)	7 (16.7)	1 (3.2)
Duration of severe neutropenia, mean (SD), days	2.1 (2.5)	2.0 (2.5)	1.8 (2.4)	2.0 (2.3)	0.6 (1.1)	0.2 (0.7)	0.3 (0.9)	0.4 (1.2)	3.0 (2.5)	3.0 (2.8)	2.8 (2.3)	3.2 (2.8)	1.0 (1.2)	0.6 (1.0)	0.6 (1.1)	0.5 (1.0)
Time to ANC recovery, mean (SD), days	13.3 (7.3)	14.2 (6.9)	13.6 (6.8)	13.9 (7.1)	6.8 (5.2)	5.4 (5.7)	5.8 (6.6)	5.1 (5.7)	12.2 (6.8)	12.1 (7.4)	14.1 (6.8)	14.0 (7.1)	6.5 (5.0)	6.3 (5.7)	6.6 (6.1)	6.3 (5.9)
Depth of ANC nadir, mean (SD) × 10^9/L	0.7 (0.9)	0.8 (0.9)	0.9 (1.0)	0.7 (1.0)	1.6 (1.6)	3.0 (2.9)	2.9 (2.7)	2.7 (2.6)	0.5 (0.7)	0.7 (0.9)	0.7 (1.0)	0.6 (0.8)	1.5 (1.8)	2.3 (2.5)	2.1 (2.0)	2.1 (2.0)

Legend: ANC absolute neutrophil count, ITT intent-to-treat, SD standard deviation.

The most common AEs are summarized in table III.4. Overall, the incidence of AEs was generally similar between lipegfilgrastim and placebo treatment groups in patients aged ≤65 years and those aged >65 years.

In both age groups, the most common AEs were alopecia, anemia, nausea, and neutropenia.

Comparing the elderly and younger lipegfilgrastim recipients, the percentage of patients experiencing any AE was generally higher for elderly patients than for younger patients.

Table III.4. Most frequent adverse events (occurring in ≥5 % of lipegfilgrastim recipients in any category)

	≤65-year population				**>65-year population**			
	Placebo *n* = 95		**Lipegfilgrastim *n* = 197**		**Placebo *n* = 30**		**Lipegfilgrastim *n* = 53**	
Adverse event	**n**	**%**	**n**	**%**	**n**	**%**	**n**	**%**
At least 1 event	81	85.3	164	84.1	25	83.3	46	86.8
Non-small cell lung cancer	3	3.2	12	6.2	1	3.3	4	7.5
Anemia	24	25.3	47	24.1	6	20.0	16	30.2
Leukopenia	12	12.6	8	4.1	2	6.7	8	15.1
Neutropenia	36	37.9	37	19.0	8	26.7	14	26.4
Thrombocytopenia	7	7.4	23	11.8	3	10.0	9	17.0
Decreased appetite	10	10.5	14	7.2	2	6.7	9	17.0
Hypokalemia	2	2.1	12	6.2	1	3.3	8	15.1
Hypophosphatemia	1	1.1	7	3.6	1	3.3	5	9.4
Dyspnea	6	6.3	7	3.6	3	10.0	4	7.5
Pulmonary embolism	0	0	2	1.0	2	6.7	1	1.9
Diarrhea	3	3.2	3	1.5	1	3.3	4	7.5

Nausea	19	20.0	46	23.6	8	26.7	13	24.5
Vomiting	11	11.6	17	8.7	4	13.3	11	20.8
Alopecia	35	36.8	78	40.0	7	23.3	23	43.4
Asthenia	14	14.7	18	9.2	9	30.0	10	18.9
Chest pain	6	6.3	12	6.2	2	6.7	2	3.8
Disease progression	4	4.2	14	7.2	1	3.3	2	3.8
Fatigue	5	5.3	10	5.1	1	3.3	6	11.3
Pyrexia	4	4.2	12	6.2	2	6.7	0	0
Weight decreased	2	2.1	7	3.6	0	0	5	9.4

I.3.2.4. Discussions

A post hoc analysis was conducted in elderly patients with NSCLC who participated in a phase 3 trial of lipegfilgrastim, a once-per-cycle glycoPEGylated G-CSF. Patients with a high individual risk of FN were excluded.

For this reason, unlike a typical NSCLC population, >75 % of the population was aged ≤65 years, and the overall incidence of FN in the ITT population was low (309).

In previously published studies of patients with lung cancer receiving a similar chemotherapy regimen, in which use of G-CSF was left to investigator discretion, a higher incidence of FN was reported (range of 10.4 to 13 %) relative to that observed in our study.

However, it is likely that a less restrictive definition of FN was used in these studies (thereby leading to higher incidences of FN), as they were designed to assess the relative efficacy and safety of two different combination chemotherapy regimens rather than the effectiveness of G-CSF prophylaxis (310-312).

Moreover, in the present placebo-controlled study, it was necessary to exclude patients at high risk for FN due to ethical concerns, which was not the case in these previously published studies.

In the subset of patients aged >65 years, there was a difference in the incidence of FN in cycle 1 for patients receiving lipegfilgrastim (0 %) versus placebo (13.3 %), which was not observed in the younger subgroup or in the overall study populations (as published previously).

Although this difference in the incidence of FN was not statistically significant, it is notable considering the small number of patients in the elderly subgroup.

The differences in patient demographics and baseline characteristics between the lipegfilgrastim and placebo groups within the >65-year population (e.g., 47/53 [89 %] vs 25/30 [83 %] male and mean time since diagnosis of 2.8 vs 5.4 months) are unlikely to have caused or contributed to the difference in neutropenia and febrile neutropenia between these groups.

The 13.3 % incidence of FN in the elderly subset of patients in the placebo group is in line with earlier published studies in which the same cisplatin/etoposide chemotherapy regimen, with or without G-CSF support, was used at similar dosages to the current study and patients at high risk for FN were not excluded, suggesting minimal treatment differences in the elderly versus overall populations (310-312).

Data for the other efficacy outcomes reported here were similar between age groups, except that lipegfilgrastim appeared to exert a greater effect in reducing the incidence of severe neutropenia in non-elderly versus elderly patients.

However, the ability of lipegfilgrastim to reduce DSN was evident in both groups, persisting for no more than 1 day with lipegfilgrastim versus 2 to 3 days with placebo (consistent with the observed DSN data for the overall population).

Data for DSN are not available for the aforementioned published studies of cisplatin/etoposide, but one of the studies reported FN requiring hospitalization for a median of 6 days with a range of 4 to 24 days.

In clinical practice, the ability to reduce the duration of neutropenic events would be expected to have a positive effect on both treatment delivery, in terms of maintaining dose intensity and scheduled treatment intervals, and cost of care (313).

Of note, in the placebo group, more delays for each cycle were to be expected and were indeed observed, due to neutropenia and febrile neutropenia developed during the previous cycle.

In both age groups, lipegfilgrastim was well tolerated, with a safety profile similar to that in patients receiving placebo. The most common AEs were consistent with the known toxicity profile of platinum-based chemotherapy. The most notable differences between

lipegfilgrastim and placebo were in the incidences of hypokalemia and hypophosphatemia, which were higher among lipegfilgrastim recipients in both age groups and were more frequent in the elderly versus younger patients.

The percentage of patients experiencing any AE was generally higher for elderly patients than for younger patients, which would be expected, considering that elderly patients are more likely to have comorbidities and be taking more medications than younger patients.

Limitations of this analysis and the interpretation of the results stem from the shortcomings that are inherent in post hoc subgroup analyses, including the reduced sample sizes when analyzing subgroups based on age or other characteristics.

I.3.2.5. Conclusions

In this placebo-controlled study, patients with an individual high risk of FN as assessed by the investigator were to be excluded because of ethical considerations. Therefore, it is not surprising that in the overall study population, the difference in FN incidence during cycle 1 versus placebo was not different.

In the elderly subpopulation, which has a higher risk of developing myelosuppression and neutropenia, the FN incidence in cycle 1 in the placebo group (13.3 %) was in the range expected based on previously published studies (314).

The efficacy of lipegfilgrastim was demonstrated in this subpopulation (FN incidence of 0 %), which is more representative of the typical at-risk population scheduled to receive primary G-CSF prophylaxis.

In patients with a higher risk, such as the elderly patients in this study, lipegfilgrastim reduced not only the duration of severe neutropenia but also the incidence of FN.

However, due to the small number of patients in this elderly subpopulation, additional prospective studies that evaluate the clinical benefits of lipegfilgrastim in the elderly population with NSCLC, as well as benefits such as greater response, longer progression-free intervals, fewer hospitalizations, and reduced overall medical costs, are warranted.

I.3.3. Phase III, randomized, double-blind, placebo-controlled, multicenter study of lipegfilgrastim in patients with non-small cell lung cancer receiving myelosuppressive therapy

I.3.3.1. Introduction

Neutropenia is a major dose-limiting toxicity in many myelosuppressive chemotherapy regimens (304, 315).

A patient's risk of developing neutropenia or febrile neutropenia (FN) depends on several factors, including the type of cancer, chemotherapy regimen (standard-dose, dose-dense, or high-dose therapy), and patient-related and disease-related factors, such as age and comorbidities (304).

Recombinant granulocyte colony-stimulating factors (G-CSFs) promote the proliferation and differentiation of neutrophils, alleviating the severity of chemotherapy-induced neutropenia and FN (316). These agents are well established as primary prophylaxis for FN and are recommended in European and US guidelines for chemotherapy patients at high (≥20%) risk of FN (295, 304-306).

Filgrastim, the first recombinant human G-CSF, requires daily subcutaneous (SC) injections (Neupogen, 2013). With the attachment of polyethylene glycol (PEG) to the G-CSF molecule, the half-life of pegfilgrastim was extended compared with filgrastim, allowing once-per-chemotherapy cycle administration (Neulasta, 2012).

Lipegfilgrastim is a glycoPEGylated, once-per-cycle recombinant human G-CSF expressed in Escherichia coli. It is approved by the European Medicines Agency for reducing the duration of neutropenia and the incidence of FN in adults treated with cytotoxic chemotherapy for malignancy (with the exception of chronic myeloid leukemia and myelodysplastic syndromes) (Lonquex, 2013).

A recent phase III trial (controlled-trials.com identifier ISRCTN56891934) demonstrated the clinical efficacy of lipegfilgrastim to be noninferior to pegfilgrastim in reducing neutropenia in breast cancer patients receiving myelosuppressive chemotherapy (317).

This trial was conducted to demonstrate superiority of once-per-cycle lipegfilgrastim versus placebo in patients with stage IIIb/IV non-small cell lung cancer (NSCLC) receiving up to four cycles of cisplatin and etoposide chemotherapy. Evaluations of efficacy, tolerability, and pharmacokinetic properties were secondary assessments.

I.3.3.2. Materials and methods

This phase III, multinational, multicenter, double-blind, randomized, placebo-controlled study (controlled-trials.com identifier ISRCTN55761467) was designed to demonstrate superiority of a fixed 6-mg dose of lipegfilgrastim (XM22, Lonquex; Teva Pharmaceuticals Ltd, Petach Tikva, Israel) versus placebo in patients with NSCLC. The study was conducted in eight European countries (Belarus, Bosnia-Herzegovina, Bulgaria, Poland, Romania, Russia, Serbia, Ukraine) and included four phases: screening and randomization, double-blind treatment (chemotherapy cycles 1–4), end-of-study (or withdrawal) visit, and antibody follow-up. The study design followed the European Medicines Agency's guidelines for a confirmatory study (EMEA 2007). Everyone involved in the conduct of the study was blinded to study medications.

Eligible patients were men and women aged ≥18 years of any ethnic origin with a diagnosis of stage IIIb/IV NSCLC, documented histologically or cytologically, and a life expectancy of at least 4 months.

Patients had to be chemotherapy naive, eligible to receive four cycles of cisplatin and etoposide as myelosuppressive chemotherapy (i.e., baseline ANC ≥1.5 × 109/L and platelets ≥100 × 109/L), have an ECOG PS ≤2, and have adequate hepatic, cardiac, and renal function. Women of childbearing potential had to use an effective method of contraception.

Because this was a placebo-controlled study, patients with an individual high risk of developing FN (i.e., ≥20%) with regard to the cisplatin and etoposide chemotherapy were excluded from the study. Potential individual high-risk factors were patient age >65 years, low ECOG PS, poor nutritional status, and liver, kidney, or cardiovascular disease.

Risk factors were considered together to determine a patient's risk of developing FN, and therefore having only one risk factor did not automatically result in exclusion from the study. Other exclusion criteria included previous exposure to any G-CSF within 6 months before randomization, treatment with systemically active antibiotics within 72 h before chemotherapy, chronic use of oral corticosteroids, prior radiation therapy within 4 weeks of randomization, prior bone marrow or stem cell transplantation, or concomitant malignancy (other than in situ melanoma, skin cancer, or cervical carcinoma) within the preceding 5 years. Women who were pregnant or breastfeeding were excluded.

All patients received chemotherapy with cisplatin and etoposide and were randomized (2:1) to receive lipegfilgrastim or placebo. Randomization was performed by Biostatistics Merckle GmbH through an interactive voice response system, using a block size of 2 and

stratified by country. Patients received up to four 21-day chemotherapy cycles. On day 1 of each cycle, patients received cisplatin 80 mg/m2 intravenously (IV), with etoposide 120 mg/m2 IV administered on days 1, 2, and 3. Patients had to have an ANC ≥1.5 × 109/L and platelet count of ≥100 × 109/L to begin the next full-dose cycle. A dose delay of up to 2 weeks was acceptable.

Absolute neutrophil counts were determined at local or regional laboratories rather than a central laboratory, for logistical reasons; all other laboratory measures were determined by two central laboratories. In addition, the patient's overall condition had to allow further chemotherapy treatment as determined by the treating investigator. Generally, any chemotherapy-related toxicity had to have resolved to at least grade 1 toxicity prior to continuation of chemotherapy.

Patients received one dose of lipegfilgrastim 6 mg or placebo SC on day 4 of each chemotherapy cycle, approximately 24 h after the last chemotherapy infusion and after blood sampling to determine ANC and body temperature. The lipegfilgrastim 6-mg dose was chosen based on findings from a phase II dose-finding study in breast cancer patients that demonstrated neutrophil support that was at least equivalent to the standard 6.0-mg fixed dose of pegfilgrastim. Patients who developed FN in any cycle were not discontinued except by investigator decision; instead, they received open-label prophylactic treatment with lipegfilgrastim in subsequent cycles, regardless of treatment group.

The primary efficacy measure was the incidence of FN in cycle 1. Febrile neutropenia was defined as an oral body temperature >38.5°C for at least 1 h (two consecutive same-day measurements, ≥60 min apart) with severe neutropenia (ANC <0.5 × 109/L) on the day before, same day, or day after the elevated temperature readings; neutropenic sepsis (sepsis with ANC <0.5 × 109/L); or serious or life-threatening neutropenic infection (infection with ANC <0.5 × 109/L).

Secondary efficacy measures included the incidence of FN in cycles 2, 3, and 4 and across all cycles; incidence and DSN (defined as grade 4 neutropenia with ANC <0.5 × 109/L); incidence and duration of very severe neutropenia (ANC <0.1 × 109/L); depth of ANC nadir (lowest ANC in each cycle); time to ANC nadir (defined as time from chemotherapy administration until occurrence of ANC nadir); time to ANC recovery (defined as time from chemotherapy administration until ANC increased to ≥2.0 × 109/L after nadir); and time to ANC recovery from ANC nadir (defined as the difference in days between day of ANC nadir to first day with ANC ≥1.5 × 109/L).

Blood samples to determine ANC were obtained daily until day 15, or longer, of each cycle, until ANC ≥2.0 × 109/L was reached. A blood sample was taken on day 4 of each cycle, before administration of study medication. Body temperature was measured orally at least twice daily (morning and evening) until day 15, or longer, of each cycle, until ANC ≥2.0 × 109/L was reached.

Other secondary efficacy measures, including hospitalizations, use of IV antibiotics, delivered versus scheduled chemotherapy, chemotherapy dose modifications (reductions, omissions, delays), quality of life, and the incidence of patients requiring prophylactic open-label treatment, as well as pharmacokinetic properties were assessed but are not reported here.

Safety was assessed using reported treatment-emergent AEs data, including intercurrent illnesses and clinically abnormal laboratory values; AEs were recorded until 3 weeks after the last injection of study medication. Adverse events were summarized by seriousness, severity, and investigator-assessed relationship to study medication.

A serious AE was one that was life-threatening or resulted in death, required hospitalization or prolongation of hospitalization, or resulted in a persistent or significant disability or incapacity that required medical or surgical intervention. Investigators assessed AEs as probably, possibly, unlikely, or not related to the study medication or chemotherapy regimen, or as not classifiable. For laboratory values, all AEs of grade 3 and higher were documented.

The AEs were assessed on days 1 and 7 of each chemotherapy cycle. Safety samples (hematology and clinical chemistry) were taken on day 15. Other safety assessments, including physical examination and vital signs, were performed within 24 h before chemotherapy administration on day 1 and on days 7 and 15 of each chemotherapy cycle.

The planned sample size was 375 patients from approximately 90 centers in nine countries, based on the assumption that the incidence of FN would be in the range of 7% to 10% in the placebo group and, at most, 1% in the lipegfilgrastim group.

For a statistical test with a two-sided significance level α of 5%, a required power of at least 80%, and a sampling rate of 2:1 (lipegfilgrastim: placebo), sample size requirements were 250 patients in the lipegfilgrastim group and 125 patients in the placebo group. As the actual incidence of FN in the placebo group was expected to be closer to 10%, a power of at least 90% was expected.

For the primary efficacy measure (incidence of FN in cycle 1), a 95% CI for the OR (placebo/lipegfilgrastim) was calculated to assess the relative efficacy of lipegfilgrastim

versus placebo. For secondary efficacy measures, no adjustment for Type I error was applied, so all secondary analyses should be interpreted as exploratory.

When applicable, for secondary efficacy measures for which regression analyses were planned, statistical models with the same explanatory variables as in the analysis of the primary measures were estimated.

Demographic and baseline characteristics, AEs, and other safety assessments were presented as descriptive statistics (continuous variables) or frequency tables (categorical variables).

The intent-to-treat population, which included all patients randomized at baseline, was also the efficacy population. The safety population included all randomized patients who received at least one dose or partial dose of study medication.

I.3.3.3. Results

The study was conducted between May 2010 and April 2011 at 72 centers in eight countries. In total, 427 patients were screened and 376 were randomized (Belarus, n = 34; Bosnia-Herzegovina, n = 2; Bulgaria, n = 16; Poland, n = 4; Romania, n = 25; Russia, n = 160; Serbia, n = 20; Ukraine, n = 115). One patient in the lipegfilgrastim group who was randomized in error and received no chemotherapy or study medication was excluded from the efficacy and safety analyses.

Thus, 250 patients in the lipegfilgrastim group and 125 in the placebo group were included in the intent-to-treat population (Figure III.1). Of these, 169 (67.6%) patients in the lipegfilgrastim and 81 (64.8%) in the placebo group completed treatment.

Two patients in the lipegfilgrastim group who died after randomization but did not receive study medication were included in the efficacy but not safety analyses.

Baseline demographics and clinical characteristics were similar between treatment groups (Table III.5). Most patients were men, had stage IV NSCLC, an Eastern Cooperative Oncology Group Performance Status (ECOG PS) of 1, and were receiving chemotherapy for metastatic disease.

The mean age was similar in both groups and was somewhat younger than is typically seen for patients with lung cancer. However, this was expected as one of the risk factors that would have contributed to the exclusion of patients at individual high risk for FN was age >65 years, leading to a relatively low percentage of patients aged >65 years (23.5%) being enrolled.

Table III.5. Patient demographics and baseline characteristics (intent-to-treat population).

Characteristic	**Placebo (*n* = 125)**	**Lipegfilgrastim 6 mg SC (*n* = 250)**
Age, years		
Mean ± SD	58.7 ± 8.5	58.2 ± 8.5
≤64, *n* (%)	94 (75.2)	193 (77.2)
65–74, *n* (%)	29 (23.2)	54 (21.6)
≥75, *n* (%)	2 (1.6)	3 (1.2)
Weight, kg		
Mean ± SD	70.4 ± 13.4	69.0 ± 12.9
≤60, *n* (%)	34 (27.2)	70 (28.0)
>60 to ≤75, *n* (%)	53 (42.4)	106 (42.4)
>75, *n* (%)	38 (30.4)	74 (29.6)
Sex, n (%)		
Female	20 (16.0)	30 (12.0)
Male	105 (84.0)	220 (88.0)
Region, *n* (%)		
Russia	54 (43.2)	106 (42.4)
Ukraine	38 (30.4)	77 (30.8)
Rest of Europe	33 (26.4)	67 (26.8)
NSCLC stage at enrolment, *n* (%)		
Stage IIIB	49 (39.2)	97 (38.8)
Stage IV	76 (60.8)	152 (60.8)
Unknown	0 (0)	1 (0.4)
Time since diagnosis, months		
Mean ± SD	3.4 ± 9.1	2.4 ± 6.2
Median (range)	1.0 (0–58.0)	1.0 (0–52.0)
ECOG PS, *n* (%)		
0	19 (15.2)	28 (11.2)
1	96 (76.8)	194 (77.6)
2	10 (8.0)	28 (11.2)
Reason for chemotherapy, *n* (%)		
Adjuvant therapy	21 (16.8)	35 (14.0)

Characteristic	Placebo (*n* = 125)	Lipegfilgrastim 6 mg SC (*n* = 250)
Treatment for metastatic disease	104 (83.2)	215 (86.0)
Lung cancer surgery		
No	98 (78.4)	215 (86.0)
Yes	27 (21.6)	35 (14.0)

Legend: ECOG PS Eastern Cooperative Oncology Group Performance Status, NSCLC non-small cell lung cancer, SC subcutaneously, SD standard deviation.

Most patients in both treatment groups received their planned chemotherapy dose in each cycle; ≤3.3% of patients receiving placebo and ≤2.3% of those receiving lipegfilgrastim had a dose reduction or omission. The total number of administered doses for both cisplatin and etoposide was similar between treatment groups (data not shown). The proportion of patients with chemotherapy dose delays was significantly lower in patients treated with lipegfilgrastim than in those receiving placebo (cycle 2, 28.5 vs. 65.1%; cycle 3, 42.1 vs. 66.3%; and cycle 4, 40.4 vs. 75.3%, respectively; all $p \leq 0.0001$). The mean duration of chemotherapy delay across all cycles also was shorter for patients receiving lipegfilgrastim (6.4 ± 7.6 days) versus those receiving placebo (12.8 ± 10.2 days).

The primary efficacy measure, incidence of FN in cycle 1, was lower in the lipegfilgrastim group compared with the placebo group (Table III.6), but the difference was not significant. Thus, the study failed to achieve its primary objective of demonstrating superiority of lipegfilgrastim versus placebo in these patients.

Table III.6. Febrile neutropenia in cycles 1, 2, 3, and 4 (intent-to-treat population).

Cycle	Placebo			Lipegfilgrastim 6 mg SC			Lipegfilgrastim 6 mg SC vs. placebo		
	N	FN	%	*N*	FN	%	OR	95% CI	*P* value*
1	125	7	5.6	250	6	2.4	0.390	0.121–1.260	0.1151
2	105	0	0	214	1	0.5	NE	NE	0.9551
3	92	1	1.1	188	1	0.5	0.642	0.234–1.762	0.3883
4	81	2	2.5	171	2	1.2	0.421	0.119–1.489	0.1787

Legend: CI confidence interval, FN febrile neutropenia, NE not evaluable, OR odds ratio, SC subcutaneously.

Seven investigator-assessed cases of FN were observed during cycles 2, 3, and 4 (Table III.6), but no significant differences in the incidence of FN between treatment groups were observed ($p > 0.05$). None of the patients switched to open-label lipegfilgrastim experienced FN during chemotherapy cycles 2, 3, and 4.

Patients receiving lipegfilgrastim experienced a significantly shorter duration of severe neutropenia (DSN) in cycle 1 compared with patients receiving placebo ($p < 0.0001$; Table III.7). Similarly, the DSN in cycles 2, 3, and 4 was consistently and significantly shorter in the lipegfilgrastim group compared with the placebo group ($p < 0.0001$, all cycles).

The incidence of severe neutropenia was significantly lower in the lipegfilgrastim group versus the placebo group overall ($p < 0.0001$) and in each cycle ($p < 0.0001$, each cycle; Table III.8). Notably, in cycles 2, 3, and 4, approximately 80% of patients in the lipegfilgrastim group experienced no severe neutropenia compared with approximately 40% in the placebo group.

Table III.7. Incidence of severe and very severe neutropenia in cycles 1, 2, 3, and 4 (ITT population)

Cycle	**Duration of severe neutropenia (days)**	**Placebo**	**Lipegfilgrastim 6 mg SC**
1	*N*	125	250
	Mean ± SD	2.3 ± 2.5	0.6 ± 1.1
	Median (range)	2.0 (0–11.0)	0 (0–5.0)
	LSM*	−1.661	
	95% CI*	−2.089 to −1.232	
	P value*	<0.0001	
2	*N*	122	244
	Mean ± SD	2.2 ± 2.6	0.3 ± 0.7
	Median (range)	1.0 (0–11.0)	0 (0–4.0)
	LSM*	−1.915	
	95% CI*	−2.317 to −1.512	
	P value*	<0.0001	
3	*N*	122	245
	Mean ± SD	2.0 ± 2.4	0.4 ± 0.9
	Median (range)	1.0 (0–11.0)	0 (0–5.0)
	LSM*	−1.640	
	95% CI*	−2.053 to −1.227	
	P value*	<0.0001	
4	*N*	123	246
	Mean ± SD	2.3 ± 2.5	0.5 ± 1.1
	Median (range)	1.0 (0–11.0)	0 (0–0.8)

Cycle	Duration of severe neutropenia (days)	Placebo	Lipegfilgrastim 6 mg SC
	LSM*	−1.844	
	95% CI*	−2.281 to −1.407	
	P value*	<0.0001	

Legend: CI confidence interval, ITT intent to treat, LSM least squares mean, SC subcutaneously, SD standard deviation.

Table III.8. Pregnancy outcomes for the two groups of patients included in the study.

Cycle	Placebo			Lipegfilgrastim 6 mg SC			Lipegfilgrastim 6 mg SC vs. placebo		
	N	***n***	**%**	***N***	***n***	**%**	**Odds ratio**	**95% CI**	***P* value***
Severe neutropenia (grade 4, ANC <0.5 × 10^9/L)									
1	125	74	59.2	249	80	32.1	0.325	0.206–0.512	<0.0001
2	105	55	52.4	215	36	16.7	0.156	0.086–0.282	<0.0001
3	92	47	51.1	188	26	13.8	0.115	0.057–0.229	<0.0001
4	81	45	55.6	169	25	14.8	0.121	0.062–0.238	<0.0001
All	125	100	80.0	249	103	41.4	0.176	0.105–0.294	<0.0001
Very severe neutropenia (ANC <0.1 × 10^9/L)									
1	125	18	14.4	249	27	10.8	0.700	0.365–1.342	NS
2	105	10	9.5	215	8	3.7	0.298	0.099–0.895	0.031
3	92	9	9.8	188	9	4.8	0.421	0.156–1.138	NS
4	81	11	13.6	169	8	4.7	0.260	0.098–0.687	0.007
All	125	33	26.4	249	40	16.1	0.516	0.300–0.888	0.017

Legend: ANC absolute neutrophil count, CI confidence interval, ITT intent to treat, NS not significant, SC subcutaneously.

Patients treated with lipegfilgrastim experienced a shorter mean duration of very severe neutropenia [absolute neutrophil count (ANC) <0.1 × 109/L] versus patients receiving placebo in cycle 1: 0.3 ± 0.9 days versus 0.2 ± 0.6 days for lipegfilgrastim and placebo, respectively.

The mean duration of very severe neutropenia was also shorter for patients in the lipegfilgrastim group compared with the placebo group in cycles 2, 3, and 4.

Patients receiving lipegfilgrastim had a significantly lower incidence of very severe neutropenia over all cycles versus those receiving placebo ($p = 0.017$).

Differences between groups also were significant in cycles 2 ($p = 0.031$) and 4 ($p = 0.007$), with the lipegfilgrastim group having a lower incidence (Table III.8).

The time course of median ANC during cycle 1 is shown in Figure III.1. The mean depth of the ANC nadir in both treatment groups was lowest in cycle 1, but was significantly higher in patients treated with lipegfilgrastim ($1.6 \pm 1.6 \times 109/L$) versus patients receiving placebo ($0.7 \pm 0.9 \times 109/L$); $p < 0.0001$).

In cycles 2, 3, and 4, the mean ANC nadir was greater than $2.5 \times 109/L$ for the lipegfilgrastim group, but remained below $1.0 \times 109/L$ for the placebo group (mean 2.8 vs. 0.8, 2.8 vs. 0.8, and 2.6 vs. $0.7 \times 109/L$, respectively; $p < 0.0001$ in each case).

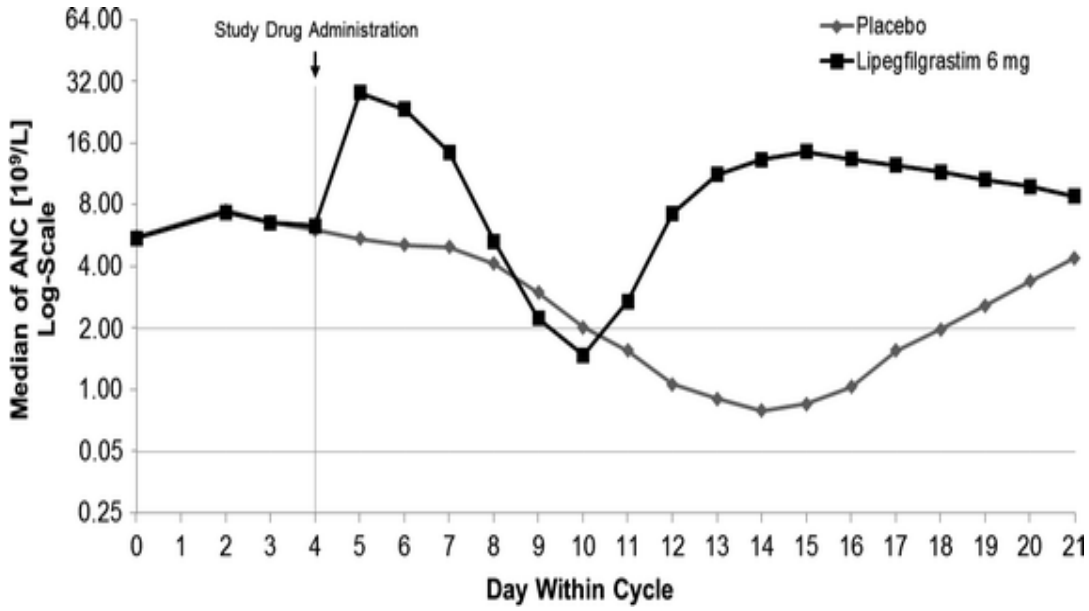

Figure III.1. Time course of measured median absolute neutrophil count in cycle 1 (intent-to-treat population). ANC absolute neutrophil count.

The mean time to ANC nadir was consistently shorter in the lipegfilgrastim group compared with the placebo group in each cycle (cycle 1: 8.2 vs. 13.7; cycle 2: 9.6 vs. 13.6; cycle 3: 9.8 vs. 13.6; cycle 4: 9.6 vs. 14.2 days).

In addition, the mean time to ANC recovery from ANC nadir was significantly shorter in the lipegfilgrastim versus placebo group in each cycle (cycle 1: 1.1 vs. 2.7; cycle 2: 0.6 vs. 2.6; cycle 3: 0.8 vs. 2.3; cycle 4: 0.7 vs. 2.6 days; $p < 0.0001$ between groups in each cycle).

Patients treated with lipegfilgrastim also experienced a significantly shorter mean time to ANC recovery after chemotherapy in each chemotherapy cycle compared with patients receiving placebo (cycle 1: 6.8 vs. 13.0; cycle 2: 5.6 vs. 13.8; cycle 3: 6.0 vs. 13.7; cycle 4: 5.4 vs. 14.0 days, respectively; $p < 0.0001$ between groups in each cycle).

During the double-blind phase, 171 (69.0%) patients in the lipegfilgrastim group and 81 (64.8%) in the placebo group received four doses of study medication. The mean total amount of study medication administered was 19.9 ± 6.7 mg and 19.3 ± 7.0 mg in the lipegfilgrastim and placebo groups, respectively.

Adverse events (AEs) were similar between treatment groups. The most common AEs (total incidence of ≥10% in either treatment group) in the lipegfilgrastim and placebo groups were alopecia (40.7 and 33.6%), anemia (25.4 and 24.0%), nausea (23.8 and 21.6%), neutropenia (20.6 and 35.2%), thrombocytopenia (12.9 and 8.0%), asthenia (11.3 and 18.4%), vomiting (11.3 and 12.0%), and leukopenia (6.5 and 11.2%), respectively (Table III.9). In total, 57 (23.0%) patients in the lipegfilgrastim group and 33 (26.4%) patients in the placebo group experienced an AE that led to discontinuation from the study.

Table III.9. Most frequent TEAEs (≥5% of patients) in either treatment group across all cycles (safety population).

AE by preferred term	**Placebo (*N* = 125)**		**Lipegfilgrastim 6 mg SC (*N* = 248)**	
	n	***%***	***n***	***%***
Alopecia	42	33.6	101	40.7
Anemia	30	24.0	63	25.4
Nausea	27	21.6	59	23.8
Neutropenia	44	35.2	51	20.6
Thrombocytopenia	10	8.0	32	12.9
Asthenia	23	18.4	28	11.3
Vomiting	15	12.0	28	11.3
Decreased appetite	12	9.6	23	9.3
Hypokalemia	3	2.4	20	8.1
Leukopenia	14	11.2	16	6.5
Fatigue	6	4.8	16	6.5
Disease progression	5	4.0	16	6.5
NSCLC	4	3.2	16	6.5

AE by preferred term	Placebo (*N* = 125)		Lipegfilgrastim 6 mg SC (*N* = 248)	
	n	***%***	***n***	***%***
Chest pain	8	6.4	14	5.6
Febrile neutropenia	10	8.0	11	4.4
Dyspnea	9	7.2	11	4.4

Legend: AE adverse event, NSCLC non-small cell lung cancer, SC subcutaneously, TEAEs treatment-emergent adverse events.

Bone-pain-related symptoms (defined as arthralgia, back pain, bone pain, myalgia, noncardiac chest pain, and pain in extremity) were reported in 21 (8.5%) patients treated with lipegfilgrastim and 8 (6.4%) patients receiving placebo. These events were generally mild or moderate in severity and led to study discontinuation in only two patients (both receiving placebo).

Serious AEs in the lipegfilgrastim and placebo groups included anemia (3.2 and 1.6%), NSCLC (3.2 and 0.8%), disease progression (2.4 and 0%), FN (2.0 and 4.0%), neutropenia (1.6 and 0.8%), pulmonary embolism (1.2 and 1.6%), cardio-respiratory arrest (1.2% and 0), thrombocytopenia (1.2% and 0), pneumonia (0.8 and 2.4%), pulmonary hemorrhage (0.8% and 0), renal failure (0.8% and 0), and sudden death (0.8% and 0), respectively.

A total of 31 (12.5%) patients treated with lipegfilgrastim and nine (7.2%) patients receiving placebo died during the course of the study or up to 30 days after the last study drug injection.

General disorders and administration site conditions accounted for eight deaths in the lipegfilgrastim group and two in the placebo group; benign, malignant, and unspecified neoplasms for eight in the lipegfilgrastim group and two in the placebo group; respiratory, thoracic, and mediastinal disorders for five in the lipegfilgrastim group and three in the placebo group; cardiac disorders for four in the lipegfilgrastim group and one in the placebo group; vascular disorders for two in the lipegfilgrastim group; renal and urinary disorders for two in the lipegfilgrastim group; nervous system disorders for one in the lipegfilgrastim group and one in the placebo group; and metabolism and nutrition disorders for one in the lipegfilgrastim group.

Changes over time in laboratory assessments were consistent with the underlying disease and with the chemotherapy treatment received and, in the lipegfilgrastim group, with G-CSF therapy.

I.3.3.4. Discussions and conclusions

In this study, patients with NSCLC and a low individual risk of FN who received lipegfilgrastim had a lower incidence of FN during cycle 1 (2.4%) compared with patients receiving placebo (5.6%). The incidence of FN was in line with previously published results for pegfilgrastim (318). Because the difference between treatment groups was not statistically significant, the study did not achieve its primary efficacy measure of demonstrating the superiority of lipegfilgrastim versus placebo. Nevertheless, the reduction in the incidence of FN in cycle 1 of >50% in the lipegfilgrastim group versus the placebo group is clinically important, particularly when considering the potential serious effects of FN on the overall health of patients.

The actual incidence of FN was lower than anticipated for the placebo group and higher than anticipated for the lipegfilgrastim group, affecting the statistical power of the study. The use of prophylactic G-CSFs is not recommended by treatment guidelines unless a patient's risk for developing FN is high (≥20%); however, the current study used chemotherapy with a reported incidence of FN <20% and excluded patients with an individual high risk of developing FN (≥20% risk). Thus, the use of prophylactic G-CSF therapy in this study was experimental in nature and provides additional evidence for the recommendation that prophylactic G-CSFs should not be used in patients with a risk of FN <20% (295, 304-306).

The use of cisplatin and etoposide, along with the strict definition of FN, may have contributed to the overall rate of FN being lower than the rate reported for patients receiving placebo in previously published lung cancer studies using the same chemotherapy regimen (311, 312, 319, 320).

In particular, excluding patients thought to be at high risk for FN led to a relatively low percentage of patients aged ≥65 years (24.8%). In a similar study of patients with NSCLC receiving myelosuppressive chemotherapy and adjuvant filgrastim therapy or placebo, 41.1% of all patients were aged ≥65 years. Of these patients, 71 and 43% experienced FN in the placebo and filgrastim groups, respectively (321).

The study design and statistical assumptions of this phase III trial may have contributed to not achieving the primary measure of demonstrating superiority to placebo in the incidence of FN in cycle 1. The existence of effective G-CSF supportive care and the uniformity of treatment guidelines for the use of G-CSFs in patients at risk for developing chemotherapy-induced neutropenia mean that a placebo-controlled trial in this setting is now

uncommon. In addition, the strict definition of FN used in this study may have excluded patients who otherwise may have been reported as having FN. Moreover, the incidence of FN in cycle 1 was used as the primary measure, whereas G-CSF studies often use DSN in cycle 1 as the primary measure.

At the time the study was conducted, cisplatin and etoposide chemotherapy at the doses used was recommended for patients with stage IIIb/IV NSCLC (Belani et al. 2005). The reported incidence of FN for this regimen ranged from 8 to 12% in a population with an average risk of FN, permitting the placebo-controlled study design (311, 312, 319, 320). After the completion of this study, a systematic review and meta-analysis of the use of G-CSFs for FN prophylaxis following chemotherapy was published (Cooper et al. 2011). Although a broad range of studies was included, no study of patients with NSCLC receiving cisplatin and etoposide chemotherapy was included. The meta-analysis reported a risk ratio for FN of 0.30 [95% confidence interval (CI), 0.14–0.65] for pegfilgrastim and 0.57 (95% CI, 0.48–0.69) for filgrastim. In the current study, the odds ratio (OR) for FN in cycle 1 of 0.39 (95% CI, 0.121–1.260) for the comparison of lipegfilgrastim with placebo is in line with these results.

Secondary objectives of this study included the duration and incidence of severe neutropenia, and ANC profile (including depth of and time to ANC nadir, and time to ANC recovery). For most of these secondary measures, treatment with lipegfilgrastim was superior to placebo. In each of the four chemotherapy cycles, DSN was significantly shorter in the lipegfilgrastim group versus the placebo group ($p < 0.0001$), and in cycles 2, 3, and 4; approximately 80% of the lipegfilgrastim group experienced no severe neutropenia compared with approximately 40% of the placebo group.

The incidence of severe neutropenia also was significantly lower in the lipegfilgrastim group versus the placebo group ($p < 0.0001$). A commonly used primary measure in studies with G-CSFs, DSN in cycle 1 was used as a primary measure in a recently published study that found lipegfilgrastim to be noninferior to pegfilgrastim in patients with breast cancer (317).

In the current study, the depth of ANC nadir was significantly lower in patients treated with lipegfilgrastim versus patients receiving placebo ($p < 0.0001$), and time to ANC nadir was shorter with lipegfilgrastim treatment. Time to ANC recovery also was shorter in the lipegfilgrastim group compared with the placebo group. Furthermore, significantly fewer patients receiving lipegfilgrastim had chemotherapy dose delays compared with those

receiving placebo. These results add further support to data indicating the clinical benefits of lipegfilgrastim (317, 322).

The high incidence of AEs was anticipated in this population of patients with stage IIIb/IV NSCLC receiving chemotherapy, and AEs were consistent with the underlying disease and chemotherapy regimen administered. In addition to neutropenia, the most common AEs (≥10% in either group) were alopecia, anemia, nausea, thrombocytopenia, asthenia, vomiting, and leukopenia—all known to be associated with the chemotherapy agents used in this study. The incidence of study medication-related AEs was relatively low. Bone-pain-related symptoms, known AEs associated with G-CSF therapy, were generally mild or moderate in severity.

The mortality rate in this study was low, considering that the study population had advanced-stage disease. Most deaths were related to NSCLC or to other underlying conditions and were not considered to be related to lipegfilgrastim treatment. Deaths occurred early in and did not increase during the study; no difference in mortality was observed at the end of the 12-month follow-up, suggesting that the difference in mortality between the lipegfilgrastim and placebo groups at the end of the study was likely a chance effect.

The incidence of FN in patients with NSCLC receiving lipegfilgrastim or placebo in this study is similar to those reported in two placebo-controlled studies of pegfilgrastim in patients with advanced or metastatic colorectal cancer receiving chemotherapy regimens reported to have a low risk of FN (allowing the use of a placebo group). Again, the use of prophylactic G-CSF therapy in this setting is experimental, as the main chemotherapy regimens administered (oxaliplatin, fluorouracil, and leucovorin [FOLFOX4] or irinotecan, fluorouracil [infusion], and leucovorin [FOLFIRI]) have been reported to have a 6 and 9% incidence of FN, respectively, in patients with advanced colorectal cancer (306).

In the large phase III trial (N = 845), grade 3/4 FN was reported in 2.4% of patients receiving pegfilgrastim and in 5.7% of patients receiving placebo after four cycles of chemotherapy ($p = 0.014$) (323). In a phase II study (n = 252), grade 3/4 FN was reported in 2% of pegfilgrastim recipients and 8% of placebo recipients after four cycles of chemotherapy ($p = 0.04$) (324).

In this study in patients with stage IIIb/IV NSCLC, treatment with lipegfilgrastim did not demonstrate superiority to placebo in terms of the incidence of FN in cycle 1. Use of a G-CSF in this setting was investigational in that it was administered to patients contrary to current treatment guidelines (311, 312, 319, 320), yet treatment with lipegfilgrastim was

consistently more effective than placebo in reducing the duration and incidence of severe neutropenia and time to ANC recovery, with an acceptable safety and tolerability profile in this patient population.

I.3.4. Efficacy and safety of balugrastim compared with pegfilgrastim in patients with breast cancer receiving chemotherapy

I.3.4.1. Introduction

Neutropenia is a significant dose-limiting toxicity of myelosuppressive chemotherapy (325). Although neutropenia per se is asymptomatic, it is associated with many clinical sequelae, including increased risk for opportunistic infection, febrile neutropenia, sepsis, and related morbidity and mortality. Severe neutropenia may also delay subsequent cycles of chemotherapy.

In the absence of supportive therapy, the incidence of grade 4 or severe neutropenia (absolute neutrophil count [ANC] < 0.5 109/L) is almost 100% in patients with breast cancer receiving doxorubicin and docetaxel, and the incidence of febrile neutropenia ranges from 23% to 34% (306). The mean duration of severe neutropenia (DSN) is 3.8 days during the first cycle of treatment for these patients (326).

Recombinant granulocyte-colony stimulating factor (G-CSF) products have emerged as effective adjunct therapies for reducing the incidence and duration of chemotherapy-induced neutropenia and febrile neutropenia by stimulating neutrophil proliferation and differentiation in patients with cancer. Placebo-controlled clinical studies have shown significant reductions in the incidence of febrile neutropenia in patients treated with recombinant G-CSF products,4-8 and guidelines recommend that they be used alongside chemotherapy when the risk of febrile neutropenia is 20% or higher (297, 315, 318, 327, 328).

Filgrastim, the first recombinant human G-CSF (r-metHuGCSF), was introduced to clinical practice in 1991. However, filgrastim and similar G-CSFs require daily subcutaneous (s.c.) injections throughout the chemotherapy cycle. Attachment of a polyethylene glycol molecule (pegylation) to filgrastim to create pegfilgrastim decreases plasma clearance and extends the drug’s halflife in the body, allowing for less frequent dosing (329). Data from randomized controlled studies demonstrate similar efficacy in patients treated with once-per-cycle pegfilgrastim or twice-daily filgrastim,7,8 and pegfilgrastim is approved as an adjunct therapy in patients with nonmyeloid malignancies receiving myelosuppressive anticancer drugs (330).

Balugrastim is a recombinant protein composed of human serum albumin and human G-CSF, which allows for once-per-cycle administration without pegylation. Data from a phase II/III study demonstrated the noninferiority of balugrastim to pegfilgrastim for reducing DSN in patients with breast cancer who received doxorubicin and docetaxel (331).

The primary objective of this confirmatory phase III study was to evaluate the efficacy and safety of balugrastim compared with pegfilgrastim in patients with breast cancer who received doxorubicin and docetaxel, as evidenced by DSN in the first cycle of chemotherapy.

I.3.4.2. Materials and methods

This was a phase III double-blind randomized noninferiority study (clinical trials registration number NCT01126190) conducted by 59 investigators in 5 countries—Bulgaria, Romania, Russia, Serbia, and Ukraine.

The study was conducted in 2 phases: (1) a randomized doubleblind active-comparator phase, which was powered to evaluate whether a fixed dose of balugrastim was noninferior to pegfilgrastim in terms of safety and efficacy when given to patients with breast cancer alongside doxorubicin and docetaxel and (2) a further openlabel single-arm phase in which additional patients received balugrastim.

Patients who were enrolled in the open-label phase were included in the safety analysis. A limited number of blood samples for the analysis of balugrastim or pegfilgrastim were collected in cycles 1 and 4. Samples were obtained before study drug administration and after administration at 24, 72, and 144 hours after the dose was administered. In addition, a drug-drug interaction substudy was conducted in a subset of patients during the randomized phase of the study.

A comparison of the pharmacokinetics (PK) of doxorubicin and its main metabolite doxorubicinol was performed between treatment groups: doxorubicin/doxorubicinol with balugrastim vs. doxorubicin/doxorubicinol with pegfilgrastim. An echocardiographic (ECG) substudy was also conducted to define the ECG changes in intervals and morphologic features caused by balugrastim or pegfilgrastim and to define the relationship of the change in the duration of the QT interval corrected using Fridericia’s formula with serum concentration of balugrastim or pegfilgrastim over time.

The institutional review boards or ethics committees of the participating centers approved the protocol, and all patients gave written informed consent before any study-related procedures were performed. The study was conducted in accordance with the ethical principles of the Declaration of Helsinki and according to current International Conference

on Harmonization of Technical Requirements for Registration of Pharmaceuticals for Human Use Good Clinical Practice guidelines. The study was sponsored by Teva Pharmaceuticals, Inc.

Patients with histologically or cytologically confirmed breast cancer who were scheduled to receive doxorubicin 60 mg/m2 and docetaxel 75 mg/m2 were eligible for the study. Patients must have been 18 years of age or older and had adequate hematologic (ANC ≥ 1.5* 109 /L; platelets ≥ 100 109 /L), hepatic, and renal function (serum creatinine level < 2.0 mg/dL; alanine aminotransferase and aspartate aminotransferase levels < 1.5 the upper limit of normal; alkaline phosphatase levels < 2.5 the upper limit of normal; and total bilirubin levels within normal limits).

Patients were excluded from participating in the study if they had received 1 or more previous chemotherapy regimens (including adjuvant or neoadjuvant therapy, or both, if given ≤ 12 months before the study chemotherapy), had a previous lifetime cumulative anthracycline dose of > 240 mg/m2 of doxorubicin (or equivalent), or had received previous chemotherapy, immunotherapy, G-CSF, granulocyte macrophage-colony stimulating factor, erythropoietin, or any investigational agent ≤ 30 days before study commencement.

In the randomized double-blind active-comparator phase of this study, patients were randomized in a 1:1 ratio to receive s.c. injections of balugrastim 40 mg or pegfilgrastim 6 mg. Patients were stratified by weight (< 50 kg, ≥ 50 kg, < 80 kg, or ≥ 80 kg), previous chemotherapy exposure, and regional location. Patients enrolled in the open-label single-arm phase of the study received balugrastim. All patients were treated with doxorubicin 60 mg/m2 followed by docetaxel 75 mg/m2 administered by intravenous infusion on day 1 of a 21-day cycle for up to 4 cycles. For each cycle, patients received single injections of study medication approximately 24 hours (≥ 6 hours) after chemotherapy administration. Subsequent cycles of chemotherapy were started only if a patient had an ANC of ≥ 1. 5 109 /L and a platelet count of ≥ 100 109 /L. A delay of up to 14 days for subsequent cycles of chemotherapy was acceptable to reach these levels before chemotherapy.

A 25% reduction in the dose of both chemotherapies was allowed if grade 3/4 nonhematologic toxicity or grade 4 thrombocytopenia occurred in the previous cycle, or if the patient experienced 2 grade 3/4 infectious episodes.

Patients who experienced severe hypersensitivity reactions or nonhematologic toxicities that precluded further cycles of chemotherapy were removed from study treatment.

Participants were monitored for adverse events (AEs) and concomitant medications throughout the study.

For the double-blind phase, the intent-to-treat (ITT) population included all randomized participants. For the open-label cohort, the ITT population included all enrolled participants who satisfied eligibility criteria.

Efficacy analyses, including the primary efficacy comparison, were performed on the per-protocol (PP) population of the doubleblind cohort. The PP population included all data that were obtained from randomized participants before the occurrence of major protocol violations. Safety analyses were performed on the safety population, which included all participants who received at least 1 dose of study drug.

The primary efficacy end point was DSN in cycle 1 of chemotherapy in the PP population. Severe neutropenia was defined as grade 4 neutropenia with an ANC < 0.5 109 /L. The DSN was calculated by cycle as the number of days from the first day in which the ANC fell to less than 0.5 109 /L after chemotherapy until a patient reached an ANC ≥ 0.5 109 /L within this cycle.

Secondary efficacy end points that were derived from ANC profiles included the DSN during cycles 2, 3, and 4; time to ANC recovery; ANC nadir; and time to ANC nadir. Additional efficacy end points included the incidence of febrile neutropenia, severe neutropenia, grade 3/4 neutropenia, and various types of infection. T

he safety of balugrastim was assessed by evaluation of the type, frequency, and severity of AEs; changes in clinical laboratory test results (hematology and clinical chemistry); immunogenicity; ECG evaluations; physical examinations; and the monitoring of vital signs over time.

Noncompartmental PK parameters for balugrastim and pegfilgrastim were determined from the concentration-time profiles. Maximum observed serum concentration, time of maximum concentration, and partial area under the serum concentration-time curve from time 0 to144 hours were calculated from the PK population. Terminal elimination half-life was calculated when applicable.

Patients were monitored for AEs and concomitant medication use throughout the study. Measurements of vital signs—including heart rate, respiratory rate, systolic and diastolic blood pressure, and body temperature—were collected at screening, before and at the end of docetaxel infusion, before drug administration, and at 30 and 60 minutes after administration.

Immunogenicity was assessed before each administration of study drug (day 2 of each cycle), at the end of treatment period visit (w30 days after the last dose of study drug), and during the long-term follow-up at 6 months and 1 year after initiation of study treatment.

Blood samples were collected for ANC determination during each chemotherapy cycle ≤ 24 hours before chemotherapy, on day 3, daily from days 5 to 9 or until ANC reached ≥ 2.0 109 /L after the nadir, and then twice weekly until the next chemotherapy cycle. Serum samples for PK analyses were obtained before administration of study drugs and 24, 72, and 144 hours after dose administration in cycles 1 and 4.

All patients were followed over a 1-year period for disease progression and survival. Follow-up was scheduled 30 days after the last dose of study drug and at 6, 9, and 12 months after the start of treatment.

The sample size for this study was based on a noninferiority design and the mean DSN observed in pivotal efficacy studies for pegfilgrastim combined with data from the phase II/III study.6,7,12 The primary analysis assessed noninferiority in the PP population with a procedure that provided an overall 1-sided alpha of 0.025.

The primary analysis consisted of hypothesis testing and corresponding confidence interval (CI) estimation of the difference in mean DSN in cycle 1 between the balugrastim treatment group and the pegfilgrastim control group, defined as the mean DSN in the balugrastim group minus the mean DSN in the pegfilgrastim group.

Balugrastim was considered noninferior to pegfilgrastim if in cycle 1, the upper limit of the 2-sided 95% CI for the difference in DSN was < 1 day. If noninferiority to within 1 day was established, the upper limit of the CI was compared with margins of < 1 day to establish the smallest treatment difference that could be excluded at a 1-sided alpha of 0.025.

This closed testing procedure controlled overall 1-sided alpha at 0.025. Secondary end points were assessed by descriptive statistics and exploratory analyses. Mean time to ANC recovery (ANC ≤ 1.5 109 /L), mean ANC nadir, and mean time to ANC nadir in all cycles were compared between treatment groups using a t test.

If the test was deemed significant, 95% CIs for the mean difference between treatment groups were calculated. Mean DSN was estimated and compared between treatment groups at cycles 2 to 4 by 1-way analysis of variance; 95% CI for the difference in mean DSN between treatment groups was also presented.

The Fisher exact test was used for testing the differences in incidence of febrile neutropenia, severe neutropenia (ANC < 0.5 109 /L), and grade 3/4 neutropenia between

treatment groups. If the test was deemed significant, 95% CIs for relative risk of febrile neutropenia were calculated.

I.3.4.3. Results

Between July 2010 and May 2011, 304 patients with breast cancer were enrolled and treated in the double-blind phase of the study, and 77 additional patients were enrolled and treated in the open-label phase.

All patients randomized in the double-blind phase of the study received at least 1 dose of study medication (153 received balugrastim and 151 received pegfilgrastim) and were evaluable for efficacy analysis (ITT population).

One participant who was randomized to pegfilgrastim received chemotherapy but withdrew consent before being treated with the study drug. As a result, 150 patients were evaluable for safety analysis.

Six patients had protocol violations and were excluded from the PP population; therefore, 298 patients (150 receiving balugrastim and 148 receiving pegfilgrastim) were eligible for efficacy analysis of the primary end point.

Twenty-one patients (15 [9.8%] treated with balugrastim and 6 [4.0%] treated with pegfilgrastim) did not complete the study.

The most frequent reasons for early discontinuation were withdrawal of patient consent (5 receiving balugrastim, 2 receiving pegfilgrastim), treatment failure/disease progression (4 receiving balugrastim), failure to return/lost to follow-up (3 receiving balugrastim, 1 receiving pegfilgrastim), and AEs (2 receiving balugrastim, 1 receiving pegfilgrastim).

Of the 77 patients enrolled in the open-label safety cohort, 11 patients did not complete the study. The most frequent reasons for early discontinuation were withdrawal of consent (6 patients) and AEs (4 patients).

Mean ages of patients in the double-blind phase of the study were 51.5 (standard deviation [SD], 10.28) years and 50.8 (SD, 9.65) years for the balugrastim and pegfilgrastim groups, respectively.

The 2 groups were balanced for other demographic factors and disease status at baseline (Table III.10). All patients were white women.

No clinically relevant differences between the groups were noted for the density and intensity of chemotherapy.

The majority of patients in both the double-blind and open-label phases of this study completed all 4 treatment cycles (97.9%, 93.3%, and 88.3% for the balugrastim double-blind, pegfilgrastim, and balugrastim openlabel groups, respectively).

Of the 381 patients enrolled in the open-label and double-blind phases of this study, 348 (211 who received balugrastim and 137 who received pegfilgrastim) supplied at least 1 serum sample and were included in PK analyses.

Table III.10. Demographic and Baseline Characteristics.

Parameter	**Pegfilgrastim 6 mg**	**Balugrastim 40 mg**		
		Double Blind	**Open Label**	**All**
N	151b	153c	77	230
Age, years (mean ± SD)	50.8 (9.65)	51.5 (10.28)	52.2 (10.22)	51.8 (10.24)
Height, cm (mean ± SD)	162.1 (6.31)	162.3 (6.85)	162.2 (6.75)	162.3 (6.80)
Weight, kg (mean ± SD)	70.3 (14.43)	71.8 (13.17)	73.5 (13.64)	72.4 (13.32)
BSA, m2 (mean ± SD)	1.8 (0.19)	1.8 (0.17)	1.8 (0.18)	1.8 (0.18)
BMI, kg/m2 (mean ± SD)	26.8 (5.62)	27.3 (4.97)	28.0 (5.17)	27.5 (5.04)
Time Since Histologic Diagnosis, years (mean ± SD)	0.7 (1.72)	1.1 (3.33)	0.8 (1.68)	1.0 (2.88)
Metastatic Disease, n (%)	35 (23.2)	42 (27.5)	28 (36.4)	70 (30.4)
ECOG Status, n (%)				

0	99 (65.6)	99 (64.7)	51 (66.2)	150 (65.2)
1	52 (34.4)	54 (35.3)	22 (28.6)	76 (33.0)
2	0 (0)	0 (0)	4 (5.2)	4 (1.7)
Location of Metastasis, n (%)				
Liver	10 (6.6)	11 (7.2)	4 (5.2)	15 (6.5)
Lung	10 (6.6)	14 (9.2)	10 (13.0)	24 (10.4)
Bone	12 (7.9)	19 (12.4)	11 (14.3)	30 (13.0)
Brain	0 (0)	1 (0.7)	0 (0.0)	1 (0.4)
Distant lymph nodes	14 (9.3)	10 (6.5)	11 (14.3)	21 (9.1)
Other	12 (7.9)	18 (11.8)	3 (3.9)	21 (9.1)

Legend: ANC- absolute neutrophil count; BMI- body mass index; BSA- body surface area; ECOG- Eastern Cooperative Oncology Group; SD- standard deviation.
[a]Patient demographic data were identical between the intent-to-treat (ITT) and per-protocol (PP) populations.
[b]Three patients were excluded from the PP population: 2 patients had < 5 ANC values between day 1 and day 9 of cycle 1; 1 patient withdrew consent.
[c]Three patients were excluded from the PP population because < 5 ANC values were obtained between day 1 and day 9 of cycle 1.

DSN in cycle 1 was comparable between treatment groups, with a mean of 1.0 day in the pegfilgrastim group and 1.1 days in the balugrastim group (95% 2-sided CI, 0.13-0.37 days).

Because the upper limit of the CI was 0.37, noninferiority of balugrastim to pegfilgrastim in terms of mean cycle 1 DSN was demonstrated within a margin of 0.37 at a 1-sided alpha of 0.025.

Analyses of the ITT and PP populations were consistent and supported the same conclusion—that balugrastim is noninferior to pegfilgrastim for reducing DSN in patients treated with doxorubicin and docetaxel (Table III.11).

Table III.11. Incidence and Duration of Severe Neutropenia and Incidence of Febrile Neutropenia in Cycle 1 (Double-Blind Phase).

Parameter	**Pegfilgrastim 6 mg**	**Balugrastim 40 mg**	**P Value (95% CI)**
PP Population			
N	148	150	e
Incidence of severe neutropenia, n (%)	87 (58.8)	87 (58.0)	0.907 (-11.98 to 10.41)
Mean DSN, d (SD)	1.0 (1.08)	1.1 (1.13)	(-0.13 to 0.37)
Incidence of febrile neutropenia, n (%)	4 (2.7)	2 (1.3)	0.446
ITT Population			
N	150	153	e

Incidence of severe neutropenia, n (%)	87 (58.0)	89 (58.2)	1.000 (-10.94 to 11.28)
Mean DSN, d (SD)	1.0 (1.08)	1.1 (1.14)	(-0.11 to 0.38)
Incidence of febrile neutropenia, n (%)	4 (2.6)	2 (1.3)	0.446 (0.09 to 2.65)

Legend: CI- confidence interval; DSN- duration of severe neutropenia; ITT- intent to treat; PP- per protocol; SD- standard deviation.

In the double-blind phase of this study, the incidence of severe neutropenia in the PP population was 58.0% among balugrastimtreated patients and 58.8% among pegfilgrastim-treated patients during the first cycle of treatment.

In cycles 2 to 4, the incidence of **severe** neutropenia was comparable in both treatment groups (≤ 22.6% in the ITT and PP populations), and the mean DSN was ≤ 0.4 days.

In cycle 1, the mean ANC nadir in the PP population was 0.8 X 10^9/L in both the balugrastim and pegfilgrastim groups.

Mean time to nadir and recovery were 6.8 and 2.0 days, respectively, in the balugrastim group and 6.7 and 2.1 days, respectively, in the pegfilgrastim group (Table III.12).

In cycles 2 to 4 for both treatment groups in the PP population, the ANC nadir was slightly higher and occurred slightly later than in cycle 1.

Time to ANC recovery was also slightly shorter than in cycle 1. In each of the 4 cycles, values for each secondary end point were comparable between treatment groups and consistent between the PP and ITT populations.

For the PP and ITT populations, the incidence of grade 3/4 neutropenia during cycle 1 was 75.3% and 75.2%, respectively, among balugrastim-treated patients and 76.4% and 75.3%, respectively, among pegfilgrastim-treated patients.

Mean duration of grade 3/4 neutropenia during cycle 1 was 1.6 days in the balugrastim group and 1.7 days in the pegfilgrastim group for both populations.

For cycles 2 to 4, the incidence of grade 3/4 neutropenia was comparable in the PP and ITT populations for both treatment groups. The incidence was < 50%, with a mean duration of < 1 day in both treatment groups.

Within the PP population, febrile neutropenia was observed in 2 (1.3%) patients in the balugrastim group and 4 (2.7%) patients in the pegfilgrastim group during cycle 1 of treatment (Table III.11) and was not observed in either treatment group during cycles 2 to 4.

Table III.12. Absolute Neutrophil Count Nadir, Time to Absolute Neutrophil Count Nadir, and Time to Recovery in Cycle 1 (Per-Protocol Population).

Parameter	**Double Blind**			**Balugrastim 40 mg**	
	Pegfilgrastim 6 mg	**Balugrastim 40 mg**	**P value (95% CI)b**	**Open Label**	**All**
N[a]	148	150	e	77	227
ANC nadir 3 10^9 /L, mean (SD)	0.8 (1.04)	0.8 (1.17)	0.763 (-0.21 to 0.29)	0.8 (1.01)	0.8 (1.12)
Time to ANC nadir, d, mean (SD)	6.7 (3.33)	6.8 (2.90)	0.963 (-0.69 to 0.73)	6.5 (2.32)	6.7 (2.71)
Time to ANC recovery (≥1.5 10^9 /L), d, mean (SD)	2.1 (0.96)	2.0 (0.94)	0.259 (-0.37 to 0.10)	1.9 (0.88)	1.9 (0.92)

Legend: ANC- absolute neutrophil count; CI- confidence interval; SD- standard deviation.
[a]Patient numbers for time to ANC recovery are as follows: pegfilgrastim 6 mg double blind, n = 125; balugrastim 40 mg double blind, n = 123; balugrastim 40 mg open label, n = 64; balugrastim 40 mg all, n = 187.
[b]Balugrastim (double-blind) vs. pegfilgrastim.

Overall, the type and incidence of treatment-emergent adverse events (TEAEs) was consistent with the underlying medical condition of the study population and administration of myelosuppressive chemotherapy (Table III.13).

More than 90% of patients in each treatment group experienced at least 1 TEAE. Most TEAEs (eg, alopecia, nausea, asthenia, diarrhea, and bone pain) were attributable to

myelosuppressive chemotherapy or the primary disease and occurred in similar percentages of patients in each group during the study.

In the doubleblind phase, 19.6% and 18.7% of patients in the balugrastim and pegfilgrastim groups, respectively, had TEAEs related to the study drug (Table III.14).

The most frequently reported TEAEs considered to be related to the study drug were bone pain and related symptoms (11.8% balugrastim double-blind phase; 10.7% pegfilgrastim; 18.2% balugrastim open-label phase).

Table III.13. Treatment-Emergent Adverse Events with Incidence > 10% (Safety Population).

Parameter	**Pegfilgrastim 6 mg**	**Balugrastim 40 mg**		
	Double Blind	**Double Blind**	**Open Label**	**All**
N	150	153	77	230
Alopecia	114 (76.0)	124 (81.0)	60 (77.9)	184 (80.0)
Nausea	62 (41.3)	56 (36.6)	26 (33.8)	82 (35.7)
Asthenia	33 (22.0)	42 (27.5)	22 (28.6)	64 (27.8)
Neutropenia	40 (26.7)	45 (29.4)	16 (20.8)	61 (26.5)

Leukopenia	22 (14.7)	26 (17.0)	19 (24.7)	45 (19.6)
Decreased Appetite	20 (13.3)	24 (15.7)	10 (13.0)	34 (14.8)
Bone Pain	16 (10.7)	18 (11.8)	14 (18.2)	32 (13.9)
Diarrhea	17 (11.3)	22 (14.4)	8 (10.4)	30 (13.0)
Headache	16 (10.7)	20 (13.1)	7 (9.1)	27 (11.7)
Thrombocytopenia	10 (6.7)	23 (15.0)	2 (2.6)	25 (10.9)

Bone pain-related symptoms are expected with G-CSF treatment and were well managed using standard analgesics, requiring no additional treatment. None of the bone pain-related TEAEs led to discontinuation of study participation.

The incidence of serious adverse events (SAEs) was similar for the double-blind treatment groups (3.9% balugrastim; 4.7% pegfilgrastim). None of the SAEs were considered to be related to the study drug.

However, SAEs were considered to be related to chemotherapy for 4 (2.6%) patients receiving balugrastim and 4 (2.7%) patients receiving pegfilgrastim in the double-blind phase and 4 (5.2%) patients receiving balugrastim in the open-label phase.

The incidence of TEAEs leading to discontinuation was slightly higher in the balugrastim group (2.6%) than in the pegfilgrastim group (0.7%).

However, the investigators considered all AEs leading to discontinuation in both phases of the study to be unrelated to the study drug or chemotherapy.

During cycle 1, 5 patients in the balugrastim group and 3 patients in the pegfilgrastim group had infections, most of which were bacterial. During each cycle, the incidence of infections was low and comparable between treatment groups.

Mean leukocyte counts and ANC levels increased substantially from baseline to day 3 or day 4 and then decreased through day 7 before beginning to return to baseline.

This pattern was consistent with a mean time to ANC nadir of 6.7 days in both double blind treatment groups.

Changes from baseline in other leukocyte subpopulations generally were small, and the pattern of changes was similar across treatment cycles.

The hematocrit and hemoglobin profiles were similar among treatment groups in all 4 treatment cycles. No clinically relevant changes in vital signs were observed.

Approximately half of all patients in each treatment group had a non-clinically significant abnormality in ECG readings at baseline.

Only 1 patient in the balugrastim double-blind group had a clinically significant abnormality. Heart rate and other ECG intervals were similar among treatment groups.

Table III.14. Summary of Treatment-Emergent Adverse Events (Safety Population).

Adverse events	**Pegfilgrastim 6 mg**	**Balugrastim 40 mg**		
	Double Blind	**Double Blind**	**Open Label**	**All**
N	150	153	77	230
‡1 TEAE	140 (93.3)	140 (91.5)	72 (93.5)	212 (92.2)
‡1 TEAE Related to Study Druga	28 (18.7)	30 (19.6)	12 (15.6)	42 (18.3)
‡1 TEAE Related to Chemotherapyb	138 (92.0)	140 (91.5)	72 (93.5)	212 (92.2)
‡1 Serious TEAE	7 (4.7)	6 (3.9)	6 (7.8)	12 (5.2)
‡1 Grade 3/4 TEAE	54 (36.0)	69 (45.1)	33 (42.9)	102 (44.3)

Discontinued Because of TEAEs	1 (0.7)	4 (2.6)	4 (5.2)	8 (3.5)

Legend: TEAE- treatment-emergent adverse event.

[a]TEAEs the investigator considered as having a reasonable possibility of a causal relationship to study drug.

[b]TEAEs the investigator considered having a reasonable possibility of a causal relationship to chemotherapy.

Mean balugrastim and pegfilgrastim serum concentrations were, in general, greater in cycle 1 than in cycle 4. For patients who had definable elimination-phase profiles, the mean terminal half-lives were 38.69 hours and 32.64 hours for balugrastim in cycle 1 and cycle 4, respectively, and 41.70 hours and 46.09 hours for pegfilgrastim in cycle 1 and cycle 4, respectively.

The mean maximum observed serum concentration for balugrastim 40 mg was 847 ng/mL in cycle 1 and 648 ng/mL in cycle 4. Median Tmax values for balugrastim were 23.0 hours in cycle 1 and 22.8 hours in cycle 4.

Balugrastim mean area under the curve from time 0 to 144 hours (coefficient of variance %) was 59,236 hours ng/mL (109.1%) for cycle 1, and 31,654 hours ng/mL (110.0%) for cycle 4. When the effects of balugrastim and pegfilgrastim on ANC were plotted over time, there were no differences in terms of pharmacodynamics.

I.3.4.4. Discussion

Randomized trials have demonstrated the benefit of recombinant G-CSF products when used prophylactically for chemotherapy induced neutropenia, and pegfilgrastim is approved as an adjunct therapy in patients with non-myeloid malignancies who are receiving myelosuppressive anticancer drugs.

Balugrastim is a long-acting G-CSF being developed for once-per-cycle s.c. administration to provide a safe and effective alternative to pegfilgrastim and filgrastim to decrease the incidence of infection as manifested by febrile neutropenia.

This study demonstrated that a single fixed-dose injection of 40 mg balugrastim was as safe and effective as pegfilgrastim for decreasing DSN in patients with breast cancer who were receiving myelosuppressive chemotherapy, confirming findings from a phase II/III study of balugrastim in patients with breast cancer.

In addition, balugrastim demonstrated comparable efficacy to pegfilgrastim based on additional clinical parameters, including ANC nadir, time to ANC nadir, time to ANC recovery, incidence and duration of severe neutropenia, and incidence of febrile neutropenia.

The incidence of all TEAEs, SAEs, and TEAEs considered by the investigators to be related to study drug were comparable for balugrastim and pegfilgrastim, and there were no unexpected safety findings.

The results of this study support the conclusion that balugrastim is well tolerated when administered to patients with breast cancer who are receiving myelosuppressive chemotherapy, and the safety profile is similar for balugrastim and pegfilgrastim.

I.3.4.5. Conclusions

This study demonstrates that balugrastim 40 mg is noninferior to pegfilgrastim 6 mg for reducing DSN in patients with breast cancer who are receiving a first cycle of doxorubicin and docetaxel.

Balugrastim is a safe and effective alternative to pegfilgrastim and filgrastim for reducing the incidence of infection as manifested by febrile neutropenia in patients with nonmyeloid malignancies who are receiving myelosuppressive anticancer drugs associated with a significant incidence of severe neutropenia.

Neutropenia is a significant dose-limiting toxicity of myelosuppressive chemotherapy and is associated with increased risk for opportunistic infection, febrile neutropenia, sepsis, morbidity,and mortality.

Balugrastim is a once-per-cycle, fixed-dose recombinant fusion protein composed of human serum albumin and G-CSF, which is in development for prevention of severe neutropenia in patients with cancer.

Placebo-controlled clinical studies have shown significant reductions in the incidence of febrile neutropenia in patients treated with recombinant G-CSF products, and guidelines recommend that they be used alongside chemotherapy when the risk of febrile neutropenia is 20% or higher.

In this double-blind randomized phase III trial, balugrastim 40 mg demonstrated noninferiority to pegfilgrastim 6 mg for reducing the DSN in patients with breast cancer during the first cycle of myelosuppressive chemotherapy and had a favorable safety and tolerability profile.

Balugrastim demonstrated efficacy comparable to that of pegfilgrastim based on additional clinical parameters, including ANC nadir, time to ANC nadir, time to ANC recovery, incidence and duration of severe neutropenia, and incidence of febrile neutropenia.

The incidence of all TEAEs, SAEs, and TEAEs considered to be related to study drug were comparable for balugrastim and pegfilgrastim, and there were no unexpected safety findings.

Balugrastim is a safe and effective alternative to pegfilgrastim and filgrastim for reducing the incidence of infection as manifested by febrile neutropenia in patients with nonmyeloid malignancies who are receiving myelosuppressive anticancer drugs associated with a significant incidence of severe neutropenia.

SECTION III

Directions for future professional development and scientific research

I intend to use an array of strategies that are centred on the student in order to improve the overall quality of the didactic process. These strategies will make it easier to understand difficult theoretical concepts and exercise clinical judgment.

The first strategy will involve the promotion of active-participatory methods that are centred on the student (involvement of the student in the teaching-learning process, microgroup activities, research projects, and so on). These methods will be applied to both the didactic material and the pedagogical style that is used.

The second strategy will reunite the following types of actions: the use of various modern instructional aids for practical work and courses; encouraging active student engagement; alternative points of view; constructive criticism and personal solutions; and student self-evaluation. All of these actions will be part of the second strategy.

The third strategy will involve encouraging students to engage in research activities and participatory learning through a variety of clinical activities. The encouragement of student research activities will serve as a model for this strategy. I am assuming that these strategies will help increase the students' interest and attention in oncology topics.

Additionally, I plan to write a practical guide of oncology that will summarize the most important steps in the diagnosis and treatment of various types of cancers. This practical guide will be dedicated to students and young residents, who need a clear and concise approach of this difficult matter.

With regards to the training of residents, I will continue to involve them in clinical practice and research activities, considering the good results of our collaboration until now. Moreover, I would like to develop a micro hub of innovations in oncology, where residents and young specialists will be discussing emerging therapies and onco-therapeutic strategies. I find this activity necessary given the numerous recent advances in the field of oncology.

As a short-term didactic objective, I intend to coordinate a minimum of two undergraduate theses annually for students in their final years at the University of Medicine and Pharmacy "Grigore T. Popa" Iași, encompassing both the Romanian and foreign language-speaking sections. Furthermore, I will continue to support the students' activities for medical congresses and conferences.

I will continue my research work on current international grants, and I am interested to access other research programs in the field of oncology, personalized medicine, and bioinformatics. Specifically, colorectal cancer, non-small cell lung cancer, melanoma and hepatocarcinoma will represent the main points of interest in the following years.

I would like that my research to bring novelty on the pathophysiology of metastatic colorectal cancer (mCRC), and on causes of good or negative responses to treatments in patients with inoperable mCRC.

Moreover, I would like to integrate novel techniques of bioinformatics such as artificial intelligence (AI)-based computational framework to predict patient responses to combination therapies for mCRC therapy, based on the analysis of new potential prognostic biomarkers (for example, genetic mutations, alterations epigenetics, gene expression signatures) as molecular predictors of the response to therapy, resistance to treatment, or disease progression, compared to interventions established therapeutics.

Multidisciplinary approach and inter-institutional collaboration are essential in modern research, so I would like to increase the current networking between research institutions, clinical centers, and biobanks.

Despite recent advancements in the therapeutic approaches for non-small cell lung cancer (NSCLC), the therapy options remain limited for individuals diagnosed with NSCLC carrying the KRASG12C mutation. Throughout history, the KRAS gene has been widely regarded as a challenging target for drug development. However, due to advancements in our comprehension of KRAS, researchers have begun exploring potential drug candidates.

This has led to the recent approval of a drug called sotorasib for individuals with metastatic non-small cell lung cancer (NSCLC) that carries a specific mutation in the KRAS gene known as KRASG12C. The approval was granted based on promising results, specifically an objective response rate of 37.1% observed in a study involving 124 patients (332).

Like sotorasib, adagrasib is a specific covalent inhibitor of KRASG12C. However, there are notable pharmacologic distinctions between these two compounds. Sotorasib has a drug half-life of 5 hours, whereas adagrasib has a significantly longer half-life of 23 hours. Additionally, adagrasib exhibits dose-dependent prolonged exposure, and there is a possibility of adagrasib penetrating the central nervous system (333).

I would like to evaluate the efficacy and safety profile of this drug in a cohort of Romanian patients with KRASG12C-mutated non–small-cell lung cancer (NSCLC) previously treated with platinum-based chemotherapy and anti–programmed death 1 or

programmed death ligand 1 therapy.

The other two directions of research include: a) evaluation of the safety profile and efficacy of fianlimab combined with cemiplimab compared to pembrolizumab in patients with metastatic melanoma; b) evaluation of the safety profile and efficacy of namodenoson in the treatment of advanced hepatocarcinoma.

The integration of genomics, next generation sequencing, and bioinformatics in new risk soring systems for various types of cancers represents another research direction for me and my team. We consider that artificial intelligence and machine learning algorithms will increase the predictive performance of the screening and diagnostic strategies.

SECTION IV

REFERENCES

1. Siegel RL, Miller KD, Fuchs HE, Jemal A. Cancer statistics, 2021. Ca Cancer J Clin. 2021;71(1):7-33.
2. Torre LA, Siegel RL, Ward EM, Jemal A. Global cancer incidence and mortality rates and trends—an update. Cancer epidemiology, biomarkers & prevention. 2016;25(1):16-27.
3. Yabroff KR, Wu X-C, Negoita S, Stevens J, Coyle L, Zhao J, et al. Association of the COVID-19 pandemic with patterns of statewide cancer services. JNCI: Journal of the National Cancer Institute. 2022;114(6):907-9.
4. Sung H, Ferlay J, Siegel RL, Laversanne M, Soerjomataram I, Jemal A, et al. Global Cancer Statistics 2020: GLOBOCAN Estimates of Incidence and Mortality Worldwide for 36 Cancers in 185 Countries. CA Cancer J Clin. 2021;71(3):209-49.
5. Gupta D, Bhattacharjee O, Mandal D, Sen MK, Dey D, Dasgupta A, et al. CRISPR-Cas9 system: A new-fangled dawn in gene editing. Life sciences. 2019;232:116636.
6. Sun T, Zhang YS, Pang B, Hyun DC, Yang M, Xia Y. Engineered nanoparticles for drug delivery in cancer therapy. Nanomaterials and Neoplasms. 2021:31-142.
7. Bukowski K, Kciuk M, Kontek R. Mechanisms of multidrug resistance in cancer chemotherapy. International journal of molecular sciences. 2020;21(9):3233.
8. Jabr-Milane LS, van Vlerken LE, Yadav S, Amiji MM. Multi-functional nanocarriers to overcome tumor drug resistance. Cancer treatment reviews. 2008;34(7):592-602.
9. Wei G, Yang G, Wei B, Wang Y, Zhou S. Near-infrared light switching nitric oxide nanoemitter for triple-combination therapy of multidrug resistant cancer. Acta Biomaterialia. 2019;100:365-77.
10. Keogh J. Membrane transporters in drug development. Advances in pharmacology. 2012;63:1-42.
11. Tarasov VV, Chubarev VN, Ashraf GM, Dostdar SA, Sokolov AV, Melnikova TI, et al. How Cancer Cells Resist Chemotherapy: Design and Development of Drugs Targeting. Current Topics in Medicinal Chemistry. 2019;19:1-17.
12. Chidambaram M, Manavalan R, Kathiresan K. Nanotherapeutics to overcome conventional cancer chemotherapy limitations. Journal of pharmacy & pharmaceutical sciences. 2011;14(1):67-77.
13. Ulldemolins A, Seras-Franzoso J, Andrade F, Rafael D, Abasolo I, Gener P, et al. Perspectives of nano-carrier drug delivery systems to overcome cancer drug resistance in the clinics. Cancer Drug Resistance. 2021;4(1):44.
14. Danhier F. To exploit the tumor microenvironment: Since the EPR effect fails in the clinic, what is the future of nanomedicine? Journal of Controlled Release. 2016;244:108-21.
15. Lobatto ME, Fuster V, Fayad ZA, Mulder WJ. Perspectives and opportunities for nanomedicine in the management of atherosclerosis. Nature Reviews Drug Discovery. 2011;10(11):835-52.
16. Scarano W, De Souza P, Stenzel MH. Dual-drug delivery of curcumin and platinum drugs in polymeric micelles enhances the synergistic effects: a double act for the treatment of multidrug-resistant cancer. Biomaterials science. 2015;3(1):163-74.

17. Jang M, Han HD, Ahn HJ. A RNA nanotechnology platform for a simultaneous two-in-one siRNA delivery and its application in synergistic RNAi therapy. Scientific reports. 2016;6(1):32363.
18. Eftekhari RB, Maghsoudnia N, Samimi S, Zamzami A, Dorkoosh FA. Co-delivery nanosystems for cancer treatment: a review. Pharmaceutical nanotechnology. 2019;7(2):90-112.
19. Taratula O, Garbuzenko OB, Chen AM, Minko T. Innovative strategy for treatment of lung cancer: targeted nanotechnology-based inhalation co-delivery of anticancer drugs and siRNA. Journal of drug targeting. 2011;19(10):900-14.
20. Yin F, Yang C, Wang Q, Zeng S, Hu R, Lin G. A Light-Driven Therapy of Pancreatic Adenocarcinoma Using Gold Nanorods-Based Nanocarriers for Co-Delivery of Doxorubicin and siRNA. Theranostics, 5, 818-833. J Am Chem Soc. 2015;131:8398.
21. Pho-Iam T, Punnakitikashem P, Somboonyosdech C, Sripinitchai S, Masaratana P, Sirivatanauksorn V, et al. PLGA nanoparticles containing α-fetoprotein siRNA induce apoptosis and enhance the cytotoxic effects of doxorubicin in human liver cancer cell line. Biochemical and Biophysical Research Communications. 2021;553:191-7.
22. Blank C, Brown I, Peterson AC, Spiotto M, Iwai Y, Honjo T, et al. PD-L1/B7H-1 Inhibits the Effector Phase of Tumor Rejection by T Cell Receptor (TCR) Transgenic CD8+ T Cells. Cancer Research. 2004;64(3):1140-5.
23. Chen DS, Mellman I. Elements of cancer immunity and the cancer-immune set point. Nature. 2017;541(7637):321-30.
24. Chen IX, Chauhan VP, Posada J, Ng MR, Wu MW, Adstamongkonkul P, et al. Blocking CXCR4 alleviates desmoplasia, increases T-lymphocyte infiltration, and improves immunotherapy in metastatic breast cancer. Proceedings of the National Academy of Sciences of the United States of America. 2019;116(10):4558-66.
25. Chauhan VP, Chen IX, Tong R, Ng MR, Martin JD, Naxerova K, et al. Reprogramming the microenvironment with tumorselective angiotensin blockers enhances cancer immunotherapy. Proceedings of the National Academy of Sciences of the United States of America. 2019;166(22):10674-80.
26. Ebert PJR, Cheung J, Yang Y, McNamara E, Hong R, Moskalenko M, et al. MAP Kinase Inhibition Promotes T Cell and Anti-tumor Activity in Combination with PD-L1 Checkpoint Blockade. Immunity. 2016;44(3):609-21.
27. Mariathasan S, Turley SJ, Nickles D, Castiglioni A, Yuen K, Wang Y, et al. TGFβ attenuates tumour response to PD-L1 blockade by contributing to exclusion of T cells. Nature. 2018;554(7693):544-8.
28. Galon J, Bruni D. Approaches to treat immune hot, altered and cold tumours with combination immunotherapies. Nature Reviews Drug Discovery. 2019;18(3):197-218.
29. Mlecnik B, Tosolini M, Kirilovsky A, Berger A, Bindea G, Meatchi T, et al. Histopathologic-based prognostic factors of colorectal cancers are associated with the state of the local immune reaction. Journal of Clinical Oncology. 2011;29(6):610-8.
30. Galon J, Angell H, Bedognetti D, Marincola F. The Continuum of Cancer Immunosurveillance: Prognostic, Predictive, and Mechanistic Signatures. Immunity. 2013;39(1):11-26.
31. Angell H, Galon J. From the immune contexture to the Immunoscore: The role of prognostic and predictive immune markers in cancer. Current Opinion in Immunology. 2013;25(2):261-7.
32. Galluzzi L, Senovilla L, Vacchelli E, Eggermont A, Fridman WH, Galon J, et al. Trial watch: Dendritic cell-based interventions for cancer therapy. OncoImmunology. 2012;1(7):1111-34.

33. Galon J, Mlecnik B, Bindea G, Angell HK, Berger A, Lagorce C, et al. Towards the introduction of the 'Immunoscore' in the classification of malignant tumours. Journal of Pathology. 2014;232(2):199-209.
34. Mellman I, Coukos G, Dranoff G. Cancer immunotherapy comes of age. Nature. 2011;480(7378):480-9.
35. Oiseth SJ, Aziz MS. Cancer immunotherapy: A brief review of the history, possibilities, and challenges ahead. J Cancer Metastasis Treat. 2017;3(10):250-61.
36. Sharma N, Zahoor I, Sachdeva M, Subramaniyan V, Fuloria S, Fuloria NK, et al. Deciphering the role of nanoparticles for management of bacterial meningitis: an update on recent studies. Environ Sci Pollut Res Int. 2021;28(43):60459-76.
37. Van den Bulk J, Verdegaal EME, De Miranda NFCC. Cancer immunotherapy: broadening the scope of targetable tumours. Open Biology. 2018;8(6).
38. Majzner RG, Heitzeneder S, Mackall CL. Harnessing the Immunotherapy Revolution for the Treatment of Childhood Cancers. Cancer Cell. 2017;31(4):476-85.
39. Sambi M, Bagheri L, Szewczuk MR. Current challenges in cancer immunotherapy: Multimodal approaches to improve efficacy and patient response rates. Journal of Oncology. 2019;2019.
40. Kato S, Ross JS, Gay L, Dayyani F, Roszik J, Subbiah V, et al. Analysis of MDM2 amplification: Next-generation sequencing of patients with diverse malignancies. JCO Precision Oncology. 2018(2):1-14.
41. Champiat S, Dercle L, Ammari S, Massard C, Hollebecque A, Postel-Vinay S, et al. Hyperprogressive disease is a new pattern of progression in cancer patients treated by anti-PD-1/PD-L1. Clinical Cancer Research. 2017;23(8):1920-8.
42. Russo GL, Moro M, Sommariva M, Cancila V, Boeri M, Centonze G, et al. Antibody-Fc/FcR interaction on macrophages as a mechanism for hyperprogressive disease in non-small cell lung cancer subsequent to PD-1/PD-L1 blockade. Clinical Cancer Research. 2019;25(3):989-99.
43. Van Allen EM, Miao D, Schilling B, Shukla SA, Blank C, Zimmer L, et al. Genomic correlates of response to CTLA-4 blockade in metastatic melanoma. Science. 2015;350(6257):207-11.
44. Savas P, Salgado R, Denkert C, Sotiriou C, Darcy PK, Smyth MJ, et al. Clinical relevance of host immunity in breast cancer: From TILs to the clinic. Nature Reviews Clinical Oncology. 2016;13(4):228-41.
45. Xing X, Guo J, Wen X, Ding G, Li B, Dong B, et al. Analysis of PD1, PDL1, PDL2 expression and T cells infiltration in 1014 gastric cancer patients. OncoImmunology. 2018;7(3).
46. Schalper KA, Brown J, Carvajal-Hausdorf D, McLaughlin J, Velcheti V, Syrigos KN, et al. Objective measurement and clinical significance of TILs in non-small cell lung cancer. Journal of the National Cancer Institute. 2015;107(3).
47. Shevtsov M, Sato H, Multhoff G, Shibata A. Novel approaches to improve the efficacy of immuno-radiotherapy. Frontiers in Oncology. 2019;9(MAR).
48. Galon J, Costes A, Sanchez-Cabo F, Kirilovsky A, Mlecnik B, Lagorce-Pagès C, et al. Type, density, and location of immune cells within human colorectal tumors predict clinical outcome. Science. 2006;313(5795):1960-4.
49. Cabrita R, Lauss M, Sanna A, Donia M, Skaarup Larsen M, Mitra S, et al. Tertiary lymphoid structures improve immunotherapy and survival in melanoma. Nature. 2020;577(7791):561-5.
50. Park YM, Lee SJ, Kim YS, Lee MH, Cha GS, Jung ID, et al. Nanoparticle-based vaccine delivery for cancer immunotherapy. Immune Netw. 2013;13(5):177-83.

51. Agarwal R, Jurney P, Raythatha M, Singh V, Sreenivasan SV, Shi L, et al. Effect of Shape, Size, and Aspect Ratio on Nanoparticle Penetration and Distribution inside Solid Tissues Using 3D Spheroid Models. Advanced Healthcare Materials. 2015;4(15):2269-80.

52. Fischer HC, Hauck TS, Gómez-Aristizábal A, Chan WCW. Exploring primary liver macrophages for studying quantum dot interactions with biological systems. Advanced Materials. 2010;22(23):2520-4.

53. Gordon S, Taylor PR. Monocyte and macrophage heterogeneity. Nature Reviews Immunology. 2005;5(12):953-64.

54. Patel PC, Giljohann DA, Daniel WL, Zheng D, Prigodich AE, Mirkin CA. Scavenger receptors mediate cellular uptake of polyvalent oligonucleotide-functionalized gold nanoparticles. Bioconjugate Chemistry. 2010;21(12):2250-6.

55. Maeda H, Nakamura H, Fang J. The EPR effect for macromolecular drug delivery to solid tumors: Improvement of tumor uptake, lowering of systemic toxicity, and distinct tumor imaging in vivo. Advanced Drug Delivery Reviews. 2013;65(1):71-9.

56. Pedersen JA, Boschetti F, Swartz MA. Effects of extracellular fiber architecture on cell membrane shear stress in a 3D fibrous matrix. Journal of Biomechanics. 2007;40(7):1484-92.

57. Fleischer CC, Payne CK. Secondary structure of corona proteins determines the cell surface receptors used by nanoparticles. Journal of Physical Chemistry B. 2014;118(49):14017-26.

58. Lartigue L, Wilhelm C, Servais J, Factor C, Dencausse A, Bacri JC, et al. Nanomagnetic sensing of blood plasma protein interactions with iron oxide nanoparticles: Impact on macrophage uptake. ACS Nano. 2012;6(3):2665-78.

59. Dai Q, Guo J, Yan Y, Ang CS, Bertleff-Zieschang N, Caruso F. Cell-Conditioned Protein Coronas on Engineered Particles Influence Immune Responses. Biomacromolecules. 2017;18(2):431-9.

60. Jackson MA, Werfel TA, Curvino EJ, Yu F, Kavanaugh TE, Sarett SM, et al. Zwitterionic Nanocarrier Surface Chemistry Improves siRNA Tumor Delivery and Silencing Activity Relative to Polyethylene Glycol. ACS Nano. 2017;11(6):5680-96.

61. Cedervall T, Lynch I, Lindman S, Berggård T, Thulin E, Nilsson H, et al. Understanding the nanoparticle-protein corona using methods to quntify exchange rates and affinities of proteins for nanoparticles. Proceedings of the National Academy of Sciences of the United States of America. 2007;104(7):2050-5.

62. MATSUMOTO K, YAMAMOTO T, KAMATA R, MAEDA H. Pathogenesis of serratial infection: activation of the Hageman factor-prekallikrein cascade by serratial protease. The Journal of Biochemistry. 1984;96(3):739-49.

63. Lee S, Kivimäe S, Dolor A, Szoka FC. Macrophage-based cell therapies: the long and winding road. Journal of Controlled Release. 2016;240:527-40.

64. Lee Y-R, Lee Y-H, Im S-A, Yang I-H, Ahn GW, Kim K, et al. Biodegradable nanoparticles containing TLR3 or TLR9 agonists together with antigen enhance MHC-restricted presentation of the antigen. Archives of pharmacal research. 2010;33:1859-66.

65. Colzani B, Pandolfi L, Hoti A, Iovene PA, Natalello A, Avvakumova S, et al. Investigation of antitumor activities of trastuzumab delivered by PLGA nanoparticles. International Journal of Nanomedicine. 2018:957-73.

66. Bandyopadhyay A, Fine RL, Demento S, Bockenstedt LK, Fahmy TM. The impact of nanoparticle ligand density on dendritic-cell targeted vaccines. Biomaterials. 2011;32(11):3094-105.

67. Luo L, Zhu C, Yin H, Jiang M, Zhang J, Qin B, et al. Laser immunotherapy in combination with perdurable PD-1 blocking for the treatment of metastatic tumors. ACS nano. 2018;12(8):7647-62.
68. Nanjwade BK, Bechra HM, Derkar GK, Manvi F, Nanjwade VK. Dendrimers: emerging polymers for drug-delivery systems. European Journal of Pharmaceutical Sciences. 2009;38(3):185-96.
69. Bulbake U, Doppalapudi S, Kommineni N, Khan W. Liposomal formulations in clinical use: an updated review. Pharmaceutics. 2017;9(2):12.
70. Bozzuto G, Molinari A. Liposomes as nanomedical devices. International journal of nanomedicine. 2015:975-99.
71. Peng J, Xiao Y, Li W, Yang Q, Tan L, Jia Y, et al. Photosensitizer micelles together with IDO inhibitor enhance cancer photothermal therapy and immunotherapy. Advanced science. 2018;5(5):1700891.
72. Dykman LA, Staroverov SA, Fomin AS, Khanadeev VA, Khlebtsov BN, Bogatyrev VA. Gold nanoparticles as an adjuvant: Influence of size, shape, and technique of combination with CpG on antibody production. International Immunopharmacology. 2018;54:163-8.
73. Chen J, Wang D, Xi J, Au L, Siekkinen A, Warsen A, et al. Immuno gold nanocages with tailored optical properties for targeted photothermal destruction of cancer cells. Nano letters. 2007;7(5):1318-22.
74. Rezaei M, Hosseini SN, Khavari-Nejad RA, Najafi F, Mahdavi M. HBs antigen and mannose loading on the surface of iron oxide nanoparticles in order to immuno-targeting: Fabrication, characterization, cellular and humoral immunoassay. Artificial Cells, Nanomedicine, and Biotechnology. 2019;47(1):1543-58.
75. Warheit DB, Hartsky MA. Role of alveolar macrophage chemotaxis and phagocytosis in pulmonary clearance responses to inhaled particles: comparisons among rodent species. Microscopy research and technique. 1993;26(5):412-22.
76. Slowing II, Vivero-Escoto JL, Wu C-W, Lin VS-Y. Mesoporous silica nanoparticles as controlled release drug delivery and gene transfection carriers. Advanced drug delivery reviews. 2008;60(11):1278-88.
77. Vallhov H, Gabrielsson S, Strømme M, Scheynius A, Garcia-Bennett AE. Mesoporous silica particles induce size dependent effects on human dendritic cells. Nano letters. 2007;7(12):3576-82.
78. Hassan HA, Smyth L, Wang JT-W, Costa PM, Ratnasothy K, Diebold SS, et al. Dual stimulation of antigen presenting cells using carbon nanotube-based vaccine delivery system for cancer immunotherapy. Biomaterials. 2016;104:310-22.
79. Dash BS, Jose G, Lu Y-J, Chen J-P. Functionalized reduced graphene oxide as a versatile tool for cancer therapy. International journal of molecular sciences. 2021;22(6):2989.
80. Gurunathan S, Han JW, Eppakayala V, Kim J-H. Green synthesis of graphene and its cytotoxic effects in human breast cancer cells. International journal of nanomedicine. 2013:1015-27.
81. Liu Y, Luo Y, Wu J, Wang Y, Yang X, Yang R, et al. Graphene oxide can induce in vitro and in vivo mutagenesis. Scientific reports. 2013;3(1):3469.
82. Yang K, Wan J, Zhang S, Zhang Y, Lee S-T, Liu Z. In vivo pharmacokinetics, long-term biodistribution, and toxicology of PEGylated graphene in mice. ACS nano. 2011;5(1):516-22.
83. Wang L, Wang M, Zhou B, Zhou F, Murray C, Towner RA, et al. PEGylated reduced-graphene oxide hybridized with Fe 3 O 4 nanoparticles for cancer photothermal-immunotherapy. Journal of Materials Chemistry B. 2019;7(46):7406-14.

84. Duan W, Shi-Mei Y, Zhi-Wei S, Jing X, De-Gang Z, Hong-Bin W, et al. Genome-Wide Analysis of the Fatty Acid Desaturase Gene Family Reveals the Key Role of PfFAD3 in α-Linolenic Acid Biosynthesis in Perilla Seeds. Front Genet. 2021;12:735862.
85. Farley MM, Hu B, Margolin W, Liu J. Minicells, back in fashion. Journal of Bacteriology. 2016;198(8):1186-95.
86. Lara-Tejero M, Kato J, Wagner S, Liu X, Galán JE. A sorting platform determines the order of protein secretion in bacterial type III systems. Science. 2011;331(6021):1188-91.
87. Möller A, Lobb RJ. The evolving translational potential of small extracellular vesicles in cancer. Nature Reviews Cancer. 2020;20(12):697-709.
88. Théry C, Witwer KW, Aikawa E, Alcaraz MJ, Anderson JD, Andriantsitohaina R, et al. Minimal information for studies of extracellular vesicles 2018 (MISEV2018): a position statement of the International Society for Extracellular Vesicles and update of the MISEV2014 guidelines. Journal of extracellular vesicles. 2018;7(1):1535750.
89. Yang H, Fu H, Wang B, Zhang X, Mao J, Li X, et al. Exosomal miR-423-5p targets SUFU to promote cancer growth and metastasis and serves as a novel marker for gastric cancer. Molecular carcinogenesis. 2018;57(9):1223-36.
90. Zitvogel L, Regnault A, Lozier A, Wolfers J, Flament C, Tenza D, et al. Eradication of established murine tumors using a novel cell-free vaccine: dendritic cell derived exosomes. Nature medicine. 1998;4(5):594-600.
91. Smith DM, Simon JK, Baker Jr JR. Applications of nanotechnology for immunology. Nature Reviews Immunology. 2013;13(8):592-605.
92. Lizotte P, Wen A, Sheen M, Fields J, Rojanasopondist P, Steinmetz N, et al. In situ vaccination with cowpea mosaic virus nanoparticles suppresses metastatic cancer. Nature nanotechnology. 2016;11(3):295-303.
93. Bommareddy PK, Shettigar M, Kaufman HL. Integrating oncolytic viruses in combination cancer immunotherapy. Nature Reviews Immunology. 2018;18(8):498-513.
94. El-Shemi AG, Ashshi AM, Na Y, Li Y, Basalamah M, Al-Allaf FA, et al. Combined therapy with oncolytic adenoviruses encoding TRAIL and IL-12 genes markedly suppressed human hepatocellular carcinoma both in vitro and in an orthotopic transplanted mouse model. Journal of Experimental & Clinical Cancer Research. 2016;35:1-16.
95. Goel A, Carlson SK, Classic KL, Greiner S, Naik S, Power AT, et al. Radioiodide imaging and radiovirotherapy of multiple myeloma using VSV (Δ51)-NIS, an attenuated vesicular stomatitis virus encoding the sodium iodide symporter gene. Blood, The Journal of the American Society of Hematology. 2007;110(7):2342-50.
96. Macedo N, Miller DM, Haq R, Kaufman HL. Clinical landscape of oncolytic virus research in 2020. Journal for immunotherapy of cancer. 2020;8(2).
97. Andtbacka RH, Kaufman HL, Collichio F, Amatruda T, Senzer N, Chesney J, et al. Talimogene laherparepvec improves durable response rate in patients with advanced melanoma. Journal of clinical oncology. 2015;33(25):2780-8.
98. Goracci M, Pignochino Y, Marchiò S. Phage display-based nanotechnology applications in cancer immunotherapy. Molecules. 2020;25(4):843.
99. Akiyama Y, Miyata H, Komiyama M, Nogami M, Ozawa K, Oshita C, et al. The identification of affinity peptide ligands specific to the variable region ofhuman antibodies. Biomedical Research. 2014;35(2):105-16.
100. Jafari N, Abediankenari S. Phage particles as vaccine delivery vehicles: concepts, applications and prospects. Asian Pac J Cancer Prev. 2015;16:8019-29.

101. Zhao X, Yang K, Zhao R, Ji T, Wang X, Yang X, et al. Inducing enhanced immunogenic cell death with nanocarrier-based drug delivery systems for pancreatic cancer therapy. Biomaterials. 2016;102:187-97.

102. Chatterjee DK, Fong LS, Zhang Y. Nanoparticles in photodynamic therapy: an emerging paradigm. Advanced drug delivery reviews. 2008;60(15):1627-37.

103. Bonvalot S, Rutkowski PL, Thariat J, Carrère S, Ducassou A, Sunyach M-P, et al. NBTXR3, a first-in-class radioenhancer hafnium oxide nanoparticle, plus radiotherapy versus radiotherapy alone in patients with locally advanced soft-tissue sarcoma (Act. In. Sarc): a multicentre, phase 2–3, randomised, controlled trial. The Lancet Oncology. 2019;20(8):1148-59.

104. Taylor CT, Colgan SP. Regulation of immunity and inflammation by hypoxia in immunological niches. Nature Reviews Immunology. 2017;17(12):774-85.

105. Barsoum IB, Smallwood CA, Siemens DR, Graham CH. A mechanism of hypoxia-mediated escape from adaptive immunity in cancer cells. Cancer research. 2014;74(3):665-74.

106. Chen Q, Feng L, Liu J, Zhu W, Dong Z, Wu Y, et al. Intelligent albumin–MnO2 nanoparticles as pH-/H2O2-responsive dissociable nanocarriers to modulate tumor hypoxia for effective combination therapy. Advanced materials. 2016;28(33):7129-36.

107. Sallusto F, Lanzavecchia A. Efficient presentation of soluble antigen by cultured human dendritic cells is maintained by granulocyte/macrophage colony-stimulating factor plus interleukin 4 and downregulated by tumor necrosis factor alpha. The Journal of experimental medicine. 1994;179(4):1109-18.

108. Bonehill A, Van Nuffel AM, Corthals J, Tuyaerts S, Heirman C, François V, et al. Single-step antigen loading and activation of dendritic cells by mRNA electroporation for the purpose of therapeutic vaccination in melanoma patients. Clinical Cancer Research. 2009;15(10):3366-75.

109. Prendergast GC, Malachowski WP, DuHadaway JB, Muller AJ. Discovery of IDO1 inhibitors: from bench to bedside. Cancer research. 2017;77(24):6795-811.

110. Zanganeh S, Hutter G, Spitler R, Lenkov O, Mahmoudi M, Shaw A, et al. Iron oxide nanoparticles inhibit tumour growth by inducing pro-inflammatory macrophage polarization in tumour tissues. Nature nanotechnology. 2016;11(11):986-94.

111. Swartz MA, Hirosue S, Hubbell JA. Engineering approaches to immunotherapy. Science translational medicine. 2012;4(148):148rv9-rv9.

112. Thomas SN, Vokali E, Lund AW, Hubbell JA, Swartz MA. Targeting the tumor-draining lymph node with adjuvanted nanoparticles reshapes the anti-tumor immune response. Biomaterials. 2014;35(2):814-24.

113. Kahlert C, Kalluri R. Exosomes in tumor microenvironment influence cancer progression and metastasis. Journal of molecular medicine. 2013;91:431-7.

114. Wolf P. The Nature and Significance of Platelet Products in Human Plasma. British Journal of Haematology. 1967;13(3):269-88.

115. Munro N. Immunology and Immunotherapy in Critical Care: An Overview. AACN Adv Crit Care. 2019;30(2):113-25.

116. de Visser KE, Eichten A, Coussens LM. Paradoxical roles of the immune system during cancer development. Nature Reviews Cancer. 2006;6(1):24-37.

117. Lin W-W, Karin M. A cytokine-mediated link between innate immunity, inflammation, and cancer. The Journal of clinical investigation. 2007;117(5):1175-83.

118. Nishimura T, Iwakabe K, Sekimoto M, Ohmi Y, Yahata T, Nakui M, et al. Distinct role of antigen-specific T helper type 1 (Th1) and Th2 cells in tumor eradication in vivo. The Journal of experimental medicine. 1999;190(5):617-28.

119. DeNardo DG, Coussens LM. Inflammation and breast cancer. Balancing immune response: crosstalk between adaptive and innate immune cells during breast cancer progression. Breast cancer research. 2007;9:1-10.
120. Mailliard RB, Egawa S, Cai Q, Kalinska A, Bykovskaya SN, Lotze MT, et al. Complementary dendritic cell–activating function of CD8+ and CD4+ T cells: helper role of CD8+ T cells in the development of T helper type 1 responses. The Journal of experimental medicine. 2002;195(4):473-83.
121. Srivastava MK, Sinha P, Clements VK, Rodriguez P, Ostrand-Rosenberg S. Myeloid-derived suppressor cells inhibit T-cell activation by depleting cystine and cysteine. Cancer research. 2010;70(1):68-77.
122. Gabrilovich DI, Nagaraj S. Myeloid-derived suppressor cells as regulators of the immune system. Nature reviews immunology. 2009;9(3):162-74.
123. Mantovani A, Sica A. Macrophages, innate immunity and cancer: balance, tolerance, and diversity. Current opinion in immunology. 2010;22(2):231-7.
124. Solinas G, Germano G, Mantovani A, Allavena P. Tumor-associated macrophages (TAM) as major players of the cancer-related inflammation. Journal of leukocyte biology. 2009;86(5):1065-73.
125. Schreiber RD, Old LJ, Smyth MJ. Cancer immunoediting: integrating immunity's roles in cancer suppression and promotion. Science. 2011;331(6024):1565-70.
126. Lesterhuis WJ, Haanen JB, Punt CJ. Cancer immunotherapy–revisited. Nature reviews Drug discovery. 2011;10(8):591-600.
127. Cobaleda-Siles M, Henriksen-Lacey M, de Angulo AR, Bernecker A, Vallejo VG, Szczupak B, et al. An iron oxide nanocarrier for dsRNA to target lymph nodes and strongly activate cells of the immune system. Small. 2014;10(24):5054-67.
128. Khalil DN, Smith EL, Brentjens RJ, Wolchok JD. The future of cancer treatment: immunomodulation, CARs and combination immunotherapy. Nature reviews Clinical oncology. 2016;13(5):273-90.
129. Rosalia RA, Cruz LJ, van Duikeren S, Tromp AT, Silva AL, Jiskoot W, et al. CD40-targeted dendritic cell delivery of PLGA-nanoparticle vaccines induce potent anti-tumor responses. Biomaterials. 2015;40:88-97.
130. Yuba E, Yamaguchi A, Yoshizaki Y, Harada A, Kono K. Bioactive polysaccharide-based pH-sensitive polymers for cytoplasmic delivery of antigen and activation of antigen-specific immunity. Biomaterials. 2017;120:32-45.
131. Waeckerle-Men Y, Groettrup M. PLGA microspheres for improved antigen delivery to dendritic cells as cellular vaccines. Advanced drug delivery reviews. 2005;57(3):475-82.
132. Torchilin VP. Recent advances with liposomes as pharmaceutical carriers. Nature reviews Drug discovery. 2005;4(2):145-60.
133. Li H, Li Y, Wang X, Hou Y, Hong X, Gong T, et al. Rational design of polymeric hybrid micelles to overcome lymphatic and intracellular delivery barriers in cancer immunotherapy. Theranostics. 2017;7(18):4383.
134. Zhao Y, Zhao X, Cheng Y, Guo X, Yuan W. Iron oxide nanoparticles-based vaccine delivery for cancer treatment. Molecular pharmaceutics. 2018;15(5):1791-9.
135. Raposo G, Nijman HW, Stoorvogel W, Liejendekker R, Harding CV, Melief C, et al. B lymphocytes secrete antigen-presenting vesicles. The Journal of experimental medicine. 1996;183(3):1161-72.
136. Guo ZS, Liu Z, Bartlett DL. Oncolytic immunotherapy: dying the right way is a key to eliciting potent antitumor immunity. Frontiers in oncology. 2014;4:74.

137. Round JL, Mazmanian SK. Inducible Foxp3+ regulatory T-cell development by a commensal bacterium of the intestinal microbiota. Proceedings of the National Academy of Sciences. 2010;107(27):12204-9.

138. Cebula A, Seweryn M, Rempala GA, Pabla SS, McIndoe RA, Denning TL, et al. Thymus-derived regulatory T cells contribute to tolerance to commensal microbiota. Nature. 2013;497(7448):258-62.

139. Ivanov II, Atarashi K, Manel N, Brodie EL, Shima T, Karaoz U, et al. Induction of intestinal Th17 cells by segmented filamentous bacteria. Cell. 2009;139(3):485-98.

140. Tomkovich S, Jobin C. Microbiota and host immune responses: a love–hate relationship. Immunology. 2016;147(1):1-10.

141. Maeda H. Tumor-selective delivery of macromolecular drugs via the EPR effect: background and future prospects. Bioconjugate chemistry. 2010;21(5):797-802.

142. Marshall JS, Green AM, Pensky J, Williams S, Zinn A, Carlson DM. Measurement of circulating desialylated glycoproteins and correlation with hepatocellular damage. The Journal of Clinical Investigation. 1974;54(3):555-62.

143. Campbell RB, Fukumura D, Brown EB, Mazzola LM, Izumi Y, Jain RK, et al. Cationic charge determines the distribution of liposomes between the vascular and extravascular compartments of tumors. Cancer research. 2002;62(23):6831-6.

144. Park J, Choi Y, Chang H, Um W, Ryu JH, Kwon IC. Alliance with EPR effect: combined strategies to improve the EPR effect in the tumor microenvironment. Theranostics. 2019;9(26):8073.

145. Grossmannm V, Schmitt VH, Zeller T, Panova-Noeva M, Schulz A, Laubert-Reh D, et al. Profile of the immune and inflammatory response in individuals with prediabetes and type 2 diabetes. Diabetes Care. 2015;38(7):1356-64.

146. Barbero F, Russo L, Vitali M, Piella J, Salvo I, Borrajo ML, et al., editors. Formation of the protein corona: the interface between nanoparticles and the immune system. Seminars in immunology; 2017: Elsevier.

147. Xu J, Wang H, Xu L, Chao Y, Wang C, Han X, et al. Nanovaccine based on a protein-delivering dendrimer for effective antigen cross-presentation and cancer immunotherapy. Biomaterials. 2019;207:1-9.

148. Li L, Goedegebuure S, Gillanders WE. Preclinical and clinical development of neoantigen vaccines. Annals of Oncology. 2017;28:xii11-xii7.

149. Stone JD, Harris DT, Kranz DM. TCR affinity for p/MHC formed by tumor antigens that are self-proteins: impact on efficacy and toxicity. Current opinion in immunology. 2015;33:16-22.

150. Atif SM, Gibbings SL, Redente EF, Camp FA, Torres RM, Kedl RM, et al. Immune surveillance by natural IgM is required for early neoantigen recognition and initiation of adaptive immunity. American Journal of Respiratory Cell and Molecular Biology. 2018;59(5):580-91.

151. Li Q, Zhang D, Zhang J, Jiang Y, Song A, Li Z, et al. A Three-in-One Immunotherapy Nanoweapon via Cascade-Amplifying Cancer-Immunity Cycle against Tumor Metastasis, Relapse, and Postsurgical Regrowth. Nano Lett. 2019;19(9):6647-57.

152. Sahin U, Derhovanessian E, Miller M, Kloke BP, Simon P, Löwer M, et al. Personalized RNA mutanome vaccines mobilize poly-specific therapeutic immunity against cancer. Nature. 2017;547(7662):222-6.

153. Nonomura C, Otsuka M, Kondou R, Iizuka A, Miyata H, Ashizawa T, et al. Identification of a neoantigen epitope in a melanoma patient with good response to anti-PD-1 antibody therapy. Immunol Lett. 2019;208:52-9.

154. Kreiter S, Selmi A, Diken M, Koslowski M, Britten CM, Huber C, et al. Intranodal vaccination with naked antigen-encoding RNA elicits potent prophylactic and therapeutic antitumoral immunity. Cancer Res. 2010;70(22):9031-40.

155. Hilf N, Kuttruff-Coqui S, Frenzel K, Bukur V, Stevanović S, Gouttefangeas C, et al. Actively personalized vaccination trial for newly diagnosed glioblastoma. Nature. 2019;565(7738):240-5.

156. Robbins PF, Morgan RA, Feldman SA, Yang JC, Sherry RM, Dudley ME, et al. Tumor regression in patients with metastatic synovial cell sarcoma and melanoma using genetically engineered lymphocytes reactive with NY-ESO-1. J Clin Oncol. 2011;29(7):917-24.

157. Bencherif SA, Warren Sands R, Ali OA, Li WA, Lewin SA, Braschler TM, et al. Injectable cryogel-based whole-cell cancer vaccines. Nat Commun. 2015;6:7556.

158. Hassani Najafabadi A, Zhang J, Aikins ME, Najaf Abadi ZI, Liao F, Qin Y, et al. Cancer Immunotherapy via Targeting Cancer Stem Cells Using Vaccine Nanodiscs. Nano Lett. 2020;20(10):7783-92.

159. Zheng F, Dang J, Zhang H, Xu F, Ba D, Zhang B, et al. Cancer Stem Cell Vaccination With PD-L1 and CTLA-4 Blockades Enhances the Eradication of Melanoma Stem Cells in a Mouse Tumor Model. J Immunother. 2018;41(8):361-8.

160. Aggarwal S. Adverse effects of immuno-oncology drugs-Awareness, diagnosis, and management: A literature review of immune-mediated adverse events. Indian J Cancer. 2019;56(Supplement):S10-s22.

161. Li Y, Fang M, Zhang J, Wang J, Song Y, Shi J, et al. Hydrogel dual delivered celecoxib and anti-PD-1 synergistically improve antitumor immunity. Oncoimmunology. 2016;5(2):e1074374.

162. Wang C, Ye Y, Hochu GM, Sadeghifar H, Gu Z. Enhanced Cancer Immunotherapy by Microneedle Patch-Assisted Delivery of Anti-PD1 Antibody. Nano Lett. 2016;16(4):2334-40.

163. Ordikhani F, Uehara M, Kasinath V, Dai L, Eskandari SK, Bahmani B, et al. Targeting antigen-presenting cells by anti-PD-1 nanoparticles augments antitumor immunity. JCI Insight. 2018;3(20).

164. Li SY, Liu Y, Xu CF, Shen S, Sun R, Du XJ, et al. Restoring anti-tumor functions of T cells via nanoparticle-mediated immune checkpoint modulation. J Control Release. 2016;231:17-28.

165. Alimohammadi R, Alibeigi R, Nikpoor AR, Chalbatani GM, Webster TJ, Jaafari MR, et al. Encapsulated Checkpoint Blocker Before Chemotherapy: The Optimal Sequence of Anti-CTLA-4 and Doxil Combination Therapy. Int J Nanomedicine. 2020;15:5279-88.

166. Zhang YX, Zhao YY, Shen J, Sun X, Liu Y, Liu H, et al. Nanoenabled Modulation of Acidic Tumor Microenvironment Reverses Anergy of Infiltrating T Cells and Potentiates Anti-PD-1 Therapy. Nano Lett. 2019;19(5):2774-83.

167. Hei Y, Teng B, Zeng Z, Zhang S, Li Q, Pan J, et al. Multifunctional Immunoliposomes Combining Catalase and PD-L1 Antibodies Overcome Tumor Hypoxia and Enhance Immunotherapeutic Effects Against Melanoma. Int J Nanomedicine. 2020;15:1677-91.

168. Mishchenko T, Mitroshina E, Balalaeva I, Krysko O, Vedunova M, Krysko DV. An emerging role for nanomaterials in increasing immunogenicity of cancer cell death. Biochim Biophys Acta Rev Cancer. 2019;1871(1):99-108.

169. Obeid M, Panaretakis T, Joza N, Tufi R, Tesniere A, van Endert P, et al. Calreticulin exposure is required for the immunogenicity of gamma-irradiation and UVC light-induced apoptosis. Cell Death Differ. 2007;14(10):1848-50.

170. Garg AD, Martin S, Golab J, Agostinis P. Danger signalling during cancer cell death: origins, plasticity and regulation. Cell Death Differ. 2014;21(1):26-38.

171. Min Y, Roche KC, Tian S, Eblan MJ, McKinnon KP, Caster JM, et al. Antigen-capturing nanoparticles improve the abscopal effect and cancer immunotherapy. Nature Nanotechnology. 2017;12(9):877-82.

172. Seth A, Heo MB, Lim YT. Poly (γ-glutamic acid) based combination of water-insoluble paclitaxel and TLR7 agonist for chemo-immunotherapy. Biomaterials. 2014;35(27):7992-8001.

173. Deng H, Tan S, Gao X, Zou C, Xu C, Tu K, et al. Cdk5 knocking out mediated by CRISPR-Cas9 genome editing for PD-L1 attenuation and enhanced antitumor immunity. Acta Pharm Sin B. 2020;10(2):358-73.

174. Tzeng SY, Patel KK, Wilson DR, Meyer RA, Rhodes KR, Green JJ. In situ genetic engineering of tumors for long-lasting and systemic immunotherapy. Proc Natl Acad Sci U S A. 2020;117(8):4043-52.

175. Guan X, Lin L, Chen J, Hu Y, Sun P, Tian H, et al. Efficient PD-L1 gene silence promoted by hyaluronidase for cancer immunotherapy. J Control Release. 2019;293:104-12.

176. Hamdy S, Molavi O, Ma Z, Haddadi A, Alshamsan A, Gobti Z, et al. Co-delivery of cancer-associated antigen and Toll-like receptor 4 ligand in PLGA nanoparticles induces potent CD8+ T cell-mediated anti-tumor immunity. Vaccine. 2008;26(39):5046-57.

177. Zhang Z, Tongchusak S, Mizukami Y, Kang YJ, Ioji T, Touma M, et al. Induction of anti-tumor cytotoxic T cell responses through PLGA-nanoparticle mediated antigen delivery. Biomaterials. 2011;32(14):3666-78.

178. Rodell CB, Arlauckas SP, Cuccarese MF, Garris CS, Li R, Ahmed MS, et al. TLR7/8-agonist-loaded nanoparticles promote the polarization of tumour-associated macrophages to enhance cancer immunotherapy. Nat Biomed Eng. 2018;2(8):578-88.

179. Chen Q, Wang C, Zhang X, Chen G, Hu Q, Li H, et al. In situ sprayed bioresponsive immunotherapeutic gel for post-surgical cancer treatment. Nat Nanotechnol. 2019;14(1):89-97.

180. Alupei MC, Licarete E, Patras L, Banciu M. Liposomal simvastatin inhibits tumor growth via targeting tumor-associated macrophages-mediated oxidative stress. Cancer Lett. 2015;356(2 Pt B):946-52.

181. Qian Y, Qiao S, Dai Y, Xu G, Dai B, Lu L, et al. Molecular-Targeted Immunotherapeutic Strategy for Melanoma via Dual-Targeting Nanoparticles Delivering Small Interfering RNA to Tumor-Associated Macrophages. ACS Nano. 2017;11(9):9536-49.

182. Hornyák L, Dobos N, Koncz G, Karányi Z, Páll D, Szabó Z, et al. The Role of Indoleamine-2,3-Dioxygenase in Cancer Development, Diagnostics, and Therapy. Front Immunol. 2018;9:151.

183. Orabona C, Pallotta MT, Volpi C, Fallarino F, Vacca C, Bianchi R, et al. SOCS3 drives proteasomal degradation of indoleamine 2,3-dioxygenase (IDO) and antagonizes IDO-dependent tolerogenesis. Proc Natl Acad Sci U S A. 2008;105(52):20828-33.

184. Shou D, Wen L, Song Z, Yin J, Sun Q, Gong W. Suppressive role of myeloid-derived suppressor cells (MDSCs) in the microenvironment of breast cancer and targeted immunotherapies. Oncotarget. 2016;7(39):64505-11.

185. Zhao Q, Kuang DM, Wu Y, Xiao X, Li XF, Li TJ, et al. Activated CD69+ T cells foster immune privilege by regulating IDO expression in tumor-associated macrophages. J Immunol. 2012;188(3):1117-24.

186. Cheng K, Ding Y, Zhao Y, Ye S, Zhao X, Zhang Y, et al. Sequentially Responsive Therapeutic Peptide Assembling Nanoparticles for Dual-Targeted Cancer Immunotherapy. Nano Lett. 2018;18(5):3250-8.

187. Ye Y, Wang J, Hu Q, Hochu GM, Xin H, Wang C, et al. Synergistic Transcutaneous Immunotherapy Enhances Antitumor Immune Responses through Delivery of Checkpoint Inhibitors. ACS Nano. 2016;10(9):8956-63.

188. Aoki CA, Borchers AT, Li M, Flavell RA, Bowlus CL, Ansari AA, et al. Transforming growth factor beta (TGF-beta) and autoimmunity. Autoimmun Rev. 2005;4(7):450-9.

189. Zheng Y, Tang L, Mabardi L, Kumari S, Irvine DJ. Enhancing Adoptive Cell Therapy of Cancer through Targeted Delivery of Small-Molecule Immunomodulators to Internalizing or Noninternalizing Receptors. ACS Nano. 2017;11(3):3089-100.

190. Kang M, Hong J, Jung M, Kwon SP, Song SY, Kim HY, et al. T-Cell-Mimicking Nanoparticles for Cancer Immunotherapy. Adv Mater. 2020;32(39):e2003368.

191. Shi Y, Lammers T. Combining Nanomedicine and Immunotherapy. Acc Chem Res. 2019;52(6):1543-54.

192. Xu Z, Wang Y, Zhang L, Huang L. Nanoparticle-delivered transforming growth factor-β siRNA enhances vaccination against advanced melanoma by modifying tumor microenvironment. ACS Nano. 2014;8(4):3636-45.

193. Kohlhapp FJ, Kaufman HL. Molecular Pathways: Mechanism of Action for Talimogene Laherparepvec, a New Oncolytic Virus Immunotherapy. Clin Cancer Res. 2016;22(5):1048-54.

194. Conry RM, Westbrook B, McKee S, Norwood TG. Talimogene laherparepvec: First in class oncolytic virotherapy. Hum Vaccin Immunother. 2018;14(4):839-46.

195. Puzanov I, Milhem MM, Minor D, Hamid O, Li A, Chen L, et al. Talimogene Laherparepvec in Combination With Ipilimumab in Previously Untreated, Unresectable Stage IIIB-IV Melanoma. J Clin Oncol. 2016;34(22):2619-26.

196. Chesney J, Puzanov I, Collichio F, Singh P, Milhem MM, Glaspy J, et al. Randomized, Open-Label Phase II Study Evaluating the Efficacy and Safety of Talimogene Laherparepvec in Combination With Ipilimumab Versus Ipilimumab Alone in Patients With Advanced, Unresectable Melanoma. J Clin Oncol. 2018;36(17):1658-67.

197. Chari RVJ. Targeted cancer therapy: Conferring specificity to cytotoxic drugs. Accounts of Chemical Research. 2008;41(1):98-107.

198. Park K. Controlled drug delivery systems: Past forward and future back. Journal of Controlled Release. 2014;190:3-8.

199. Kuen CY, Galen T, Fakurazi S, Othman SS, Masarudin MJ. Increased cytotoxic efficacy of protocatechuic acid in A549 human lung cancer delivered via hydrophobically modified-chitosan nanoparticles as an anticancer modality. Polymers. 2020;12(9).

200. Pertici V, Pin-Barre C, Rivera C, Pellegrino C, Laurin J, Gigmes D, et al. Degradable and Injectable Hydrogel for Drug Delivery in Soft Tissues. Biomacromolecules. 2019;20(1):149-63.

201. Sultankulov B, Berillo D, Sultankulova K, Tokay T, Saparov A. Progress in the development of chitosan-based biomaterials for tissue engineering and regenerative medicine. Biomolecules. 2019;9(9).

202. Ailincai D, Dorobanu AM, Dima B, Irimiciuc TA, Lupacu C, Agop M, et al. Poly(vinyl alcohol boric acid)-Diclofenac Sodium Salt Drug Delivery Systems: Experimental and Theoretical Studies. Journal of Immunology Research. 2020;2020.

203. Pantziarka P, Sukhatme V, Bouche G, Meheus L, Sukhatme VP. Repurposing Drugs in Oncology (ReDO) - Diclofenac as an anti-cancer agent. ecancermedicalscience. 2016;10.
204. Isanbor C, O'Hagan D. Fluorine in medicinal chemistry: A review of anti-cancer agents. Journal of Fluorine Chemistry. 2006;127(3):303-19.
205. Marin L, Popescu MC, Zabulica A, Uji-I H, Fron E. Chitosan as matrix for bio-polymer dispersed liquid crystal systems. Carbohydrate Polymers. 2013;95(1):16-24.
206. Ailincai D, Mititelu-Tartau L, Marin L. Citryl-imine-PEG-ylated chitosan hydrogels – Promising materials for drug delivery applications. International Journal of Biological Macromolecules. 2020;162:1323-37.
207. Fisher OZ, Khademhosseini A, Peppas NA. Drug delivery: nanoscale devices. Encyclopedia of materials: science and technology. 2010:1-9.
208. Peppas NA, Brannon-Peppas L. Drug delivery biomaterials. Encyclopedia of Materials: Science and Technology. 2001:2351-5.
209. Tiwari G, Tiwari R, Sriwastawa B, Bhati L, Pandey S, Pandey P, et al. Drug delivery systems: An updated review. Int J Pharm Invest. 2012;2(1):2-11.
210. Patra JK, Das G, Fraceto LF, Campos EVR, Rodriguez-Torres MDP, Acosta-Torres LS, et al. Nano based drug delivery systems: Recent developments and future prospects. Journal of Nanobiotechnology. 2018;16(1).
211. Kosmidis K, Argyrakis P, Macheras P. Fractal kinetics in drug release from finite fractal matrices. Journal of Chemical Physics. 2003;119(12):6373-7.
212. Agop M, Merches I. Operational procedures describing physical systems. 2019.
213. Nottale L. Scale relativity and fractal space-time: A new approach to unifying relativity and quantum mechanics2011. 1-743 p.
214. Agop M, Paun VP. On the new perspectives of fractal theory. Fundaments and Applications. 2017.
215. Cobzeanu BM, Irimiciuc S, Vaideanu D, Grigorovici A, Popa O. Possible dynamics of polymer chains by means of a Ricatti's procedure-an exploitation for drug release at large time intervals. Materiale Plastice. 2017;54(3):531-4.
216. Iftime MM, Dobreci DL, Irimiciuc SA, Agop M, Petrescu T, Doroftei B. A theoretical mathematical model for assessing diclofenac release from chitosan-based formulations. Drug Delivery. 2020;27(1):1125-33.
217. Iancu R, Irimiciuc SA, Agop M, Frasila M, Paun MA, Paun VA, et al. 5-Fluorouracil release from chitosan-based matrix. Experimental and theoretical aspects. Materiale Plastice. 2020;57(3):180-9.
218. Cristescu CP. Nonlinear Dynamics and Chaos Theoretical Fundaments and Applications. Nonlinear Dynamics and Chaos: Theoretical Fundaments and Applications. 2008.
219. Mandelbrot BB. The Fractal Geometry of Nature. 1982.
220. Merches I, Agop M. Differentiability and fractality in dynamics of physical systems2015. 1-299 p.
221. Mazilu N, Agop M, Merches I. The Mathematical Principles of Scale Relativity Physics: The Concept of Interpretation. 2019.
222. Mazilu N, Skyrmions AM. A great finishing touch to classical Newtonian philosophy. 2012.
223. Penrose R. A spinor approach to general relativity. Annals of Physics. 1960;10(2):171-201.
224. Barbilian D. Elementary Algebra, the Didactic Works of Dan Barbilian. 1971.

225. Barbilian D. Geometry and the Theory of Functions, in "The Didactic Works of Dan Barbilian". Geometry and the Theory of Functions, the Didactic Works of Dan Barbilian. 1974.
226. Cartan E. Riemannian Geometry in an Orthogonal Frame. 2001.
227. Misner CW, Thorne KS, Wheeler JA. 2017.
228. Jackson EA. Perspectives of Nonlinear Dynamics. 1991.
229. Skyrme THR. Selected papers with commentary. World scientific series in 20th century physics. 1994;3.
230. Angheluță T. Theory of Functions with Complex Variations. 1957.
231. Iftime MM, Morariu S, Marin L. Salicyl-imine-chitosan hydrogels: Supramolecular architecturing as a crosslinking method toward multifunctional hydrogels. Carbohydrate Polymers. 2017;165:39-50.
232. Olaru AM, Marin L, Morariu S, Pricope G, Pinteala M, Tartau-Mititelu L. Biocompatible chitosan based hydrogels for potential application in local tumour therapy. Carbohydrate Polymers. 2018;179:59-70.
233. Craciun AM, Mititelu Tartau L, Pinteala M, Marin L. Nitrosalicyl-imine-chitosan hydrogels based drug delivery systems for long term sustained release in local therapy. Journal of Colloid and Interface Science. 2019;536:196-207.
234. Iftime MM, Mititelu Tartau L, Marin L. New formulations based on salicyl-imine-chitosan hydrogels for prolonged drug release. International Journal of Biological Macromolecules. 2020;160:398-408.
235. Morgensztern D, Ng SH, Gao F, Govindan R. Trends in stage distribution for patients with non-small cell lung cancer: a National Cancer Database survey. J Thorac Oncol. 2010;5(1):29-33.
236. Siegel RL, Miller KD, Fuchs HE, Jemal A. Cancer statistics, 2022. CA Cancer J Clin. 2022;72(1):7-33.
237. Thomas A, Liu SV, Subramaniam DS, Giaccone G. Refining the treatment of NSCLC according to histological and molecular subtypes. Nat Rev Clin Oncol. 2015;12(9):511-26.
238. Chaft JE, Rimner A, Weder W, Azzoli CG, Kris MG, Cascone T. Evolution of systemic therapy for stages I-III non-metastatic non-small-cell lung cancer. Nat Rev Clin Oncol. 2021;18(9):547-57.
239. Remon J, Soria JC, Peters S. Early and locally advanced non-small-cell lung cancer: an update of the ESMO Clinical Practice Guidelines focusing on diagnosis, staging, systemic and local therapy. Ann Oncol. 2021;32(12):1637-42.
240. Brahmer J, Reckamp KL, Baas P, Crinò L, Eberhardt WE, Poddubskaya E, et al. Nivolumab versus Docetaxel in Advanced Squamous-Cell Non-Small-Cell Lung Cancer. N Engl J Med. 2015;373(2):123-35.
241. Borghaei H, Paz-Ares L, Horn L, Spigel DR, Steins M, Ready NE, et al. Nivolumab versus Docetaxel in Advanced Nonsquamous Non-Small-Cell Lung Cancer. N Engl J Med. 2015;373(17):1627-39.
242. Arnold M, Sierra MS, Laversanne M, Soerjomataram I, Jemal A, Bray F. Global patterns and trends in colorectal cancer incidence and mortality. Gut. 2017;66(4):683-91.
243. González-Mariscal L, Betanzos A, Nava P, Jaramillo BE. Tight junction proteins. Prog Biophys Mol Biol. 2003;81(1):1-44.
244. Pope JL, Bhat AA, Sharma A, Ahmad R, Krishnan M, Washington MK, et al. Claudin-1 regulates intestinal epithelial homeostasis through the modulation of Notch-signalling. Gut. 2014;63(4):622-34.

245. Lee JW, Lee SJ, Seo J, Song SY, Ahn G, Park CS, et al. Increased expressions of claudin-1 and claudin-7 during the progression of cervical neoplasia. Gynecol Oncol. 2005;97(1):53-9.
246. Sauer T, Pedersen MK, Ebeltoft K, Naess O. Reduced expression of Claudin-7 in fine needle aspirates from breast carcinomas correlate with grading and metastatic disease. Cytopathology. 2005;16(4):193-8.
247. Usami Y, Chiba H, Nakayama F, Ueda J, Matsuda Y, Sawada N, et al. Reduced expression of claudin-7 correlates with invasion and metastasis in squamous cell carcinoma of the esophagus. Hum Pathol. 2006;37(5):569-77.
248. Quan JC, Peng J, Guan X, Liu Z, Jiang Z, Chen HP, et al. Evaluation of clinical significance of claudin 7 and construction of prognostic grading system for stage II colorectal cancer. World J Clin Cases. 2020;8(11):2190-200.
249. Pardoll DM. The blockade of immune checkpoints in cancer immunotherapy. Nat Rev Cancer. 2012;12(4):252-64.
250. Niezgoda A, Niezgoda P, Czajkowski R. Novel Approaches to Treatment of Advanced Melanoma: A Review on Targeted Therapy and Immunotherapy. Biomed Res Int. 2015;2015:851387.
251. Bansal P, Osman D, Gan GN, Simon GR, Boumber Y. Recent Advances in Immunotherapy in Metastatic NSCLC. Front Oncol. 2016;6:239.
252. Gill DM, Agarwal N, Vaishampayan U. Evolving Treatment Paradigm in Metastatic Renal Cell Carcinoma. Am Soc Clin Oncol Educ Book. 2017;37:319-29.
253. Wang C, Thudium KB, Han M, Wang XT, Huang H, Feingersh D, et al. In vitro characterization of the anti-PD-1 antibody nivolumab, BMS-936558, and in vivo toxicology in non-human primates. Cancer Immunol Res. 2014;2(9):846-56.
254. Renner A, Burotto M, Rojas C. Immune Checkpoint Inhibitor Dosing: Can We Go Lower Without Compromising Clinical Efficacy? J Glob Oncol. 2019;5:1-5.
255. Agrawal S, Feng Y, Roy A, Kollia G, Lestini B. Nivolumab dose selection: challenges, opportunities, and lessons learned for cancer immunotherapy. J Immunother Cancer. 2016;4:72.
256. Yoo SH, Keam B, Kim M, Kim SH, Kim YJ, Kim TM, et al. Low-dose nivolumab can be effective in non-small cell lung cancer: alternative option for financial toxicity. ESMO Open. 2018;3(5):e000332.
257. Zhang J, Sanghavi K, Shen J, Zhao X, Feng Y, Statkevich P, et al. Population Pharmacokinetics of Nivolumab in Combination With Ipilimumab in Patients With Advanced Malignancies. CPT Pharmacometrics Syst Pharmacol. 2019;8(12):962-70.
258. Payne RB, Little AJ, Williams RB, Milner JR. Interpretation of serum calcium in patients with abnormal serum proteins. Br Med J. 1973;4(5893):643-6.
259. Cusato J, Genova C, Tomasello C, Carrega P, Ottonello S, Pietra G, et al. Influence of Vitamin D in Advanced Non-Small Cell Lung Cancer Patients Treated with Nivolumab. Cancers (Basel). 2019;11(1).
260. Barta JA, Powell CA, Wisnivesky JP. Global Epidemiology of Lung Cancer. Ann Glob Health. 2019;85(1).
261. Tamura T, Kurishima K, Nakazawa K, Kagohashi K, Ishikawa H, Satoh H, et al. Specific organ metastases and survival in metastatic non-small-cell lung cancer. Mol Clin Oncol. 2015;3(1):217-21.
262. Crinò L, Bronte G, Bidoli P, Cravero P, Minenza E, Cortesi E, et al. Nivolumab and brain metastases in patients with advanced non-squamous non-small cell lung cancer. Lung Cancer. 2019;129:35-40.

263. Karantanos T, Karanika S, Seth B, Gignac G. The absolute lymphocyte count can predict the overall survival of patients with non-small cell lung cancer on nivolumab: a clinical study. Clin Transl Oncol. 2019;21(2):206-12.

264. Pantano F, Russano M, Berruti A, Mansueto G, Migliorino MR, Adamo V, et al. Prognostic clinical factors in patients affected by non-small-cell lung cancer receiving Nivolumab. Expert Opin Biol Ther. 2020;20(3):319-26.

265. Lee CS, Devoe CE, Zhu X, Fishbein JS, Seetharamu N. Pretreatment nutritional status and response to checkpoint inhibitors in lung cancer. Lung Cancer Manag. 2020;9(2):Lmt31.

266. Brown KGM, Koh CE. Surgical management of recurrent colon cancer. Journal of Gastrointestinal Oncology. 2020;11(3):513-25.

267. Nomura M, Takahashi H, Fujii M, Miyoshi N, Haraguchi N, Hata T, et al. Clinical significance of invasion distance relative to prognosis in pathological T3 colorectal cancer. Oncology Letters. 2019;18(5):5614-20.

268. Mathonnet M, Perraud A, Christou N, Akil H, Melin C, Battu S, et al. Hallmarks in colorectal cancer: Angiogenesis and cancer stem-like cells. World Journal of Gastroenterology. 2014;20(15):4189-96.

269. Zhou M, Fu L, Zhang J. Who will benefit more from maintenance therapy of metastatic colorectal cancer? Oncotarget. 2018;9(15):12479-86.

270. Li W, Xu C, Wang K, Ding Y, Ding L. Non-tight junction-related function of claudin-7 in interacting with integrinβ1 to suppress colorectal cancer cell proliferation and migration. Cancer Management and Research. 2019;11:1443-51.

271. Xu C, Wang X, Li W, Wang K, Ding L. Expression and clinical significance of claudin-7 in patients with colorectal cancer. Technology in Cancer Research and Treatment. 2018;17.

272. Wang K, Xu C, Li W, Ding L. Emerging clinical significance of claudin-7 in colorectal cancer: A review. Cancer Management and Research. 2018;10:3741-52.

273. Kim WK, Kwon Y, Jang M, Park M, Kim J, Cho S, et al. β-catenin activation down-regulates cell-cell junction-related genes and induces epithelial-to-mesenchymal transition in colorectal cancers. Scientific Reports. 2019;9(1).

274. Kuhn S, Koch M, Nübel T, Ladwein M, Antolovic D, Klingbeil P, et al. A complex of EpCAM, claudin-7, CD44 variant isoforms, and tetraspanins promotes colorectal cancer progression. Molecular Cancer Research. 2007;5(6):553-67.

275. Gowrikumar S, Primeaux M, Pravoverov K, Wu C, Szeglin BC, Sauvé CEG, et al. A claudin-based molecular signature identifies high-risk, chemoresistant colorectal cancer patients. Cells. 2021;10(9).

276. Koni M, Pinnarò V, Brizzi MF. The wnt signalling pathway: A tailored target in cancer. International Journal of Molecular Sciences. 2020;21(20):1-26.

277. Yoshida N, Kinugasa T, Ohshima K, Yuge K, Ohchi T, Fujino S, et al. Analysis of Wnt and β-catenin expression in advanced colorectal cancer. Anticancer Research. 2015;35(8):4403-10.

278. Sawicki T, Ruszkowska M, Danielewicz A, Niedźwiedzka E, Arłukowicz T, Przybyłowicz KE. A review of colorectal cancer in terms of epidemiology, risk factors, development, symptoms and diagnosis. Cancers. 2021;13(9).

279. Wang Y, He X, Nie H, Zhou J, Cao P, Ou C. Application of artificial intelligence to the diagnosis and therapy of colorectal cancer. Am J Cancer Res. 2020;10(11):3575-98.

280. Gründner J, Prokosch HU, Stürzl M, Croner R, Christoph J, Toddenroth D. Predicting clinical outcomes in colorectal cancer using machine learning. Studies in Health Technology and Informatics2018. p. 101-5.

281. Misawa M, Kudo SE, Mori Y, Cho T, Kataoka S, Yamauchi A, et al. Artificial Intelligence-Assisted Polyp Detection for Colonoscopy: Initial Experience. Gastroenterology. 2018;154(8):2027-9.e3.

282. Amirkhah R, Farazmand A, Gupta SK, Ahmadi H, Wolkenhauer O, Schmitz U. Naïve Bayes classifier predicts functional microRNA target interactions in colorectal cancer. Molecular BioSystems. 2015;11(8):2126-34.

283. Ladwein M, Pape UF, Schmidt DS, Schnölzer M, Fiedler S, Langbein L, et al. The cell-cell adhesion molecule EpCAM interacts directly with the tight junction protein claudin-7. Experimental Cell Research. 2005;309(2):345-57.

284. Bornholdt J, Friis S, Godiksen S, Poulsen SS, Santoni-Rugiu E, Bisgaard HC, et al. The level of claudin-7 is reduced as an early event in colorectal carcinogenesis. BMC Cancer. 2011;11.

285. Oshima T, Kunisaki C, Yoshihara K, Yamada R, Yamamoto N, Sato T, et al. Reduced expression of the claudin-7 gene correlates with venous invasion and liver metastasis in colorectal cancer. Oncology Reports. 2008;19(4):953-9.

286. Darido C, Buchert M, Pannequin J, Bastide P, Zalzali H, Mantamadiotis T, et al. Defective claudin-7 regulation by Tcf-4 and Sox-9 disrupts the polarity and increases the tumorigenicity of colorectal cancer cells. Cancer Research. 2008;68(11):4258-68.

287. Wang K, Ding Y, Xu C, Hao M, Li H, Ding L. Cldn-7 deficiency promotes experimental colitis and associated carcinogenesis by regulating intestinal epithelial integrity. OncoImmunology. 2021;10(1).

288. Xu C, Ding YH, Wang K, Hao M, Li H, Ding L. Claudin-7 deficiency promotes stemness properties in colorectal cancer through Sox9-mediated Wnt/β-catenin signalling. Journal of Translational Medicine. 2021;19(1).

289. Hou Y, Hou L, Liang Y, Zhang Q, Hong X, Wang Y, et al. The p53-inducible CLDN7 regulates colorectal tumorigenesis and has prognostic significance. Neoplasia (United States). 2020;22(11):590-603.

290. Van Domburg R, Hoeks S, Kardys I, Lenzen M, Boersma E. Tools and techniques - Statistics: How many variables are allowed in the logistic and Cox regression models? EuroIntervention. 2014;9(12):1472-3.

291. Peduzzi P, Concato J, Kemper E, Holford TR, Feinstem AR. A simulation study of the number of events per variable in logistic regression analysis. Journal of Clinical Epidemiology. 1996;49(12):1373-9.

292. Heuser M, Ganser A, Bokemeyer C. Use of colony-stimulating factors for chemotherapy-associated neutropenia: review of current guidelines. Semin Hematol. 2007;44(3):148-56.

293. Pettengell R, Schwenkglenks M, Leonard R, Bosly A, Paridaens R, Constenla M, et al. Neutropenia occurrence and predictors of reduced chemotherapy delivery: results from the INC-EU prospective observational European neutropenia study. Support Care Cancer. 2008;16(11):1299-309.

294. Kuderer NM, Dale DC, Crawford J, Cosler LE, Lyman GH. Mortality, morbidity, and cost associated with febrile neutropenia in adult cancer patients. Cancer. 2006;106(10):2258-66.

295. Aapro MS, Bohlius J, Cameron DA, Dal Lago L, Donnelly JP, Kearney N, et al. 2010 update of EORTC guidelines for the use of granulocyte-colony stimulating factor to reduce the incidence of chemotherapy-induced febrile neutropenia in adult patients with lymphoproliferative disorders and solid tumours. Eur J Cancer. 2011;47(1):8-32.

296. Ozer H, Armitage JO, Bennett CL, Crawford J, Demetri GD, Pizzo PA, et al. 2000 update of recommendations for the use of hematopoietic colony-stimulating factors:

evidence-based, clinical practice guidelines. American Society of Clinical Oncology Growth Factors Expert Panel. J Clin Oncol. 2000;18(20):3558-85.

297. Smith TJ, Khatcheressian J, Lyman GH, Ozer H, Armitage JO, Balducci L, et al. 2006 update of recommendations for the use of white blood cell growth factors: an evidence-based clinical practice guideline. J Clin Oncol. 2006;24(19):3187-205.

298. Yang BB, Kido A. Pharmacokinetics and pharmacodynamics of pegfilgrastim. Clin Pharmacokinet. 2011;50(5):295-306.

299. Buchner A, Lammerich A, Abdolzade-Bavil A, Müller U, Bias P. Lipegfilgrastim: pharmacodynamics and pharmacokinetics for body-weight-adjusted and 6 mg fixed doses in two randomized studies in healthy volunteers. Curr Med Res Opin. 2014;30(12):2523-33.

300. Halpern W, Riccobene TA, Agostini H, Baker K, Stolow D, Gu ML, et al. Albugranin, a recombinant human granulocyte colony stimulating factor (G-CSF) genetically fused to recombinant human albumin induces prolonged myelopoietic effects in mice and monkeys. Pharm Res. 2002;19(11):1720-9.

301. Gladkov O, Moiseyenko V, Bondarenko IN, Shparyk Y, Barash S, Adar L, et al. A Phase III Study of Balugrastim Versus Pegfilgrastim in Breast Cancer Patients Receiving Chemotherapy With Doxorubicin and Docetaxel. Oncologist. 2016;21(1):7-15.

302. Balducci L, Hardy CL, Lyman GH. Hematopoietic growth factors in the older cancer patient. Current Opinion in Hematology. 2001;8(3):170-87.

303. Smith BD, Smith GL, Hurria A, Hortobagyi GN, Buchholz TA. Future of cancer incidence in the United States: Burdens upon an aging, changing nation. Journal of Clinical Oncology. 2009;27(17):2758-65.

304. Crawford J, Armitage J, Balducci L, Becker PS, Blayney DW, Cataland SR, et al. Myeloid growth factors. JNCCN Journal of the National Comprehensive Cancer Network. 2013;11(10):1266-90.

305. Crawford J, Caserta C, Roila F. Hematopoietic growth factors: ESMO Clinical Practice Guidelines for the applications. Annals of Oncology. 2010;21(SUPPL. 5):v248-v51.

306. Smith TJ, Khatcheressian J, Lyman GH, Ozer H, Armitage JO, Balducci L, et al. 2006 Update of recommendations for the use of white blood cell growth factors: An evidence-based clinical practice guideline. Journal of Clinical Oncology. 2006;24(19):3187-205.

307. Balducci L, Al-Halawani H, Charu V, Tam J, Shahin S, Dreiling L, et al. Elderly cancer patients receiving chemotherapy benefit from first-cycle pegfilgrastim. Oncologist. 2007;12(12):1416-24.

308. Buchner A, Elsässer R, Bias P. A randomized, double-blind, active control, multicenter, dose-finding study of lipegfilgrastim (XM22) in breast cancer patients receiving myelosuppressive therapy. Breast Cancer Research and Treatment. 2014;148(1):107-16.

309. Volovat C, Bondarenko IM, Gladkov OA, Elsässer R, Buchner A, Bias P, et al. Phase III, randomized, double-blind, placebo-controlled, multicenter study of lipegfilgrastim in patients with non-small cell lung cancer receiving myelosuppressive therapy. SpringerPlus. 2015;4(1).

310. Mavroudis D, Papadakis E, Veslemes M, Tsiafaki X, Stavrakakis J, Kouroussis C, et al. A multicenter randomized clinical trial comparing paclitaxel-cisplatin-etoposide versus cisplatin-etoposide as first-line treatment in patients with small-cell lung cancer. Annals of Oncology. 2001;12(4):463-70.

311. Cardenal F, Paz López-Cabrerizo M, Antón A, Alberola V, Massuti B, Carrato A, et al. Randomized phase III study of gemcitabine-cisplatin versus etoposide-

cisplatin in the treatment of locally advanced or metastatic non-small-cell lung cancer. Journal of Clinical Oncology. 1999;17(1):12-8.

312. Hanna N, Bunn Jr PA, Langer C, Einhorn L, Guthrie Jr T, Beck T, et al. Randomized phase III trial comparing irinotecan/cisplatin with etoposide/cisplatin in patients with previously untreated extensive-stage disease small-cell lime cancer. Journal of Clinical Oncology. 2006;24(13):2038-43.

313. Lyman GH. Risks and Consequences of Chemotherapy-Induced Neutropenia. Clinical Cornerstone. 2006;8(SUPPL. 5):S12-S8.

314. Minisini A, Spazzapan S, Crivellari D, Aapro M, Biganzoli L. Incidence of febrile neutropenia and neutropenic infections in elderly patients receiving anthracycline-based chemotherapy for breast cancer without primary prophylaxis with colony-stimulating factors. Critical Reviews in Oncology/Hematology. 2005;53(2):125-31.

315. Holmes FA, O'Shaughnessy JA, Vukelja S, Jones SE, Shogan J, Savin M, et al. Blinded, randomized, multicenter study to evaluate single administration pegfilgrastim once per cycle versus daily filgrastim as an adjunct to chemotherapy in patients with high-risk stage II or stage III/IV breast cancer. Journal of Clinical Oncology. 2002;20(3):727-31.

316. Cooper KL, Madan J, Whyte S, Stevenson MD, Akehurst RL. Granulocyte colony-stimulating factors for febrile neutropenia prophylaxis following chemotherapy: Systematic review and meta-analysis. BMC Cancer. 2011;11.

317. Bondarenko I, Gladkov OA, Elsaesser R, Buchner A, Bias P. Efficacy and safety of lipegfilgrastim versus pegfilgrastim: A randomized, multicenter, active-control phase 3 trial in patients with breast cancer receiving doxorubicin/docetaxel chemotherapy. BMC Cancer. 2013;13.

318. Vogel CL, Wojtukiewicz MZ, Carroll RR, Tjulandin SA, Barajas-Figueroa LJ, Wiens BL, et al. First and subsequent cycle use of pegfilgrastim prevents febrile neutropenia in patients with breast cancer: A multicenter, double-blind, placebo-controlled phase III study. Journal of Clinical Oncology. 2005;23(6):1178-84.

319. Bonomi P, Kim K, Fairclough D, Cella D, Kugler J, Rowinsky E, et al. Comparison of survival and quality of life in advanced non-small-cell lung cancer patients treated with two dose levels of paclitaxel combined with cisplatin versus etoposide with cisplatin: Results of an eastern cooperative oncology group trial. Journal of Clinical Oncology. 2000;18(3):623-31.

320. Eckardt JR, Von Pawel J, Papai Z, Tomova A, Tzekova V, Crofts TE, et al. Open-label, multicenter, randomized, phase III study comparing oral topotecan/cisplatin versus etoposide/cisplatin as treatment for chemotherapy-naive patients with extensive-disease small-cell lung cancer. Journal of Clinical Oncology. 2006;24(13):2044-51.

321. Crawford J, Glaspy JA, Stoller RG. Final results of a placebo-controlled study of filgrastim in small-cell lung cancer: Exploration of risk factors for febrile neutropenia. Support Cancer Ther. 2005;3(1):36-46.

322. Buchner A, Bias P, Kaufmann M. A randomized, double-blind, active control, multicenter, dose-finding study of XM22, glycopegfilgrastim, in patients with breast cancer receiving myelosuppressive therapy [abstract 9080]. J Clin Oncol. 2011;29.

323. Pinter T, Abella S, Cesas A, Croitoru A, Decaestecker J, Gibbs P, et al. Results of a phase III, randomized, double-blind, placebo-controlled trial of pegfilgrastim (PEG) in patients (pts) receiving first-line FOLFOX or FOLFIRI and bevacizumab (B) for colorectal cancer (CRC). J Clin Oncol: Off J Am Soc Clin Oncol. 2013;30.

324. Hecht JR, Pillai M, Gollard R, Heim W, Swan F, Patel R, et al. A randomized, placebo-controlled phase II study evaluating the reduction of neutropenia and febrile neutropenia in patients with colorectal cancer receiving pegfilgrastim with every-2-week chemotherapy. Clinical Colorectal Cancer. 2010;9(2):95-101.

325. Ozer H, Armitage JO, Bennett CL, Crawford J, Demetri GD, Pizzo PA, et al. 2000 Update of recommendations for the use of hematopoietic colony-stimulating factors: Evidence-based, clinical practice guidelines. Journal of Clinical Oncology. 2000;18(20):3558-85.

326. del Giglio A, Eniu A, Ganea-Motan D, Topuzov E, Lubenau H. XM02 is superior to placebo and equivalent to Neupogen™ in reducing the duration of severe neutropenia and the incidence of febrile neutropenia in cycle 1 in breast cancer patients receiving docetaxel/doxorubicin chemotherapy. BMC Cancer. 2008;8.

327. Trillet-Lenoir V, Green J, Manegold C, Von Pawel J, Gatzemeier U, Lebeau B, et al. Recombinant granulocyte colony stimulating factor reduces the infectious complications of cytotoxic chemotherapy. European Journal of Cancer. 1993;29(3):319-24.

328. Crawford J, Ozer H, Stoller R, Johnson D, Lyman G, Tabbara I, et al. Reduction by Granulocyte Colony-Stimulating Factor of Fever and Neutropenia Induced by Chemotherapy in Patients with Small-Cell Lung Cancer. New England Journal of Medicine. 1991;325(3):164-70.

329. Molineux G, Kinstler O, Briddell B, Hartley C, McElroy P, Kerzic P, et al. A new form of Filgrastim with sustained duration in vivo and enhanced ability to mobilize PBPC in both mice and humans. Experimental Hematology. 1999;27(12):1724-34.

330. . Neulasta (Pegfilgrastim) Prescribing Information. 2002.

331. Gladkov O, Moiseyenko V, Bondarenko IN. A Randomized, Noninferiority Study of Recombinant Human G-CSF/human Serum Albumin Fusion (CG-10639) and Pegfilgrastim in Breast Cancer Patients Receiving Myelosuppressive Therapy. 2011.

332. Skoulidis F, Li BT, Dy GK, Price TJ, Falchook GS, Wolf J, et al. Sotorasib for Lung Cancers with KRAS p.G12C Mutation. N Engl J Med. 2021;384(25):2371-81.

333. Ou SI, Jänne PA, Leal TA, Rybkin, II, Sabari JK, Barve MA, et al. First-in-Human Phase I/IB Dose-Finding Study of Adagrasib (MRTX849) in Patients With Advanced KRAS(G12C) Solid Tumors (KRYSTAL-1). J Clin Oncol. 2022;40(23):2530-8.